THE THERMAL REGIME OF A STREAM IN CENTRAL ALASKA

A

THESIS

Presented to the Faculty of the

University of Alaska in partial fulfillment

of the Requirements

for the Degree of

MASTER OF SCIENCE

By

Samuel W. Corbin, B.A.

Fairbanks, Alaska

December 1977

THE THERMAL REGIME OF A STREAM IN CENTRAL ALASKA

RECOMMENDED:

Chairman, Advisory Committee

Department Head

APPROVED:

Dean of the College of Environmental Sciences

August 23, 1977
Date

Vice Chancellor for Research and Advanced Study

August 27, 1977
Date

ABSTRACT

Hydrology and thermal regimen of Goldstream Creek near Fairbanks, Alaska, was observed over the ten-year period from 1963 to 1973. During four winters, temperature cross-sections were measured in the aufeis including (in 1971) the top three meters of soil for 10 meters outward from the banks.

Depth of freezing and maximum ground surface temperature were one meter and 22°C respectively adjacent to the stream and 30 cm and 11°C beneath the streambed. The entire thickness of aufies was periodically warmed to 0°C by successive water overflows during winter.

Using: (1) Fourier analysis, (2) numerical step models, and (3) differential analysis, the thermal diffusivity of the soil was found to range from 0.004 cm^2 sec^{-1} (adjacent to stream) to over 0.015 cm^2 sec^{-1} (beneath stream). The calculations were made by assuming homogeneous material and heat conduction only. This proved inadequate, especially beneath the stream, where movement of gound water appeared to be the chief heat-transfer mechanism.

ACKNOWLEDGMENTS

I wish to express my appreciation to Dr. Carl S. Benson of the Geophysical Institute, under whose patient guidance and advice this study was made. I also extend my gratitude to other members of the Advisory Committee for their valuable time and worthwhile discussion: Dr. Gunter Weller of the Geophysical Institute, Dr. Gerd Wendler also of the Geophysical Institute, and Dr. Jan Cannon of the Department of Geology.

This project was made possible through funds from the Geophysical Institute, whose personnel were also generous in providing use of laboratory and shop facilities and for providing transportation to the field site. Appreciation is extended also to the Department of Geology for further financial support and for providing the thermocouple wire necessary for the project.

In addition, I wish to gratefully acknowledge the following individuals for use of data pertinent to the project: Mr. Timothy Hudson, Institute of Water Resources; Dr. Earl H. Beistline, Dean of the College of Mineral Industries; Mr. Larry R. Mayo of the United States Geological Survery; Mr. Donval Simpson, Institute of Arctic Biology; and Mr. John Gynch of the Alaska Department of Highways.

Special thanks is also rendered to those who patiently and unselfishly assisted me in the fieldwork at Goldstream Creek: Messrs. Robert L. Holbrook, Bjarne Holm, Stan Parker, John Larson, and Leslie Wheeler and Dr. Phillip E. Nicpon.

Finally, I wish to extend my sincere appreciation to Ms. Sandra Moseley, Ms. Mary Lee Morris and Ms. Toni Johnson who generously provided their time and skill with the typing of the manuscript, and to Mr. James Burton and Mr. Rodney March, who painstakingly drafted most of the illustrations.

TABLE OF CONTENTS

* Mention of brand names for manufactured products is for information only and should not be construed as advertisement for said products.

LIST OF PLATES

LIST OF FIGURES

LIST OF TABLES

CHAPTER 1

INTRODUCTION

The temperature distribution in the near surface layers of the earth is determined by many factors; the most important of which are the various components of the surface energy balance, proximity to bodies of water and ice, amount of insulating snow cover, topography, and the thermal properties of soil, which vary with moisture content.

In a given locality, the intrinsic thermal properties of the earth's material remain fairly constant, with the exception that the thermal diffusivity decreases significantly with decreasing moisture content and increases slightly upon freezing of the moisture. In addition, the relatively small heat flux due to the geothermal gradient is generally constant; and any changes in the uppermost portion of the earth's temperature profile are due almost entirely to changes in conditions at the ground surface.

The thermal effect of changing surface conditions (i.e., temperature amplitudes) decreases exponentially with depth below the surface at a rate that is inversely proportional to the thermal diffusivity of the ground. Where temperature changes are periodic, this exponential decrease in the range of temperatures is inversely proportional also to the period of variation. For example, daily temperature fluctuations in the soil are rarely measurable at depths greater than one meter; annual temperature fluctuations, however, can penetrate noticeably to depths of about twenty meters, while the effects of long-term climatic changes penetrate hundreds of meters.

In cold regions the amplitude caused by air temperature fluctuations is greatly moderated in the soil due to insulation by the snow cover and to latent heat exchanges resulting from the freezing and thawing of soil moisture.

1.1 Scope of study

In the literature there are many references to studies which have been devoted to thermal effects of large bodies of water on their surroundings. A book covering all aspects of microclimatology was published by R. Geiger in 1965 and has become perhaps the most important reference work on such studies. B. Michel has summarized hydrological, thermal, and engineering aspects of rivers and lakes in temperate and sub-arctic environments (Michel, 1971); and in Alaska M. C. Brewer studied the thermal regime of a shallow lake on the Alaskan Arctic slope (Brewer, 1958). Relatively little effort has been made concerning the effects of smaller bodies of water, such as creeks and streams, especially in the Arctic and sub-Arctic regions.

The problems posed for the present study are: (1) to observe the effect of a small sub-Arctic stream upon the temperature regime in the surrounding soil throughout the annual cycle, (2) to analyze the temperature data and derive the thermal parameters of the soil, using Fourier and numerical techniques, and (3) to evaluate the relative importance of various factors to the thermal regime - such as latent heat exchanges in the soil, insulation due to snow, and heat transfer by water movement in the soil. The stream system consists of five media with different thermal properties: water, ice, snow, frozen soil, and unfrozen soil.

This study was part of a broader effort devoted to a better understanding of the over-all hydrology of sub-Arctic streams (Benson, 1966; Benson, 1967; Benson and Kreitner, 1968; Kreitner, 1969; Corbin and Benson, 1971; Gilfilian et al., 1972; Gilfilian, 1973; Benson, 1973; Osterkamp et al., 1975). All field work was conducted at an experimental site of the University of Alaska, located at Goldstream Creek near Fairbanks, Alaska. Aside from its basic research aspects, this study may also be of use in view of the presently widespread development of the northern regions and the increasing need for environmental information pertaining to streams. The importance of streams in the north is realized when one considers their extensive aufeis formations acting as potential water sources and winter transportation routes, the engineering problems caused by flooding and icing over roads and bridges, and the practice of using stream beds as burial sites for oil and gas pipelines.

1.2 Location and description of site

To study the thermal regime of a subarctic stream, Goldstream Creek, a tributary of the Tanana River drainage system, was selected on account of easy accessibility from the Univeristy. Located 9 km northwest of Fairbanks, the research site is situated immediately upstream from Ballaine Road (Plate 1 and Figure 1), at an elevation of 183 meters above sea level. The stream drains a watershed of about 191 km^2, flows southwest in a broad swampy valley underlain by discontinous permafrost, and is fairly typical of streams in central Alaska. Ice wedge polygons

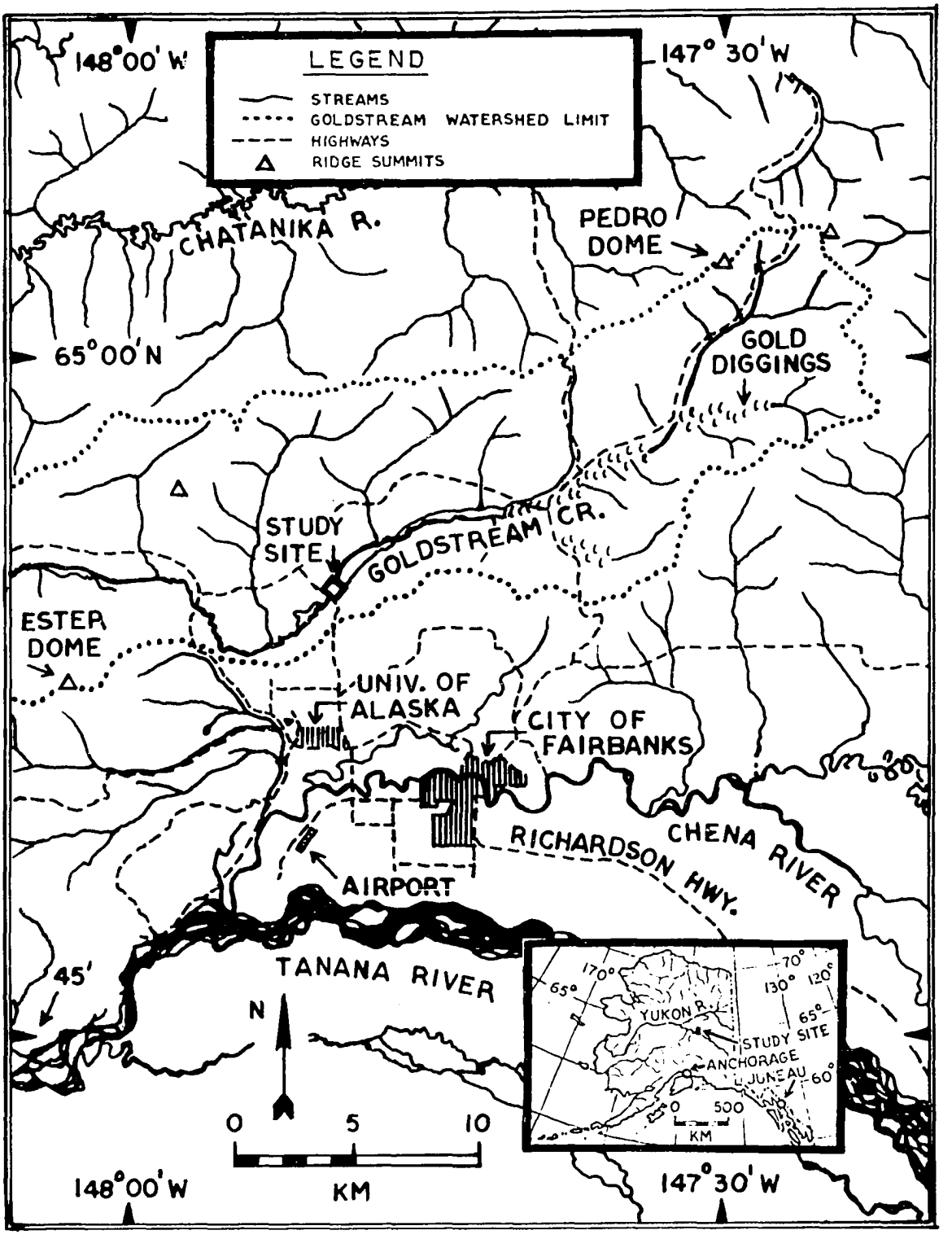

Figure 1. Location map of study site on Goldstream Creek, adjacent to Ballaine Road about 9 km northwest of Fairbanks, Alaska.

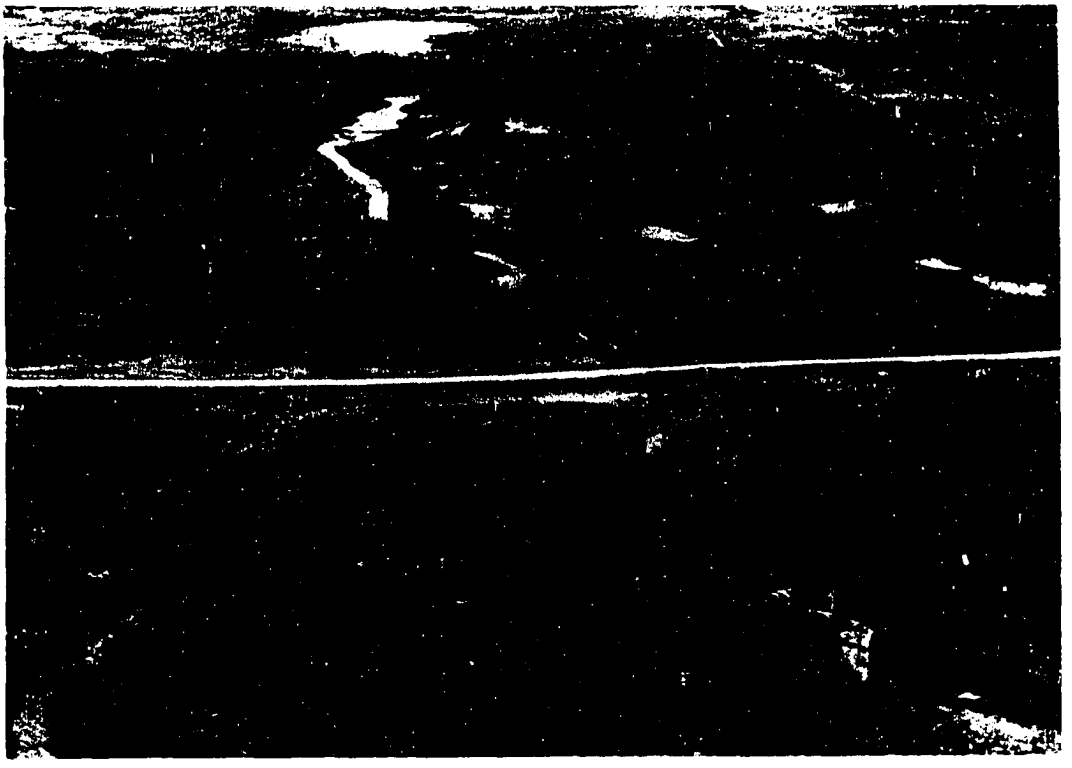

Plate 1. Aerial oblique view of Goldstream Creek, looking northeast. Photograph was taken August 1964 prior to construction of hut.

are numerous in the valley floor, and the vegetation consists mostly of willows and sparse stands of spruce.

The soil is silt with low organic content (10% or less). Sandy gravel covers the stream bottom and interbedded layers of gravel occur in the silt near the banks. Studies conducted by the Alaska Highway Department indicate a depth of 4 to 5 meters for the permafrost table. Throughout the cross-section studied, the author probed to depths of 5 meters, but did not encounter permafrost anywhere within 10 meters of the stream banks; hence, the permafrost table is apparently deeper beneath the stream bed. Data from a hole drilled by the Highway Department located about 35 meters from the east bank across from the site revealed very wet to saturated silt throughout the 7.0 meters drilled, topped by 6 cm of organic material with permafrost occurring at a depth of 4.27 meters.

1.3 Climate

Sheltered from maritime influences by the Alaska and Chugach Ranges, the climate of interior Alaska is continental. In Fairbanks, the mean annual air temperature is -3.4°C and the range extends from -50°C to +33°C, the annual precipitation averages 28.7 cm water equivalent. Winds are slight, averaging only 2.3 meters per second usually from the north, and the sky averages 30% clear (National Weather Service (NWS) 1931-1969).

During midwinter, the period of maximum sunshine is less than four hours, solar elevations are low, and the persistent snow cover reflects most of the incoming radiation. Air temperatures can drop below -50°C and steep temperature inversions form in the lowest layers of the atmosphere. The mean daily maximum and minimum temperatures throughout January, taken from the 1931-1960 National Weather Service records, are -18.2°C and -29.7°C, respectively. During July, the period with the sun above the horizon reaches 21 hours, with mean daily maximum and minimum temperatures of 22.1°C and 8.7°C. Air temperatures observed at Goldstream Creek are generally 3°C lower than at the Fairbanks airport.

Precipitation follows a regular pattern, reaching a monthly maximum of 5.6 cm for August and a minimum of 0.6 cm in April. Average annual snowfall is 178 cm, of which 40 cm makes November the month of heaviest snowfall.

1.4 Hydrology

Among sub-arctic streams, Goldstream Creek is fairly typical. At the fieldsite, the stream bed is about 8 meters wide with well-defined banks 1.8 meters high, and the stream flows in a south-south-westerly direction down an average gradient of 2.2 meters per kilometer.

The discharge rate is approximately one cubic meter per second. Measurements by the USGS indicate 0.31 and 0.38 m^3 sec^{-1} respectively during July and October 1969. Throughout October 1971, the rate varied between 0.6 and 1.3 m^3 sec^{-1} (Gilfilian, 1973). The mid-winter rate has not been determined. However, it is expected to be much less than the

lowest values cited above. The average depth of the stream is around 25 cm, giving a typical cross-section of 2.0 m^2.

The hydrological cycle of the stream can be conveniently divided into six periods: (1) supercooling and underwater ice formation, (2) freeze-up, (3) overflowing and aufeis build-up, (4) mid-winter period, (5) spring break-up, and (6) summer period. This sequence is summarized as follows.

1.4.1 Supercooling and underwater ice formation

In early or mid-October, the onset of sub-freezing air temperatures induces supercooling of the water to about -0.04°C followed by the formation of frazil and anchor ice. Supercooling has been observed at Goldstream Creek during October of 1963, 1966, and 1969 (Benson, 1967; unpublished data, 1963, 1969) but the results were questionable due to lack of calibrations. Readings taken during 1970, 1971, and 1972, however, are reliable and are tabulated as follows (Table 1) along with rate of cooling and duration of supercooling (Gilfilian, 1973; unpublished data, 1970).

Table 1. Observed Supercooling of Water at Goldstream Creek During Fall 1970, 1971, and 1972 (Gilfilian, 1973).

Date	Obs'vd Super-cooling (°C)	Ice Pt. Depress. (°C)	Actual Super-cooling (°C)	Rate of Cooling (°C min)	Duration of Super-cooling
4 Oct. 1970 *	-0.045	-	-	-0.0013	3.0 hrs
15 Oct. 1971	-0.018	-0.012	-0.006	-0.001	0.2 hrs
20 Oct. 1971	-0.035	"	-0.023	-0.0026	1.2 hrs
20 Oct. 1971	-0.029	"	-0.017	-	2.5 hrs
25 Sep. 1972	-0.030	-0.012	-0.018	-0.0030	0.7 hrs
30 Sep. 1972	-0.045	"	-0.033	-	-
1 Oct. 1972	-0.018	"	-0.006	-	-
19 Oct. 1972	-0.048	"	-0.036	-0.0017	2.1 hrs

* Unpublished data collected by Dr. Nicpon and author.

Temperature measurements by Dr. Nicpon and the author on the evening of 4 October 1970 were fairly typical and are shown in Figure 2. After declining steadily toward 0°C, supercooling proceeded from about 1845 until 2145 Alaska Daylight Time. The temperature reached a minimum of -0.045°C at 1925 ADT, at which time ice began to form. From then on, the temperature increased toward 0°C as latent heat was released from the formation of frazil, surface, and anchor ice. Deposition of ice on the thermometer bulb caused some scatter in the readings, but this was minimized by rubbing the ice off immediately before each reading. Although the thermometers used were calibrated against the triple point of water, no determinations were made of the freezing-point depression due to impurities in the stream water at this time. It was probably similar to the value of -0.012°C, found by Gilfilian (1975) using a circulating ice bath for temperature calibration.

The relative amount of ice formed has been estimated by two means: (1) analysis of heat budget of the water, and (2) measurement of increase in electrical conductance of the water due to rejection of impurities from ice crystals. Both techniques are discussed by Gilfilian (1973) and Benson (1973). At Goldstream, the first method was employed by the author for the three-hour period of supercooling on 4 October 1970, using adaptations of empirical equations from Michel (1971, pp. 26-35). The net heat flux, Q, can be represented as the sum of 10 components, which together are absorbed by the water body and results in (1) a change in temperature of the water and (2) a change in the amount of ice present:

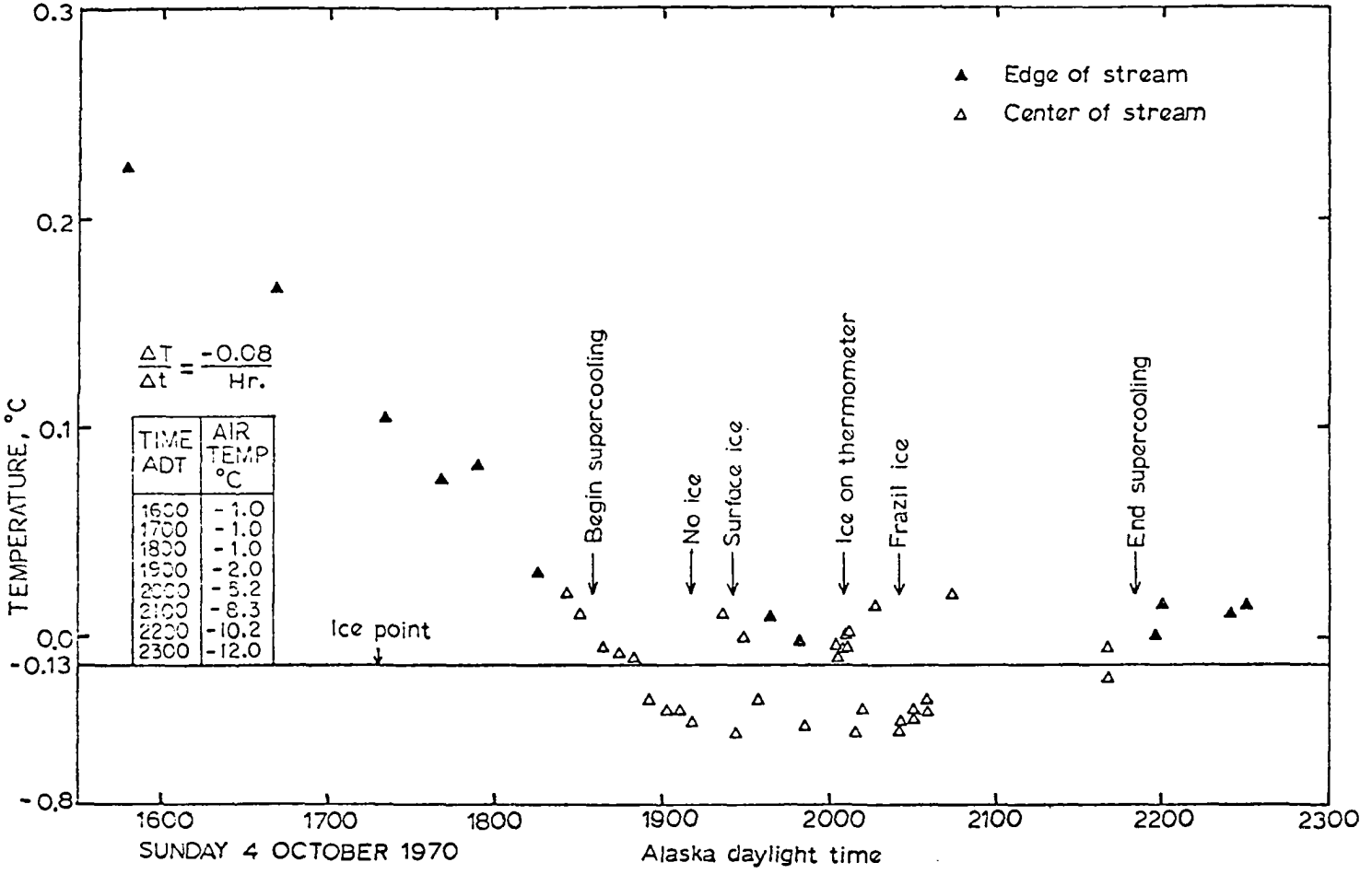

Figure 2. Supercooling of water on evening of 4 October 1970, Goldstream Creek, Fairbanks, Alaska.

$$Q = Q_c + Q_e + Q_{r1} + Q_{r2} + Q_{r3} + Q_{r4} + Q_{sp} + Q_{wp} + Q_{wg} + Q_f, \quad (1)$$

and

$$Q = Q_T - Q_L = Z\, c_w\, \rho_w \frac{dT}{dt} - L\, \rho_I \frac{dh}{dt}, \quad (2)$$

where:

Q = net heat flux,
Q_c = heat flux due to convection,
Q_e = " " " " evaporation,
Q_{r1} = " " " " direct solar radiation,
Q_{r2} = " " " " indirect solar radiation,
Q_{r3} = " " " " longwave (blackbody) radiation from the water surface,
Q_{r4} = " " " " longwave (blackbody) radiation received by the water from the atmosphere,
Q_{sp} = " " " " snowfall,
Q_{wp} = " " " " rainfall,
Q_{wg} = " " " " groundwater movement,
Q_f = " " " " friction from water movement,
Q_L = latent heat for formation of ice of thickness, dh,
Q_T = heat absorbed by water, raising the water temperature by dT,
Z = depth of water,
t = time,
T = water temperature, and
L, c_w, ρ_w, ρ_I = constants; i.e. latent heat of fusion, specific heat of water, density of water, and density of ice.

According to Equation (2), the amount of ice, dh, formed is:

$$dh = \frac{Z\, c_w\, \rho_w\, dT - Q\, dt}{L\, \rho_I}. \quad (3)$$

Using additional empirical relationships, explained by Michel (1971), values were estimated for each of the ten components of Q on the basis of meteorological conditions during the three hour period, 1900-

2200 ADT it is assumed that Q_{r1}, Q_{r2}, Q_{sp}, Q_{wp}, and Q_{wg} were negligible, due to the absence of precipitation and solar radiation, and the following values for the remaining variables were used:

Q_c	=	-0.03 (cal $cm^{-2}min^{-1}$)	Z	=	25 cm
Q_e	=	-0.04 "	$\frac{dT}{dt}$	=	+0.007°C hr^{-1} (i.e., averaged between 1900 and 2200)
Q_{r3}	=	-0.43 "			
Q_{r4}	=	+0.33 "	Q_t	=	+0.003 (cal $cm^{-2}min^{-1}$)
+ Q_f	=	+0.002 "	+ Q_L	=	-0.18 "
Q	=	-0.18 (cal $cm^{-2}min^{-1}$)	=		-0.18 (cal $cm^{-2}min^{-1}$)

The resulting value of -0.18 (cal $cm^{-2}min^{-1}$) for Q_L indicated ice formation at the rate of about 0.15 g $cm^{-2}hr^{-1}$, giving a 2.9% concentration by weight throughout the water at the end of the 3 hour period. Throughout this period, air temperature averaged -6.4°C. For the three periods of supercooling observed during the following fall (1971), both methods were employed with favorable results. Gilfilian et al. (1972) measured a radiative heat loss of 0.1 cal $cm^{-2}min^{-1}$ and calculated the heat loss from evaporation and convection with equations by Rimsha and Donchenko and got an additional 0.1 cal $cm^{-2}min^{-1}$ (Dingman et al., 1967). For these three periods of supercooling, the corresponding ice concentrations were 1.1, 1.6, and 2.3% respectively (using 150 minute time periods). Ice concentrations derived from electrical conductance measurements for these same time periods were respectively 1.8, 0.9, and 4.7% (Osterkamp et al., 1975).

The observed pattern of water temperatures during periods of supercooling at Goldstream is very similar to those observed in other studies elsewhere. The cooling rate at Goldstream (Table 1) has been almost two orders of magnitude lower than those observed experimentally in tanks by Altberg (1936) and Michel (1968), but in these classic studies, the periods of supercooling were correspondingly short - only 5 to 10 minutes. Michel observed a cooling rate of 0.016°C/min and a maximum supercooling of about -0.05°C. In experiments with water flumes, Altberg found -0.05°C to be the maximum supercooling observed in naturally occurring turbulent flows throughout his 20 years of study.

1.4.2 Freeze-up

Freeze-up is defined as the time when a persistent and continuous ice skim first forms after which it steadily increases in thickness until only a constricted channel of water flows beneath. As shown in Table 2, the correlation between date of freeze-up (item 3) and number of accumulated degree-days below freezing (item 4) is variable and is not as good as the correlation between date of freeze-up and the date when the maximum daily air temperature fell consistently below 0°C (item 1). During the fall seasons, 1965 through 1970, the calculated depth of freezing in a hypothetical soil model was found to correlate reasonably well with date of freeze-up. To calculate depth of soil freezing, Michel's (1971, p. 77, eq. 82) emperical equation for ice was modified for soil by introducing a term for soil moisture. It was applied at one

day intervals from the date when mean daily air temperature fell below 0°C until date of stream freeze-up. At any given time, t, the depth of freezing is given as:

$$Z_2 = \{(\frac{Z_s K_f}{K_s} + Z_1)^2 + \frac{2 T K_f \Delta t}{w \rho_I L}\}^{1/2} - \frac{Z_s K_f}{K_s}, \quad (4)$$

where: Δt = time increment (24 hours)
Z_2 = depth of soil freezing after Δt
Z_1 = depth of soil freezing before Δt
K_f = thermal conductivity of frozen soil
K_s = thermal conductivity of snow
Z_s = average snow thickness throughout Δt
T = average subfreezing temperature throughout Δt
w = moisture content of soil
ρ_I = density of ice
L = latent heat of fusion of ice.

Although the observed depths of soil freezing were generally less than the calculated depths (Table 2, item 5) by the above equation, one can possibly use this equation in the future to predict the approximate date of freeze-up; $Z_2 \simeq 32$ cm for the years 1965 to 1970 but the results in 1971 and 1972 were not useful.

Thermal conductivities of the frozen soil and snow were assumed to be 0.0034 and 0.00025 (cal $cm^{-1} sec^{-1} °C^{-1}$), respectively, in all cases.

The correlation, if any, between depth of soil freezing and time of freeze-up at Goldstream Creek is probably due to constriction of groundwater seepage throughout the watershed, which reduces and stabilizes stream flow and allows a permanent ice skim to form. For the sake of

consistency from year to year, the meteorological data from the National Weather Service in Fairbanks were used.

The growth of the surface ice layer in the stream was observed throughout a twelve-day period from freeze-up (19 October 1970) until the first overflow occured on 31 October. At the end of this time, the ice was 22 cm thick with 7 cm of snow on it. Using equation 2 (Michel, 1971) the ice thickness was calculated to be 16 cm (27% less than the observed thickness), using an estimated 0.0051 cal $cm^{-1}sec^{-1}{}^{\circ}C^{-1}$ for the thermal conductivity of snow. In several weeks, the ice grew solidly to the bottom across most of the stream width, leaving only a small channel of flowing water.

1.4.3 Overflowing and aufeis buildup

As freezing progressed, the available channels for water-flow were constricted, and water was periodically forced to flow over the top of the ice, forming successive layers of aufeis, which filled the entire stream bed. By late January 1971 the ice reached a total thickness of up to two meters, about 5 or 6 times the usual summer water depth, as shown in Figure 3. The date and amount of each overflow event during five winter seasons are listed in Table 2.

The exact correlation between the time of an overflow event and changes in meteorological conditions is not completely understood, but overflows have been observed to occur generally during or immediately after "warm" spells (i.e., when air temperature rises above -20°C).

1.4.4 Mid-winter period

Each year throughout February and March there has been a sharp decline in the rate of aufeis build-up. Occasionally, minor overflows have occurred from seepages along the banks and through the thin snow cover across the ice. During some seasons, a major overflow took place during late March or early April, usually stained by organic matter. Often, this froze, thus adding to the ice build-up.

Water beneath the ice has been observed to be under pressure. A pit was dug in mid-February 1971 and a 3.8 cm hole was drilled in early April 1971 through the two-meter thickness of ice, and on both occasions, water underneath welled up rapidly to the ice surface. In seconds, the drill froze solidly in place, and all efforts to retrieve it proved futile. Kane (1975) and Kane et al. (1973) observed groundwater pressure throughout the winter of 1971-72, using piezeometers in the form of iron tubes driven 1.5 to 4.5 meters into the ground and about 1 meter beneath the stream bottom. He found that the pressure was due to groundwater flow in the unfrozen soil adjacent to the stream, which became constricted by underlying permafrost and advancing seasonal frost and aufeis. Water in the peizometers, sustained by the groundwater pressure, fluctuated periodically throughout the winter between about 1.0 meters above to 1.5 meters below the ground surface, thus accounting for the periodic overflows. In support of this, a geyser of water erupted close to 2 meters above the ground surface immediately after personnel of the Alaska Department of Highways penetrated through

the seasonally frozen soil with a drill on the east bank during February 1974.

The aufeis structure has been characterized by horizontal stratification due to the frozen overflows. On the basis of crystal structure and manner of origin, Kreitner (1969) recognized five types of stream ice: (1) original ice formed from stream before overflowing, (2) snow formed from incorporation of snow crystals into overflow water, (3) block ice, (4) tabular ice, and (5) surface extrusions formed from ground water seepage along the banks.

The ice thickness from season to season has varied widely. As shown in Figure 3, covering five seasons, the thickness ranged from 126 cm (April 1969) to 200 cm (April 1971); temperature data, covered in the next chapter, revealed a correspondingly variable effect upon the thermal regime in the soil beneath. Of the freezing cycles observed between 1963 and 1973 by Benson and others, the winter of 1970-71 was the only time that the ice build-up was extensive enough to force the stream to overflow its banks.

The ice surface is generally flat with the exception of slight upwarping of the center possibly due to pressure in the water underneath. This along with thermal contraction commonly results in the formation of deep vertical cracks that form nearly every year and extend longitudinally through the center of the ice body, thus providing an additional means of heat transfer by convection of air. Other surface features include terraces along the edges formed by capillary action of

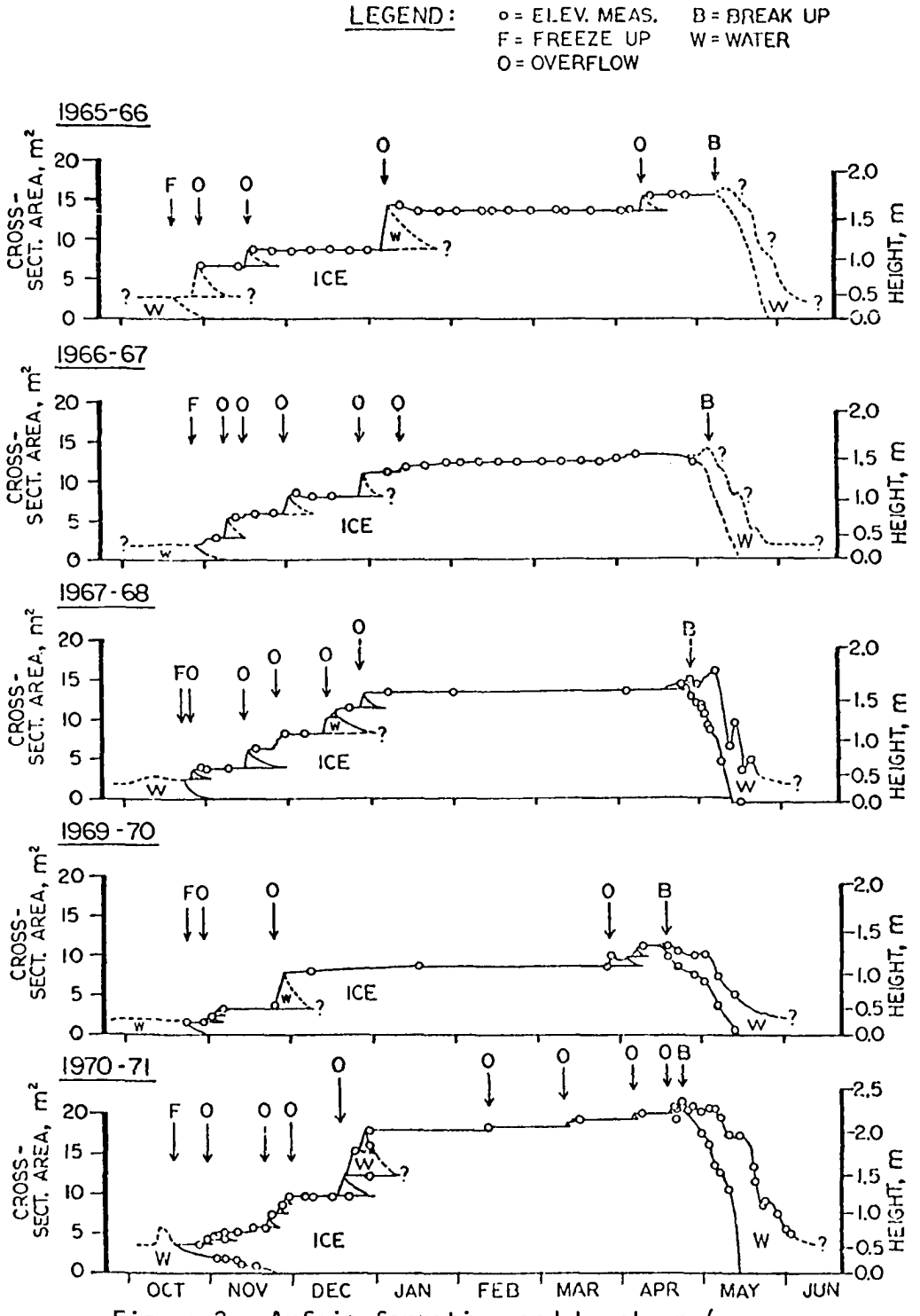

Figure 3. Aufeis formation and break-up (cross-sectional area vs. time) throughout five winter seasons - 1965-66 through 1967-68, 1969-70 and 1970-71.

flow-water in the snow (Plate 2a), ice "fans" formed by minor overflows (Plate 2c), and pingo-like frost bumps about 30 cm in diameter caused probably by localized pressure from beneath.

Topographic surveys have been made of the ice surface during seven winter periods - 1963-64 to 1970-71 (with the exception of 1968-69) and the results appear in works by Benson (1966, 1967, 1968) and Kreitner (1969). The ice surface on 19 March 1971 is shown in Plate 2b.

1.4.5 Spring break-up

By late April, meltwater reaches sufficient volume to cause melting and mechanical fragmentation of the aufeis. Within several weeks, the ice is completely removed by rafting away the overflow layers in reverse order to that in which they were formed. Through the years the duration of break-up varied from 18 days in 1968 to 29 days in 1970, as shown in Figure 3. The longest period (29 days in 1970) was in spite of an unusually thin ice cover, and can be attributed to the cool spring, when mean daily air temperatures remained below 0°C throughout April.

By the end of May, the water surface lowers to its usual summer level. In the spring of 1971, flooding occurred due to blockage of meltwater by floating chunks of ice. The force exerted by some of the larger blocks was considerable and caution had to be exercised while wading across the stream during topographic cross-section measurements.

The break-up of 1971 was photographed sequentially from the same location, looking upstream from the center of Ballaine Bridge. Shown in

Plate 2a. Aufeis surface as of 19 March 1971 with Mr. Holbrook at the plane table alidade.

Plate 2b. Ice terrace along western margin of aufeis formed by freezing of overflow water drawn into snow by capillary action.

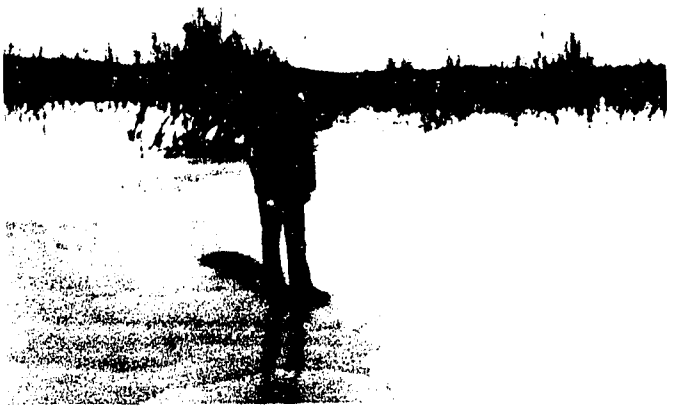

Plate 2c. Frozen overflows about 300 meters upstream from experimental site.

Plate 3, the three views selected out of many show (a) aufeis as of 19 March, (b) overflowing on 25 April, and (c) approaching summer level on 22 June.

1.4.6 Summer period

Throughout the remainder of the hydrological cycle - June through September, the stream usually remains at a depth of about 30 cm, varying according to the time and amount of precipitation. During the Fairbanks flood of August 1967, the stream overflowed its banks and deposited fresh silt in adjacent areas near the site.

A comparison of the times of various hydrological events are tabulated in Table 2 covering ten years of observation from 1963-64 to 1972-73.

Plate 3a. Maximum extent of aufeis, 8 April 1971, with ice study pit being excavated midstream near hut. Photograph sequence was taken from Old Ballaine Bridge, looking upstream.

Plate 3b. Commencement of spring break-up, 25 April, 1971, showing overflow of meltwater.

Plate 3c. Completion of break-up, 12 June 1971, with stream level approaching normal summer regimen.

Table 2. Hydrological data from ten winter seasons (1963-64 through 1972-73)

SOURCE Benson (1966, 1967, and 1973), Gilfilian (1973), Gilfilian et al (1972), Kane (1975), Kreitner (1969), NWS (1963-1973), Osterkamp et al (1975), and unpublished data (1963-1971)

EVENT	YEAR	1963-64	1964-65	1965-66	1966-67	1967-68	1968-69	1969-70	1970-71	1971-72	1972-73
1. Air temperature falls below freezing (1):											
Daily minimum		9 Oct.	1 Oct.	28 Sep.	8 Oct.	29 Sep.	20 Sep.	22 Sep.	18 Sep.	19 Oct.	17 Sep.
Daily average		9 Oct.	15 Oct.	4 Oct.	10 Oct.	16 Oct.	5 Oct.	17 Oct.	1 Oct.	20 Oct.	29 Sep.
Daily maximum		22 Oct.	15 Oct.	6 Oct.	17 Oct.	17 Oct.	15 Oct.	20 Oct.	14 Oct.	20 Oct.	22 Oct.
2. First persistent snow cover (1):		9 Oct.	16 Oct.	7 Oct.	18 Oct.	22 Oct.	17 Oct.	31 Oct.	12 Oct.	19 Oct.	29 Sep.
3. Date of freeze-up:		-	27 Oct.	19 Oct.	25 Oct.	21 Oct.	17 Oct.	22 Oct.	19 Oct.	23 Oct.	21 Oct.
4. Degree days of frost (°C) on date of freeze-up (1):		-	60	145	93	49	-	13	71	30	42
5. Depth of soil freezing (cm) on date of freeze-up:											
Calculated (2)		-	22	37	33	34	-	34	32	17	7
Observed		-	-	-	-	30±	-	-	20±	10±	-
6. Approximate dates of overflows - numbers indicate height added in centimeters (3):		-	-	29 Oct(13)	29 Oct(17)	24 Oct(19)	-	28 Oct(25)	30 Oct(15)	30 Nov(30)	-
		-	-	14 Nov(33)	8 Nov(21)	14 Nov(30)	-	24 Nov(53)	22 Nov(40)	14 Dec(21)	-
		-	-	21 Dec (3)	14 Nov (6)	24 Nov(21)	-	26 Mar(27)	17 Dec(80)	31 Dec(24)	-
				7 Jan(26)	29 Nov(17)	14 Dec(31)			11 Feb (5)	28 Mar(36)	
				29 Mar(32)	27 Dec(33)	26 Dec(18)			10 Mar(10)	16 Apr(12)	
					? Mar(24)	24 Apr (8)			4 Apr(12)		
7. Air temperature rises above freezing (1):											
Daily maximum		16 Apr.	18 Mar.	21 Mar.	31 Mar.	31 Mar.	30 Mar.	17 Mar.	12 Apr.	17 Apr.	24 Mar.
Daily average		12 May	24 Mar.	27 Apr.	24 Apr.	21 Apr.	7 Apr.	13 Apr.	13 Apr.	30 Apr.	28 Mar.
Daily minimum		16 May	18 May	29 Apr.	8 May	5 May	6 May	5 May	3 May	5 May	30 Apr.
8. First appearance of organically stained meltwater:		-	-	29 Mar.	-	17 Apr.	-	26 Mar.	20 Apr.	-	-

Table 2, cont'd

EVENT YEAR	1963-64	1964-65	1965-66	1966-67	1967-68	1968-69	1969-70	1970-71	1971-72	1972-73
9. Ice begins to break:	-	-	7 May	4 May?	27 Apr.	-	17 Apr.	23 Apr.	-	-
10. Aufeis is half-way removed:	-	-	14 May?	-	8 May	-	4 May	10 May	-	-
11. Aufeis is completely removed:	-	-	31 May?	-	13 May	-	14 May	13 May	-	-
12. Maximum thickness of aufeis:	-	-	-	147 cm	155 cm	-	126 cm	206 cm	-	-
13. Maximum cross-sectional area of aufeis:	-	-	-	13.1 m^2	13.6 m^2	-	11.2 m^2	21.0 m^2	-	-
14. Maximum snow cover(1):	41 cm	58 cm	132 cm	80 cm	83 cm	74 cm	30 cm	108 cm	76 cm	59 cm
15. Total snow fall (1):	144 cm	140 cm	312 cm	261 cm	183 cm	151 cm	92 cm	370 cm	230 cm	202 cm
16. Mean annual air temp: *July to July* (1):	-4.36°C	-4.68°C	-5.59°C	-3.80°C	-2.47°C	-3.85°C	-1.48°C	-4.79°C	-4.68°C	-2.35°C
17. Degree days of cooling: °C below 16.3°C from July to July (1):	8284	8338	8710	8080	7595	8147	7188	8453	8412	7526

(1): Data taken from National Weather Service, Fairbanks, Alaska.

(2): Depth of soil freezing was calculated by using equation (4) (see text; after Michel, 1971) on a day-to-day basis through date of freeze-up, using NWS data for mean daily air temperature and daily snow cover. Assumed values were as follows:
Thermal conductivity of frozen soil: 0.0034 cal cm $°C^{-1}sec^{-1}$;
Thermal conductivity of snow: 0.00025 cal cm $°C^{-1}sec^{-1}$;
Moisture content of frozen soil: 16 percent by weight.

(3): Data for 1971-72 taken from Kane (1975).

CHAPTER 2

EQUIPMENT AND TECHNIQUES

Facilities at the Goldstream Creek field site include a hut (2.5 x 2.5 meters) built in the fall of 1966 and situated on the west bank about 60 meters upstream from the bridge (Figures 4 and 5). It was heated by a small wood stove and a catalytic heater and was equipped with a portable electric generator, a network of copper-constantan thermocouples, a meteorological shelter, and various tools and equipment for studying the surface topography and structure of the aufeis.

2.1 Thermocouple network

All thermocouple wires were connected to a 72-junction manual switch panel built at the Geophysical Institute electronics shop. Readings were taken with a Leeds and Northrup model 8646 potentiometer with a resolution to one microvolt. With an equivalence of about 38 microvolts per 1°C, the precision of the system was = 0.03°C, and the overall accuracy was = 0.3°C. The reference temperature was established by an ice-water bath (Figure 6). This system worked well, provided due caution was exercised to insure the correct polarity when connecting the meter to the system and to keep the reference junctions well insulated from moisture to minimize spurious currents due to electrolytic action. During January 1971, a problem with electrolytic noise developed, but was eliminated by placing the reference junctions inside plastic tubing.

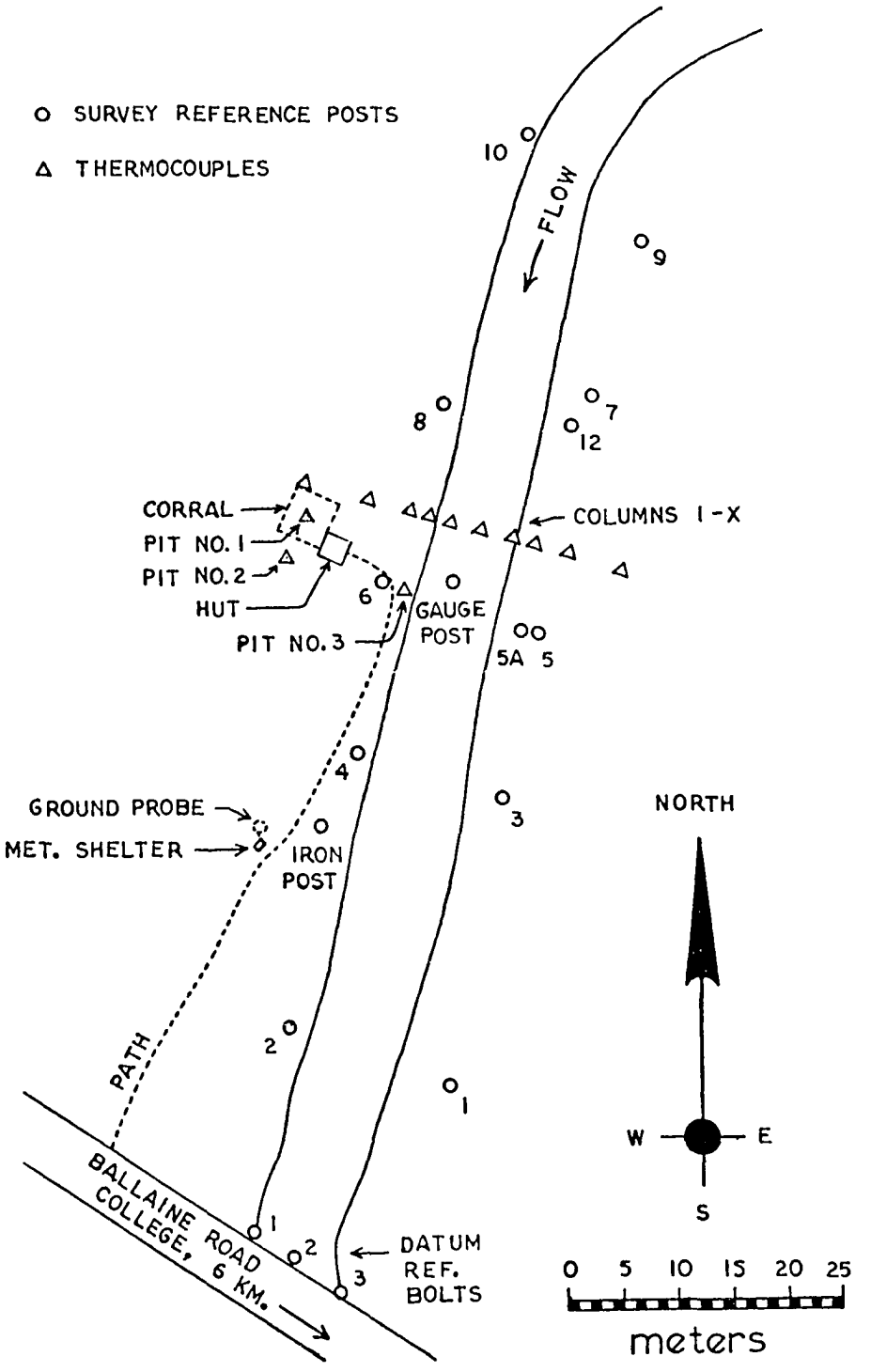

Figure 4. Goldstream experimental facility, adjacent to Ballaine Road, about 6 km north of University of Alaska, showing hut and thermocouple network.

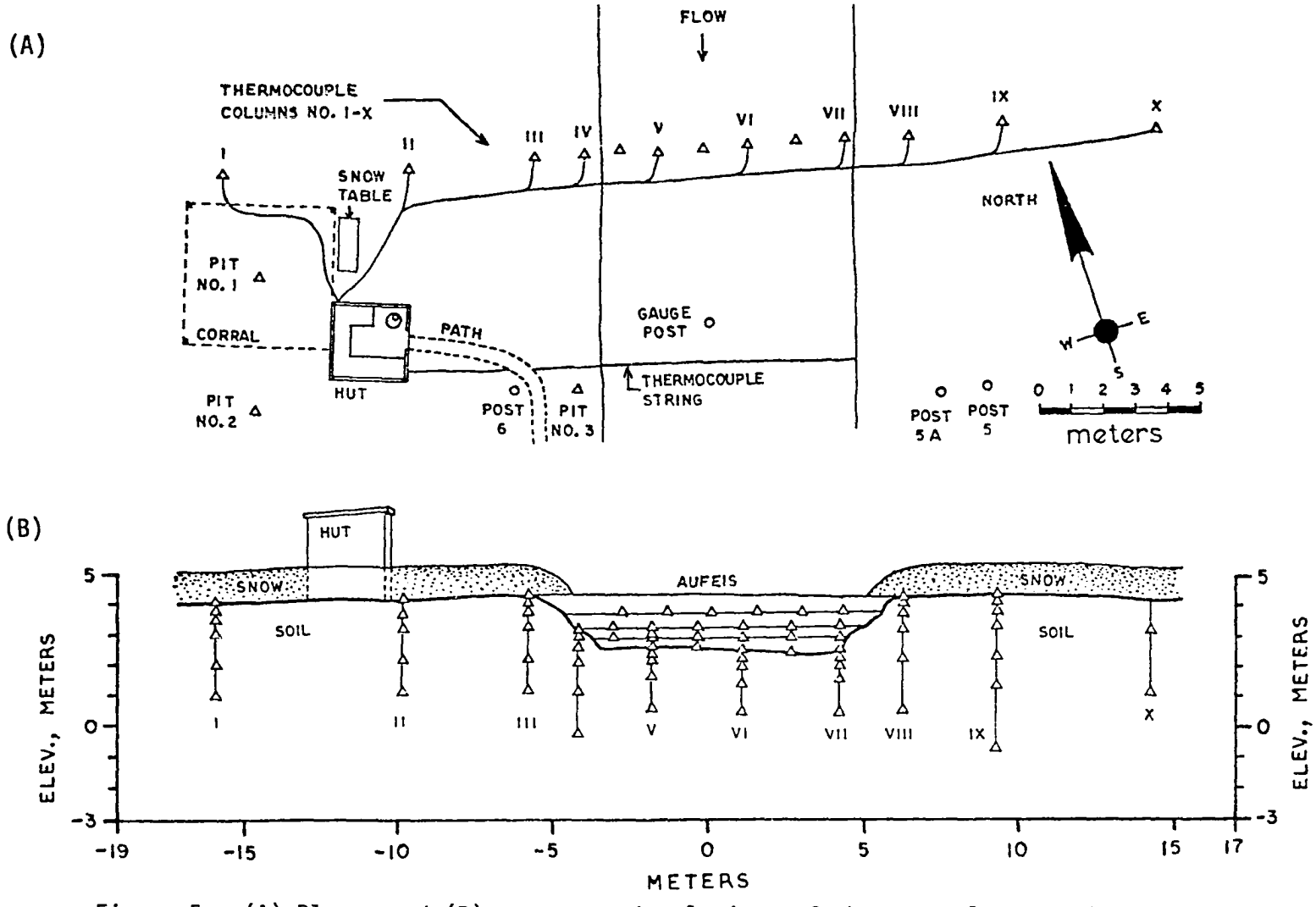

Figure 5. (A) Planar and (B) cross-sectional views of thermocouple network, consisting of pits no. 1, 2, and 3 (installed in fall 1967) and vertical columns no. I through X (installed in fall 1970).

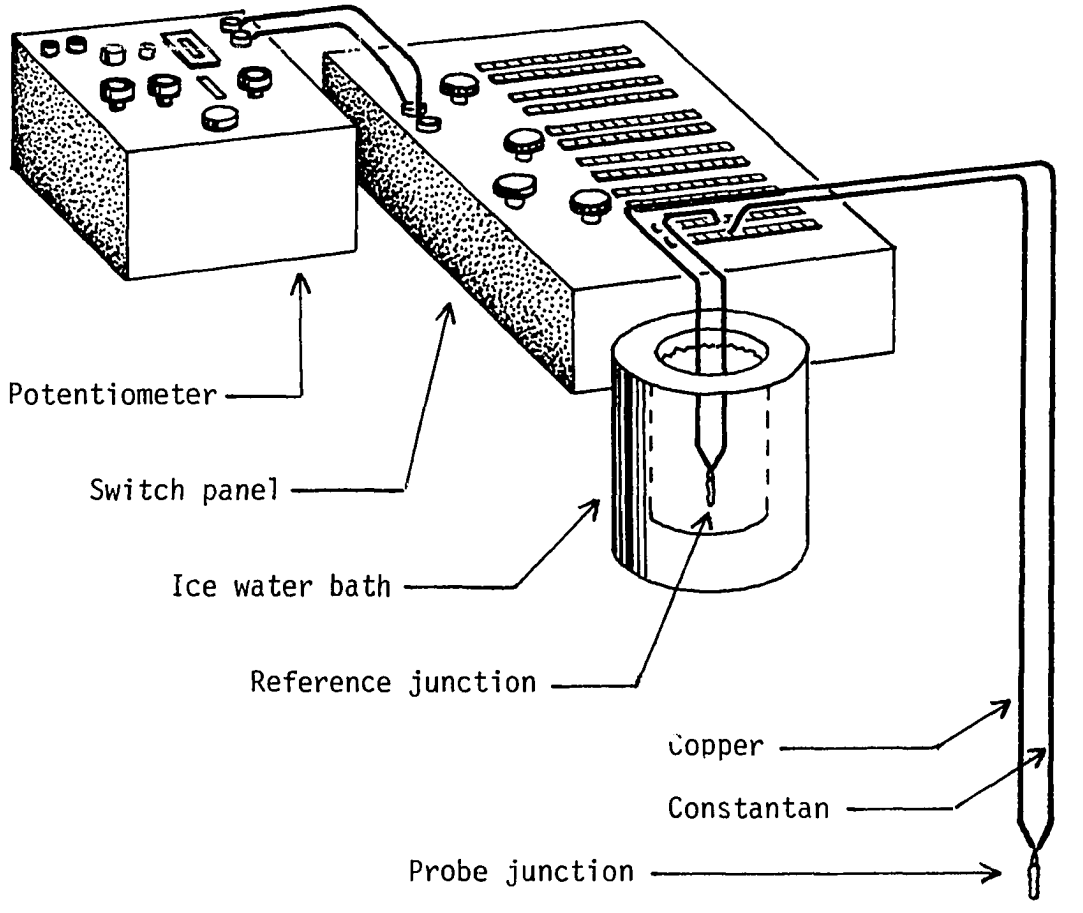

Figure 6. Instrumentation for measuring temperatures: one of 72 copper-constantan thermocouples, ice-water reference temperature bath, 72-junction switch panel, and Leeds and Northrup model 8646 potentiometer.

The main network of thermocouples consisted of 57 probes requiring about 1200 meters of wire, and was installed across the stream bed in a cross-section 30 meters wide and about 3 meters deep (Figures 5 and 6). The wires were placed in a row of 10 holes (columns I through X) sunk by means of a quarter-inch steel rod, which could be rammed easily into the soft silty gound. The rod, constructed for this purpose, consisted of five one-meter sections which could be screwed together consecutively until the desired depth was attained.

After establishing a hole, the twisted junction of each thermocouple wire was dipped into rubber-based insulator and wrapped in electrical tape for protection from moisture and abrasion. The junction was then tied to a cross-shaped piece of metal (e.g. aluminum) several centimeters across, and the arms of the cross were bent up to form a cup. The metal cup served the threefold purpose of holding, protecting, and anchoring the junction at the desired depth when retrieving the rod (Figure 7). In the soft soil layers, one probe was lodged as deep as 5 meters.

The only problem encountered with this method was the failure of the aluminum anchors in the resistent gravel layer on the stream bottom, but this was effectively overcome by using empty 9-mm Luger bullet shells as anchors instead.

Additional thermocouples for measuring soil temperatures, installed during fall 1967, were situated at pits 1, 2, and 3, all located on the west bank at various depths to 1 meter. The snow cover over pit 1 was

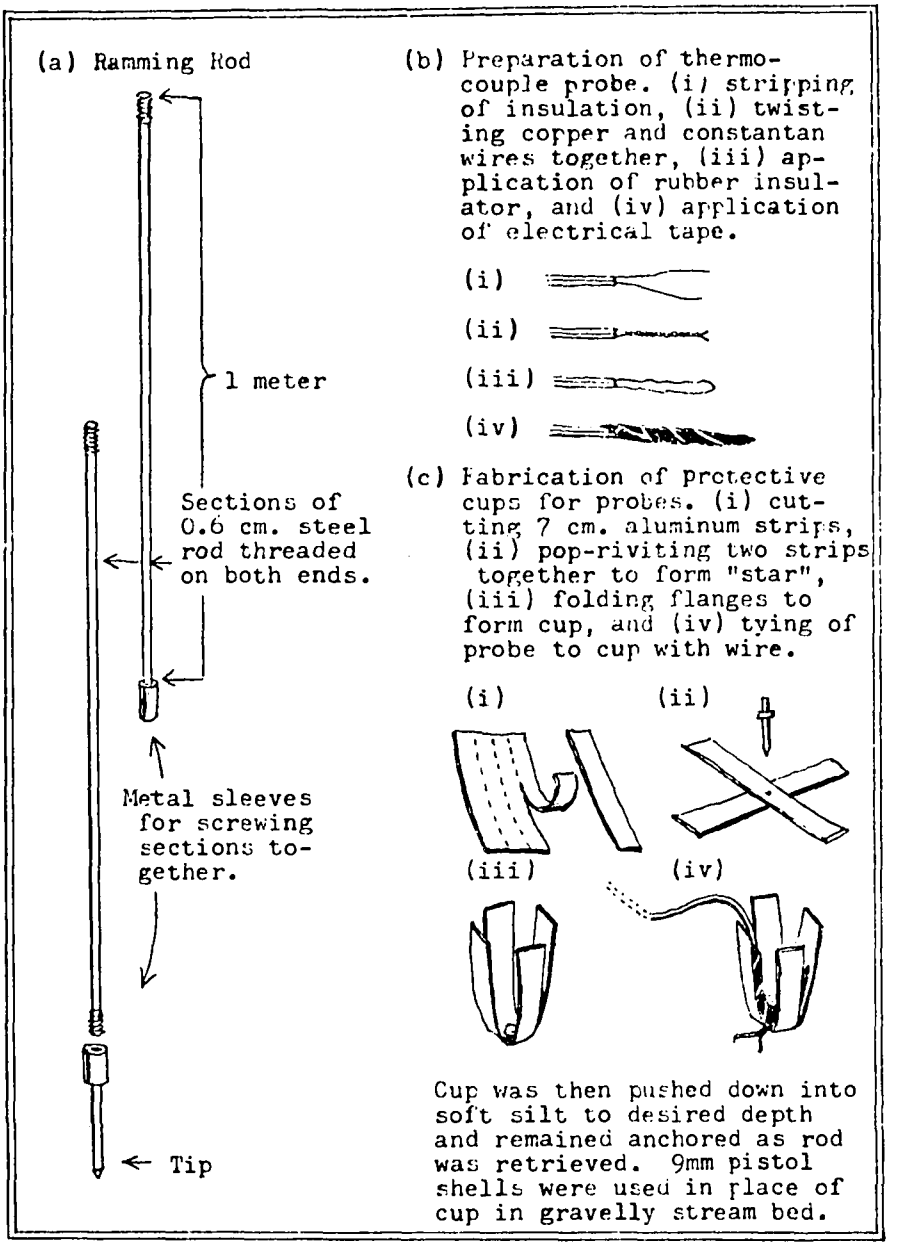

Figure 7. Method used for preparation and installation of thermocouple probes, October 1970.

protected from disturbance by a 3 meter square corral (Figure 5), while the snow was removed from the surface over pit 2 through the winter.

For measuring temperatures throughout the aufeis, a different technique was used. Approximately 30 additional thermocouple probes were tied together into five separate strings, and each string of thermocouples was, in turn, laid across the stream surface after successive over-flows, allowing the wires to freeze in place at various depths. Initiated during fall 1966, this method yielded good results during the winters of 1966-67, 1967-68, 1969-70 and 1970-71 (Figure 5b).

2.2 Other methods of temperature measurement

To determine the thermal properties of the undisturbed snow cover, temperature profiles were taken periodically during the winter 1970/71. Each time, a hole was dug in an undisturbed area, and readings were taken from the freshly exposed layers, using a dial thermometer, thermistor unit, a glass thermometer, or a thermocouple.

For measuring the degree of supercooling of the water during initial freeze-up, the temperature had to be monitored carefully and precisely. First, a thermocouple was placed in the creek, and the readings were recorded continuously for several nights on a suitable device (e.g. Esterline-Angus recorder) to ascertain the approach to 0°C. When supercooling seemed probable, readings were then taken visually at several minute intervals using precise Brooklyn mercury thermometers.

With a scale graduation of 0.005°C and a calibration check against the triple point of water, an accuracy of ≃ 0.005°C was attained.

The meteorological shelter, installed during fall 1963 on the west bank just upstream from the bridge, housed a two-pen Belfort thermograph for recording air temperature as well as the temperature of the soil/snow interface. The thermograph was calibrated against a mercury thermometer, which was also kept in the shelter.

2.3 Methods of observing aufeis formations

In addition to temperature measurements, the aufeis structure was observed. In connection with field mapping, an arbitrary level datum plane was established during fall 1965 by means of a network of twelve iron survey reference posts placed along the stream banks. Movable metal clips on the posts were adjusted to a uniform elevation before freeze-up, using either a transit or a plane table alidade and were periodically checked throughout the winter for changes due to frost heaving. A metal bolt on the north side of the Ballaine bridge served as the reference elevation and was arbitrarily taken to be 500 cm. This put the ground surface at about 410 cm and the stream bottom at around 230 cm.

A nylon chalk line stretched between opposing posts across the stream served as a reference line for measuring the ice surface topography. These observations were supplemented by readings taken from a network of ten unmarked stakes throughout the stream bed.

The SIPRE 3-inch corer and a SIPRE 1 1/2-inch drill with extension rods were used for extracting ice samples and probing the ice/water interface and the stream bottom. A complete vertical profile of the ice was exposed by means of digging a trench with the aid of a chain saw, but caution had to be exercised when approaching the bottom least water well up under pressure and fill the entire hole.

CHAPTER 3

PRESENTATION OF THE DATA

Throughout the hydrological year of 1970-71, temperature observations were made to depths of 3 meters below the soil surface along a cross-section 30 meters wide and centered on the stream (thermocouple columns I through X) as shown in Figures 11 through 17, and 20. Cross-sections of the aufeis and profiles through the snow cover were also taken.

Additional data collected during previous winter seasons include (1) cross-sections of the aufeis during the winters of 1966-67 (Benson, 1967), 1967-68 (Kreitner, 1969; Kreitner and Benson, 1970), and 1969-70 (unpublished data); and (2) profiles in the soil to depths of 1 meter (thermocouple pit no. 1 and no. 2) during the winters of 1967-68 and 1969-70 (unpublished data). The cross-sections appear in Figures 8, 9, and 10, and the profiles appear in Figures 18 and 19.

The data are presented and discussed, with emphasis placed on: (1) effect of the stream's presence upon temperature distribution in the surrounding soil, (2) changes in soil and ice temperature as a result of changes in meteorological and other surface conditions, (3) retardation of cold-pulse penetration due to latent heat exchanges and snow cover insulation, and (4) effect of water movement on the temperature distribution in the aufeis.

3.1 Cross-sections

3.1.1 Aufeis, winters 1966-67, 1967-68, and 1969-70

For the most part, isotherms throughout the aufeis were horizontal, evenly spaced, and responded readily to changes in surface temperatures (Figures 8 through 17). Thermal gradients up to 30°C per meter have been observed throughout the ice thickness (Figure 10c, 16 January 1970).

At the bottom, temperatures remained relatively constant, ranging from 0°C to several degrees below 0°C. The lowest observed beneath the ice was -8.2°C on the bottom surface on January 16, 1970. The main factor affecting the bottom temperatures is the presence or absence of running water. Throughout the winters of 1967-68 (Figure 9) and 1970-71 (Figures 11 through 17), the 0°C contour generally coincided with the bottom indicating the possibility of flowing water, although the position of the channel has not always been certain. During the winters of 1966-67 (Figure 8) and 1969-70 (Figure 10), however, the bottom was frozen across most if not all of its width. In 1966-67, water may have continued to flow along the western edge, but after the overflow in December 1969, temperatures were below 0°C to the bottom of the stream across the entire width; any streamflow, if at all, must have been confined to seepage through the underlying sediments.

3.1.2 Aufeis and surrounding soil, hydrological year 1970-71

Throughout a period of 13 months (22 October 1970 to 1 December 1971), 50 temperature cross-sections were measured, using the 56-probe

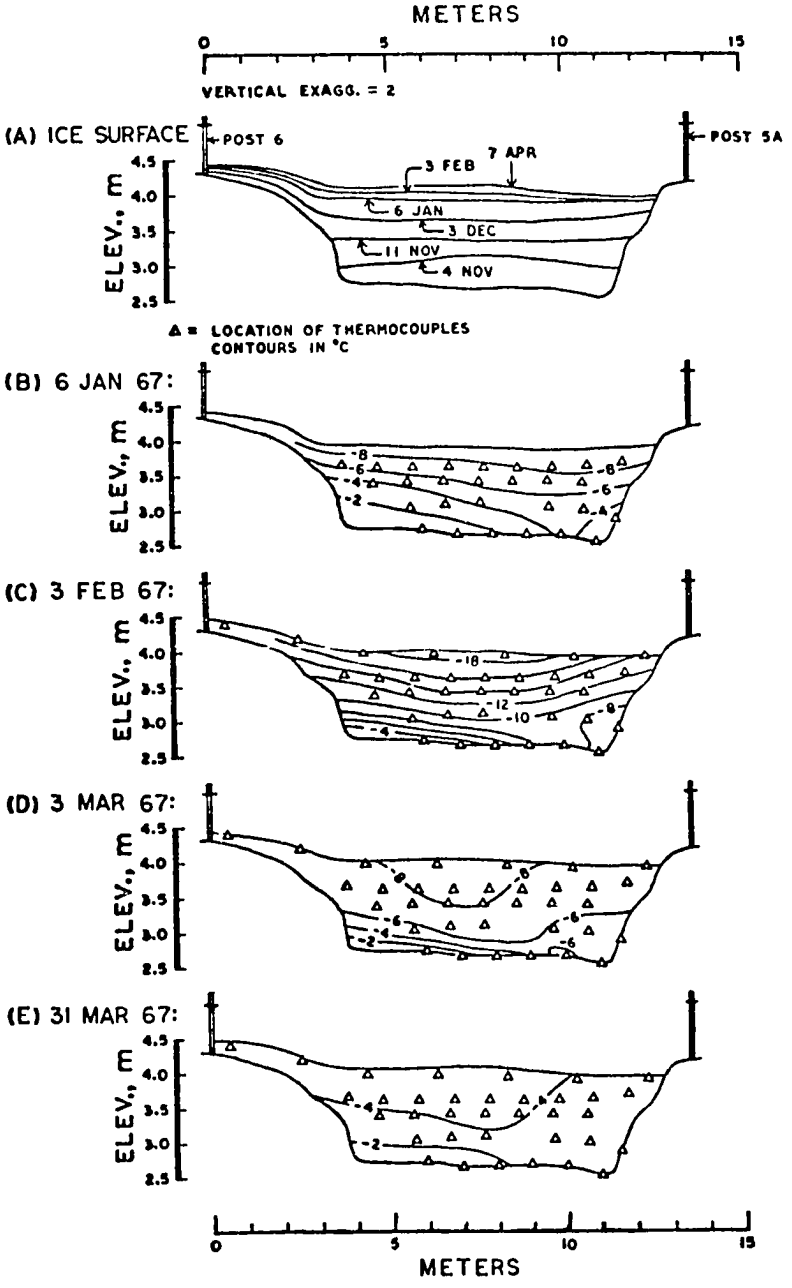

Figure 8. (A) Sequence of aufeis buildup and (B through E) temperature distributions throughout a cross-section of the aufeis during winter of 1966-67.

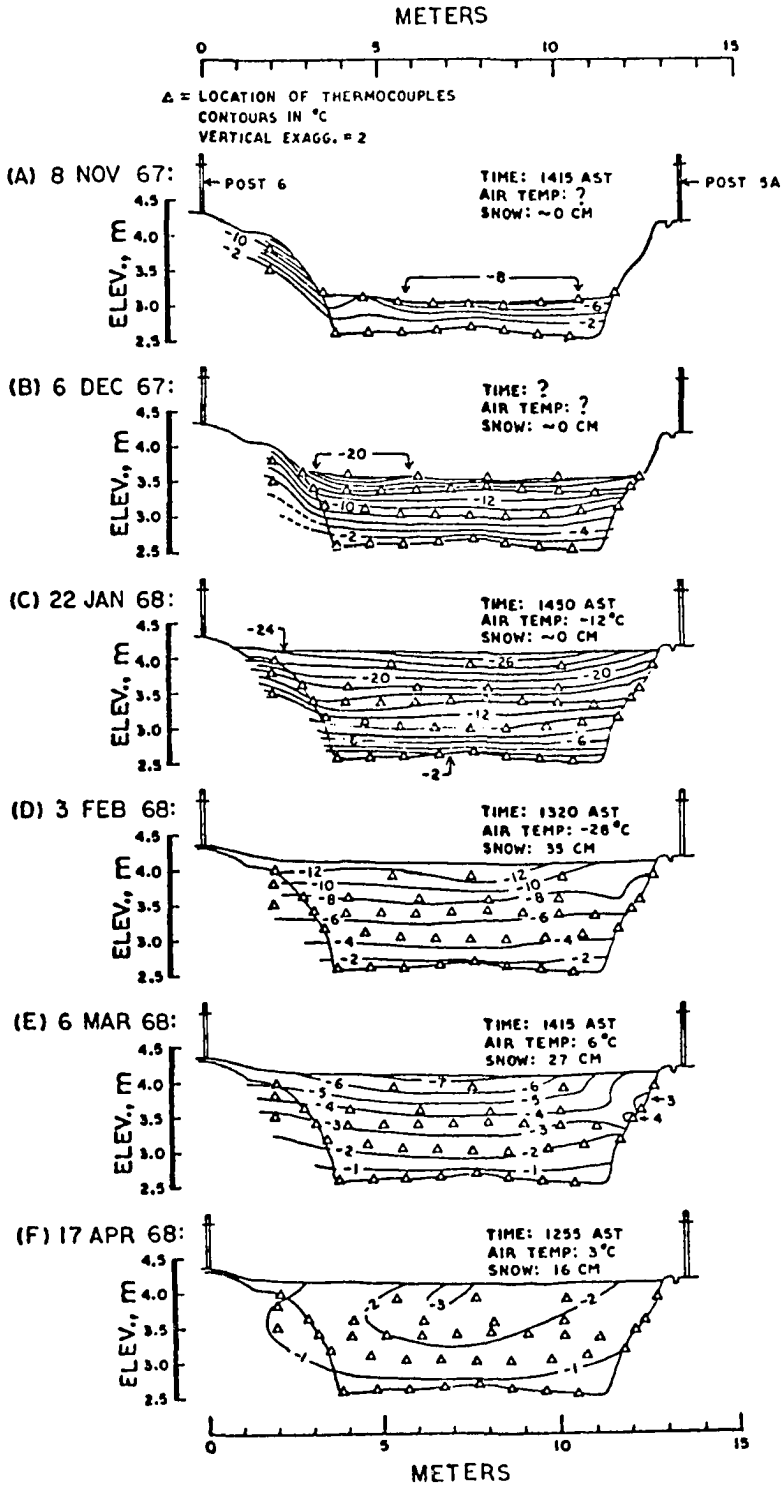

Figure 9. (A through F) Temperature distributions throughout a cross-section of the aufeis during winter of 1967-68.

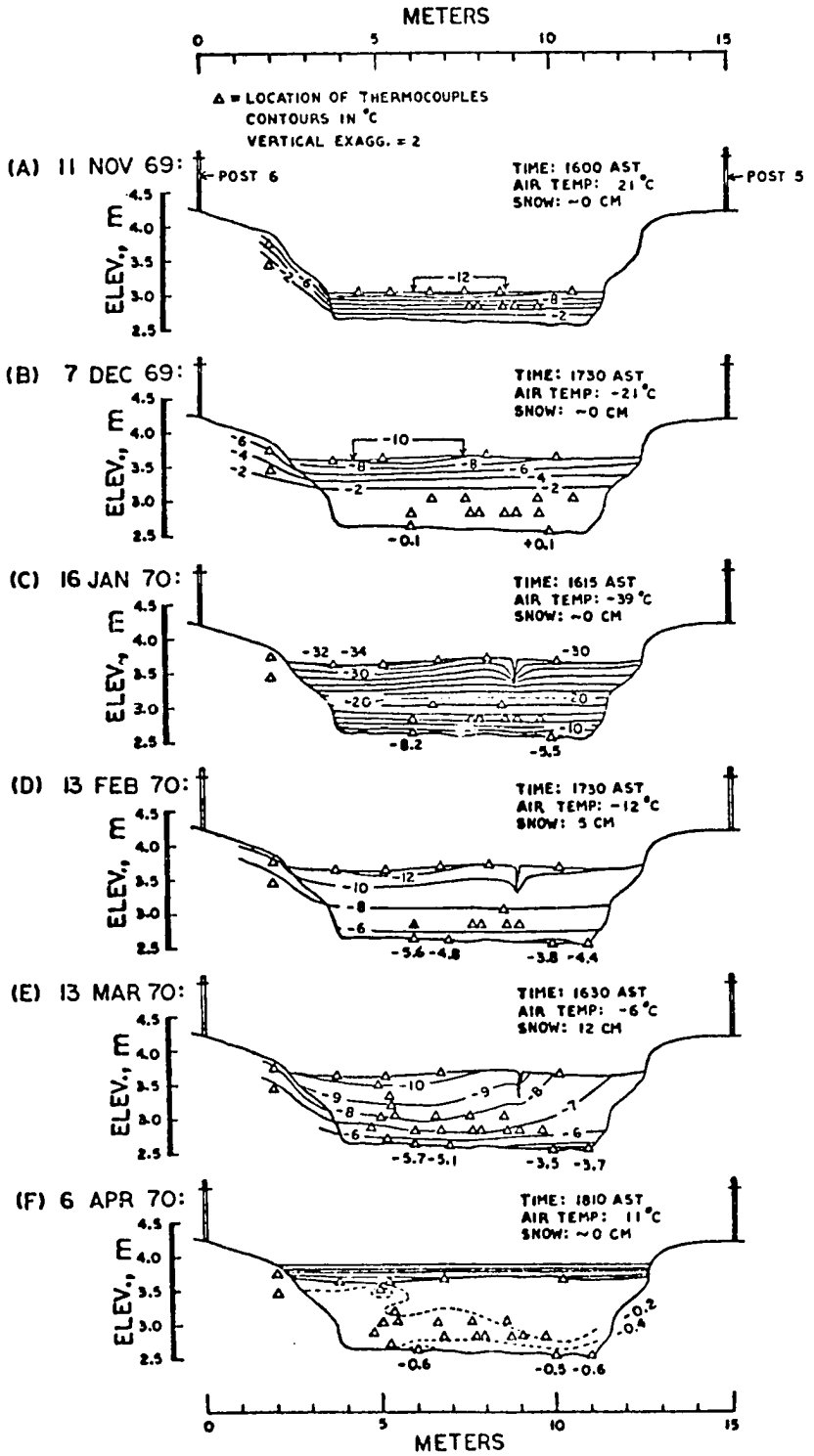

Figure 10. (A through F) Temperature distributions throughout a cross-section of the aufeis during winter of 1969-70.

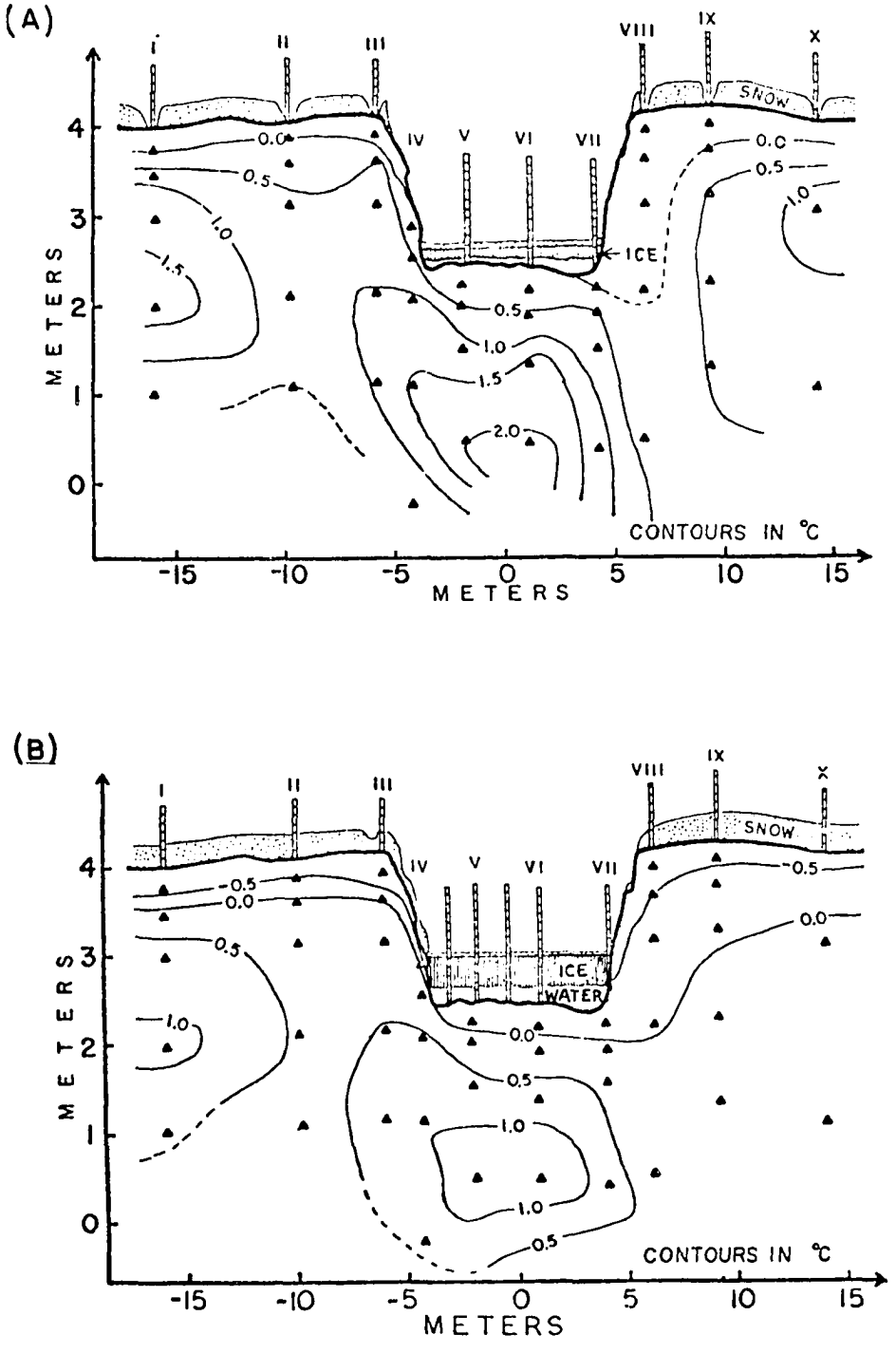

Figure 11. Temperature distributions throughout a cross-section of Goldstream Creek and surrounding soil. (A) 22 October 1970, (B) 10 November 1970.

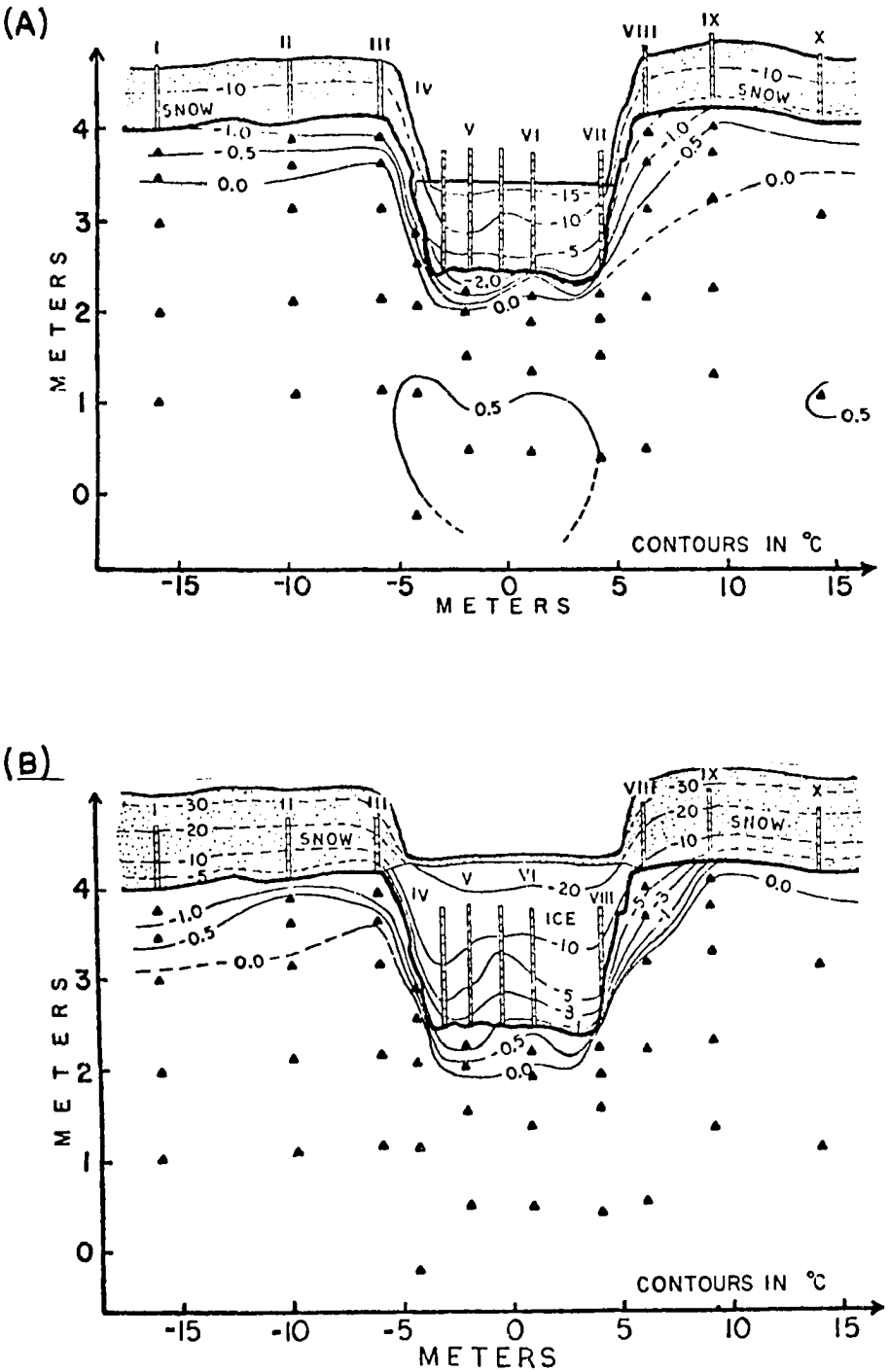

Figure 12. Temperature distributions throughout a cross-section of Goldstream Creek and surrounding soil. (A) 15 December 1970, (B) 30 January 1971.

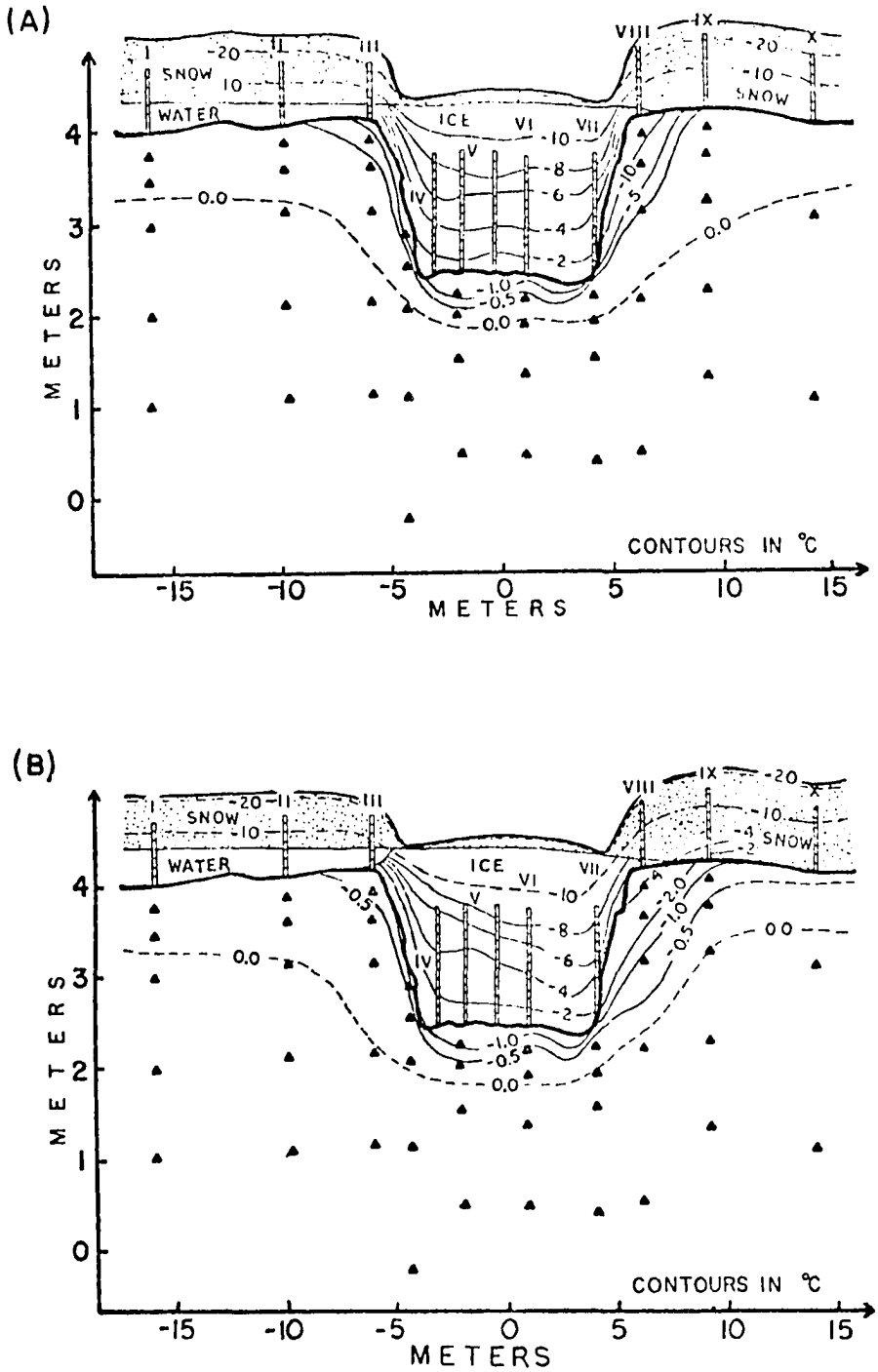

Figure 13. Temperature distributions throughout a cross-section of Goldstream Creek and surrounding soil. (A) 24 February 1971, (B) 12 March 1971.

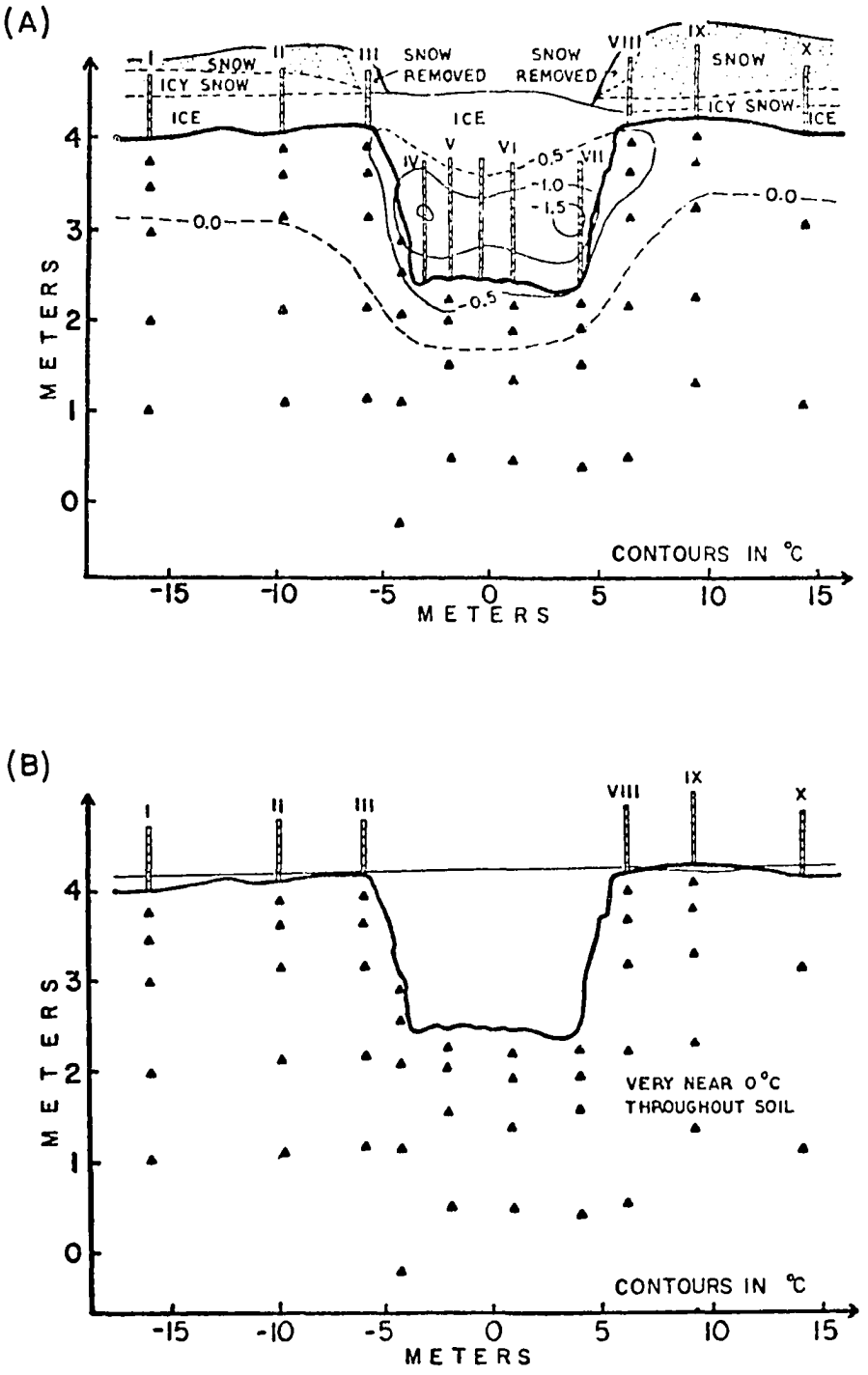

Figure 14. Temperature distributions throughout a cross-section of Goldstream Creek and surrounding soil. (A) 17 April 1971, (B) 10 May 1971.

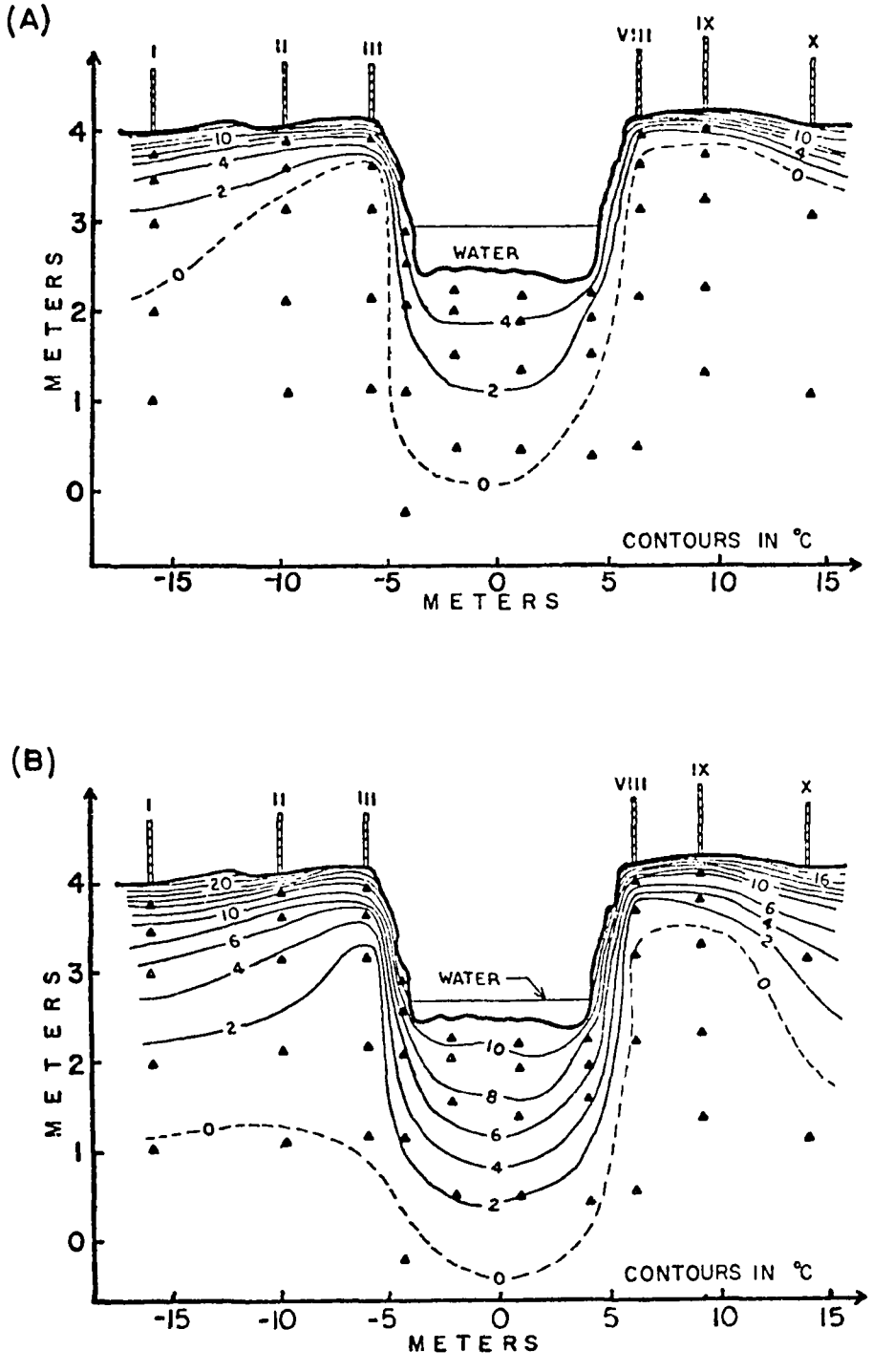

Figure 15. Temperature distributions throughout a cross-section of Goldstream Creek and surrounding soil. (A) 3 June 1971, (B) 22 June 1971.

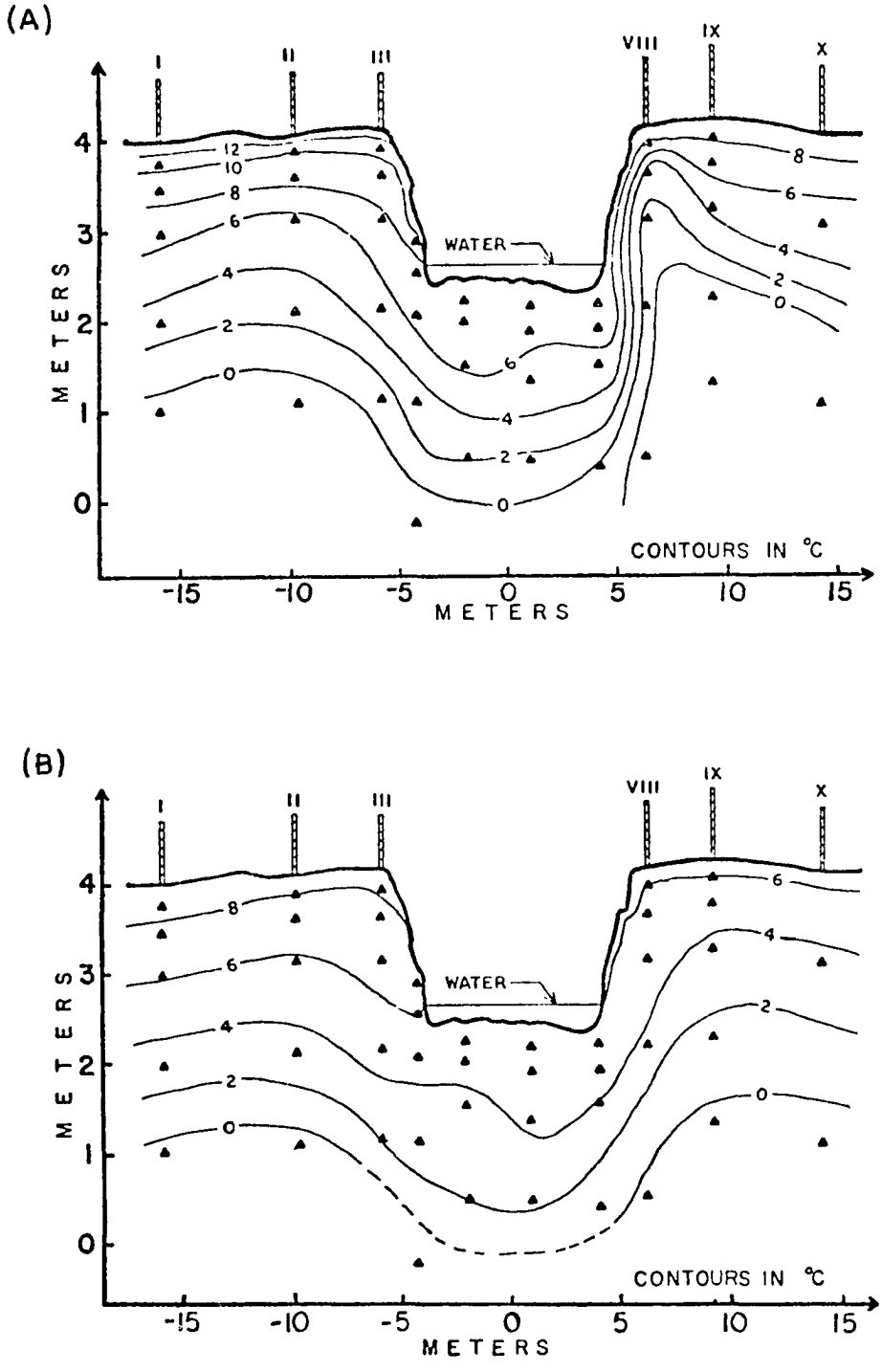

Figure 16. Temperature distributions throughout a cross-section of Goldstream Creek and surrounding soil. (A) 31 July 1971, (B) 1 September 1971.

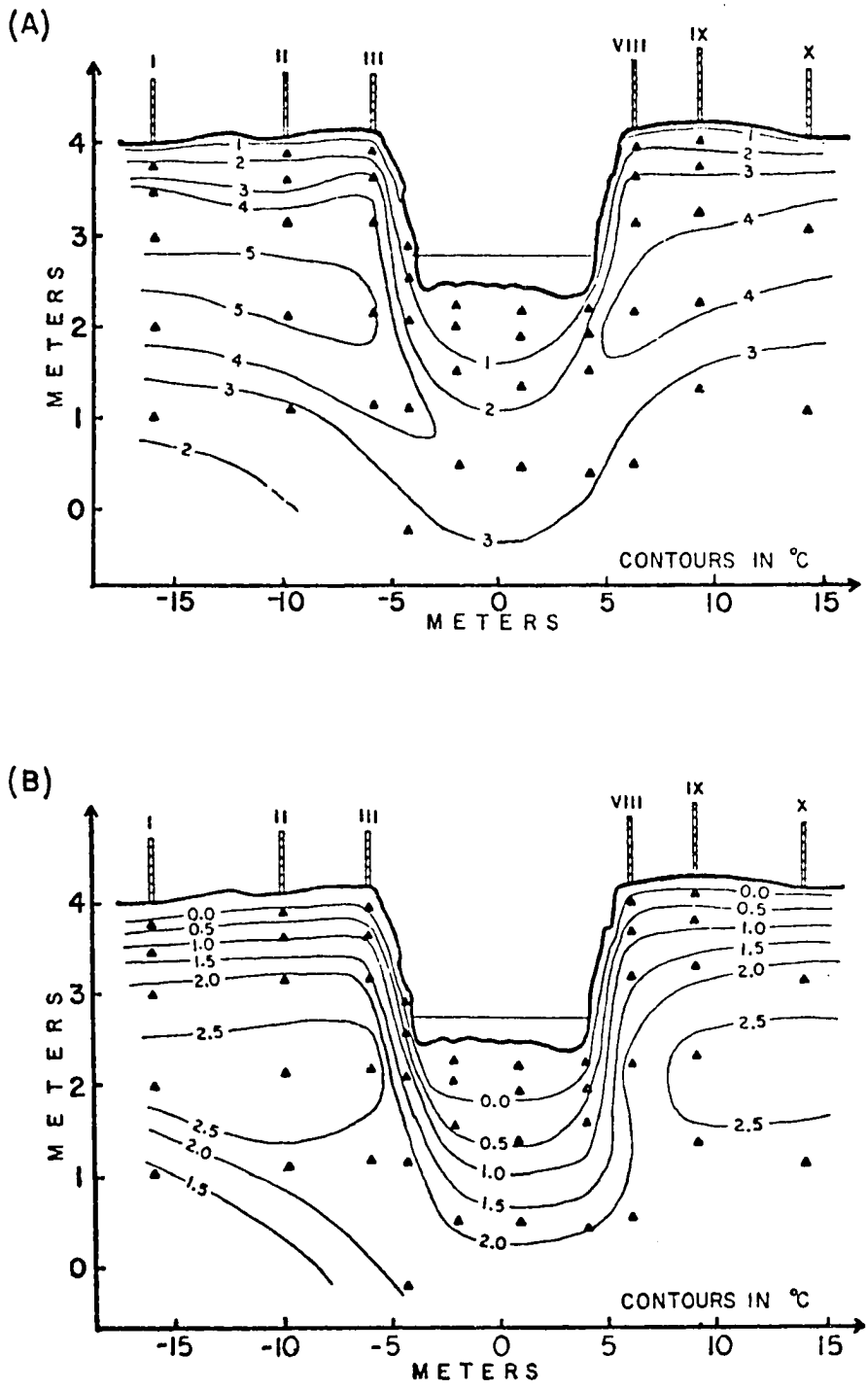

Figure 17. Temperature distributions throughout a cross-section of Goldstream Creek and surrounding soil. (A) 5 October 1971, (B) 2 November 1971.

system. Of these, 14 representative ones were selected and are presented in Figures 11 through 17, along with a summary of pertinent information in Table 3.

The 1970-71 winter at Goldstream was marked by unusually low air temperatures (-22.6°C from 1 October to 31 March; 5.2°C below the long term mean), record-breaking snowfall (370 cm), and aufeis build-up exceeding the height of the banks. The soil temperature at the snow/soil interface never got below -2°C (with the exception of -3.8°C on 22 October which was due partly to disturbance of the snow cover). The relatively high soil temperature was due to the heavy snow cover, which reached 108 cm in thickness. Due to edge effects, the soil surface temperature near the stream banks went as low as -5.0°C.

3.2 Depth versus time profiles

The effect of the stream's presence upon the thermal regime in the ground is further emphasized by the following diagrams (Figs. 18, 19, 20), each of which depicts variation through time of two selected vertical profiles - one centered in the stream and the other adjacent to the stream, but sufficiently far away to avoid thermal edge effects of the banks. In addition, meteorological data are presented, using data from the National Weather Service, Fairbanks, to cover times when data at Goldstream are missing. Also, height measurements of the snow cover and aufeis are incorporated to show their accompanying formation and dissipation throughout the winter season. The winters of 1967-68 and 1969-70 and the hydrological year of 1970-71 are discussed separately below.

Table 3. Thermal cross-sections at Goldstream Creek - Pertinent data for Hydrological Year 1970-71
Elevation of bottom = 240 cm; Elevation of bank = 415 cm

Fig.	Date	Snow Cover (cm)		Aufeis (cm)		Air Temp. (°C)	Stream Center Soil Temp.		West Bank Soil Temp.		Water Temp. (°C)	Water Level (cm)	0° Isotherm Below Ground Surf. (cm)	Comments
		On land	On ice	Elev.	Thick.		Surf.	Max.	Surf.	Max.				
11 a	22 Oct.	25	3	280	15	-15.5	0.0	2.0	-3.8	1.7	0.0	280	20±	Snow cover disturbed. Ventilation in probe holes give negative errors.
11 b	10 Nov.	28	4	296	34	-13.6	0.0	1.4	-1.7	1.1	0.0	296	45±	Stakes in stream frost-heaved 10 cm.
12 a	15 Dec.	67	1	340	95±	-20.4	-0.5	0.8	0.8	0.5	0.0	340	55±	
12 b	30 Jan.	110	10	422	185±	-37.0	-0.5	0.4	-1.5	0.1	0.0	422	?	Temperature gradients too slight to determine position of 0°C isotherm.
13 a	24 Feb.	105	16	427	190±	-27.5	-1.0	0.2	-0.3	0.0	0.0	427	?	Overflow water seeps through snow on west bank.
13 b	12 Mar.	100	18	437	200±	-21.5	-1.2	0.1	-0.2	0.0	0.0	437	?	
14 a	17 Apr.	95	0	447	210±	7.5	-0.7	0.2	-0.1	0.0	0.0	447	-	More flooding over both banks. Bottom half of snow cover densified by frozen water.
14 b	10 May	0	0	342	105	8.0	-0.1	0.1	0.0	0.0	0.0	342	-	Ice has begun melting and calving. Soil is virtually isothermal at 0°C.
15 a	3 June	0	0	-	0	16.4*	5.6	5.6	15.8	15.8	-	290	-	Return to summer regimen. Frost in soil delays penetration of warm pulse.
15 b	22 June	0	0	-	0	25.1*	11.2	11.2	22.4	22.4	-	260±	-	West bank has completely thawed. Some frozen ground still remains on east bank.
16 a	31 July	0	0	-	0	14.9*	8.5	9.6	15.8	15.8	9.7	259±	-	Summer maximum is over; surface begins to cool.
16 b	1 Sep.	0	0	-	0	8.0*	7.0	6.7	11.2	11.2	-	-	-	
17 a	5 Oct.	8	0	-	0	-3.9	1.2	3.8	1.1	5.0	1.6	-	-	Banks are warmer (5.0°C) than region beneath stream (3.8°C).
17 b	2 Nov.	12	-	-	-	17.5	-0.3	2.0	-0.8	2.8	0.0	-	20±	Ground is warmer by 1.0 to 5.0°C than it was on 22 Oct. 1970, due probably to heavy summer rainfall.

* Air temperature data taken from National Weather Service, Fairbanks, Alaska.

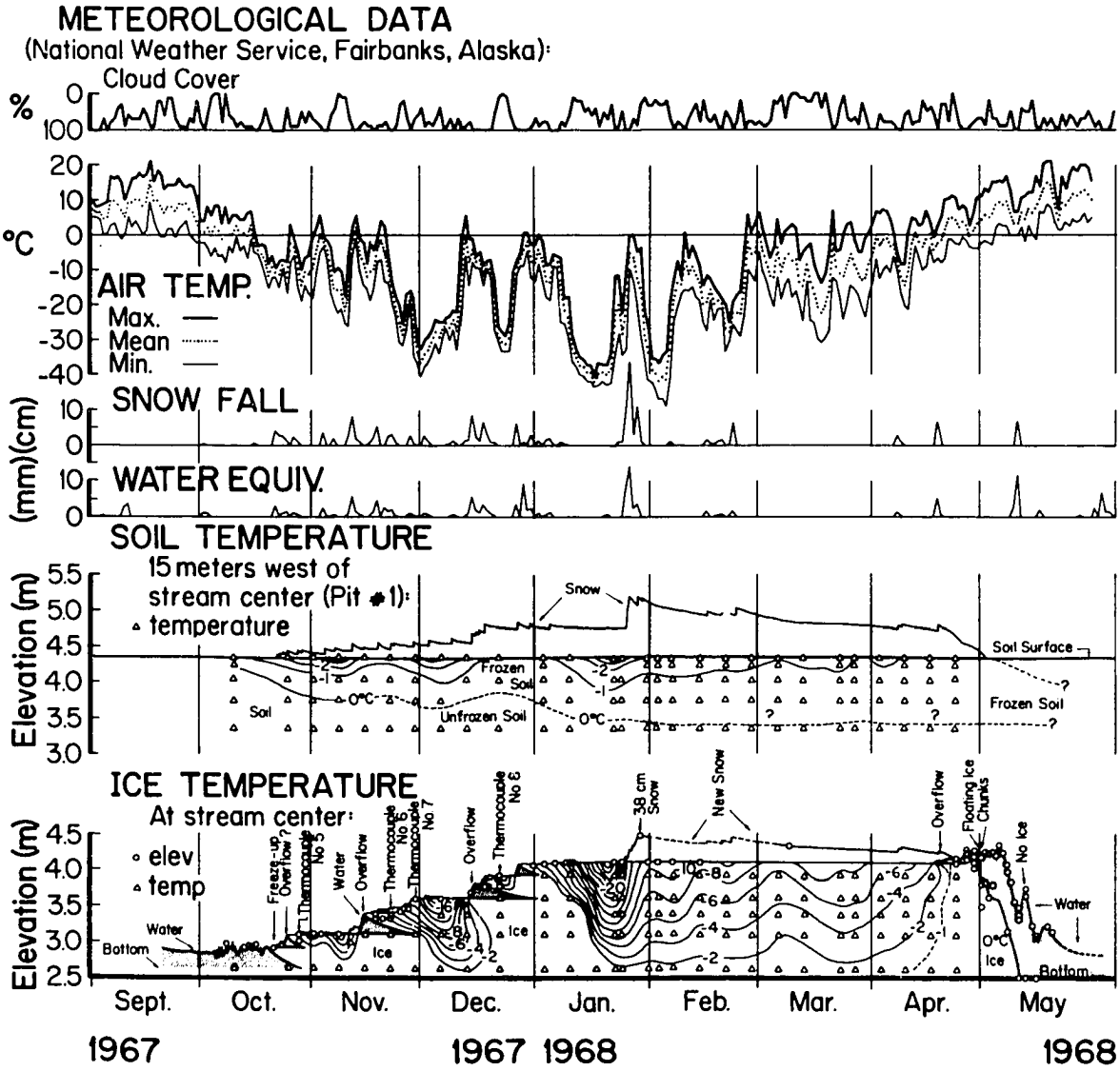

Figure 18. Comparison between temperatures in the aufeis at stream center and in the upper 1 meter of soil at thermocouple pit no. 1 (15 meters west of stream center) throughout the period September 1967 through May 1968. Supporting meteorological data (cloud cover, air temperature, snow fall, precipitation, and snow cover) is from the National Weather Service, Fairbanks.

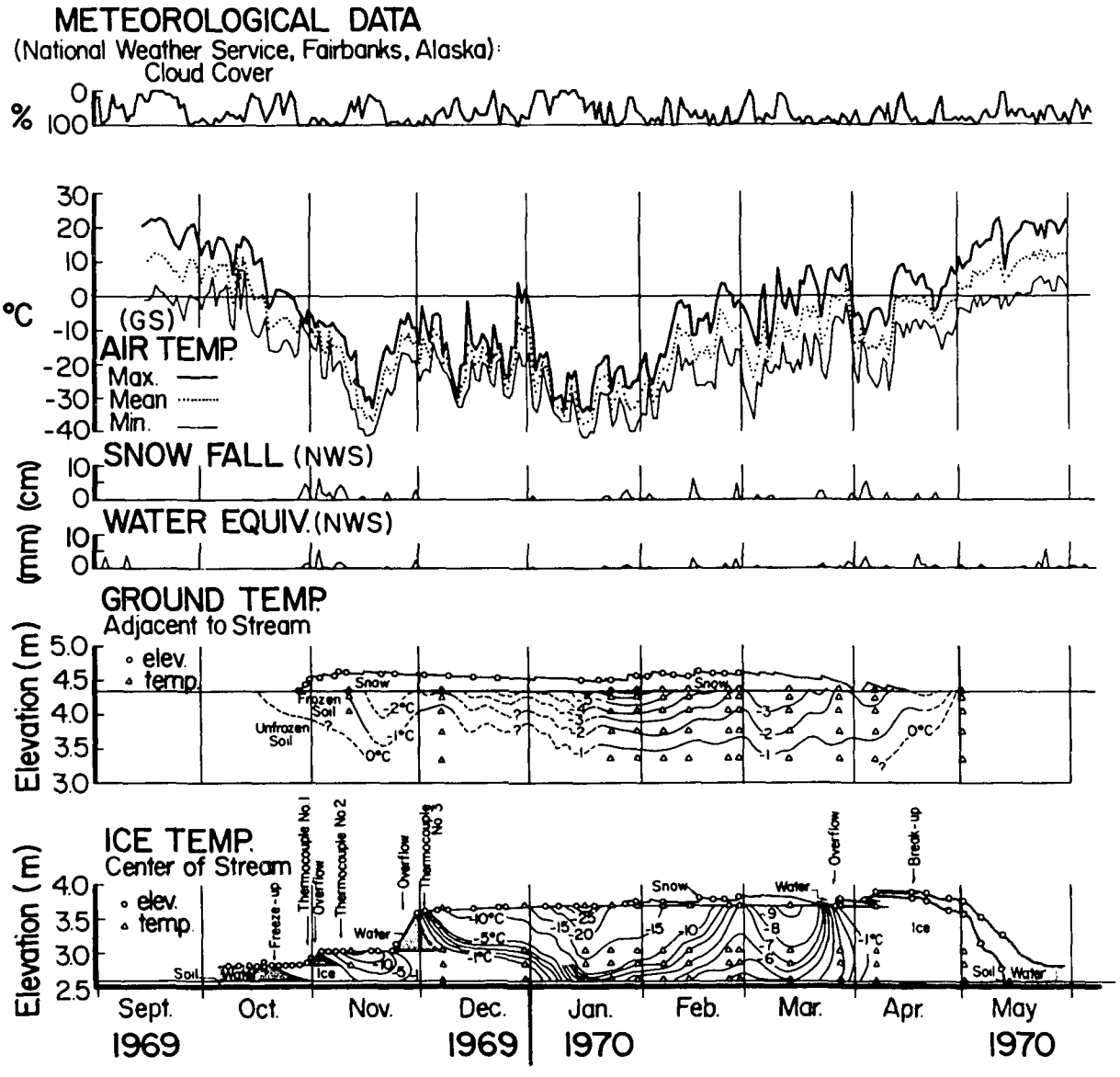

Figure 19. Comparison between temperatures in the aufeis at stream center and in the upper 1 meter of soil at thermocouple pit no. 1 (15 meters west of stream center) throughout the period September 1969 through May 1970. Supporting meteorological data is from both the Goldstream site (GS) and the National Weather Service (NWS).

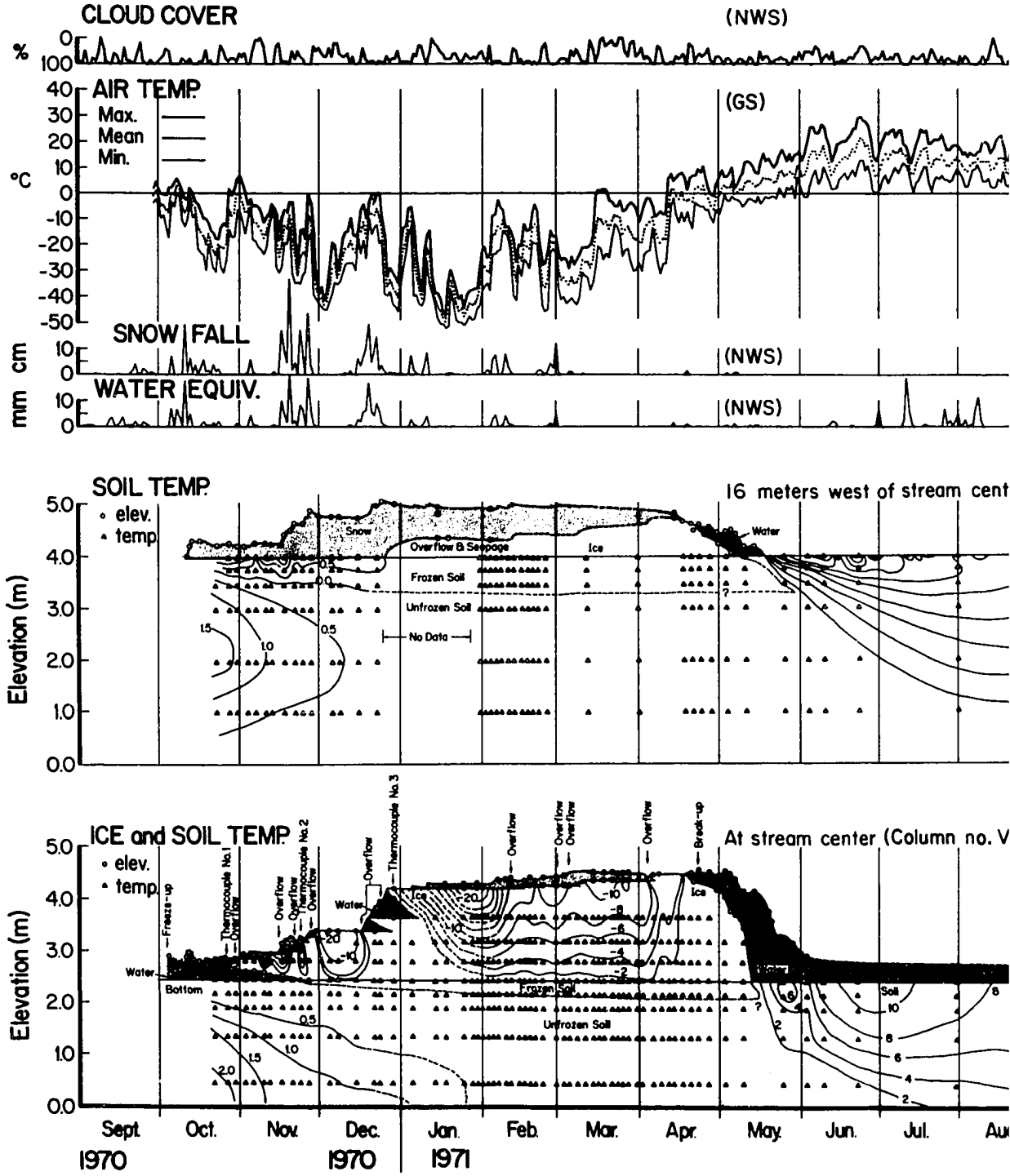

Figure 20. Comparison between temperatures in the aufeis and soil at stream and temperatures in the upper 3 meters of soil, 16 meters west of no. I) throughout the period September 1970 through December 1971 ological data is from both the Goldstream Site (GS) and the Natio Fairbanks (NWS).

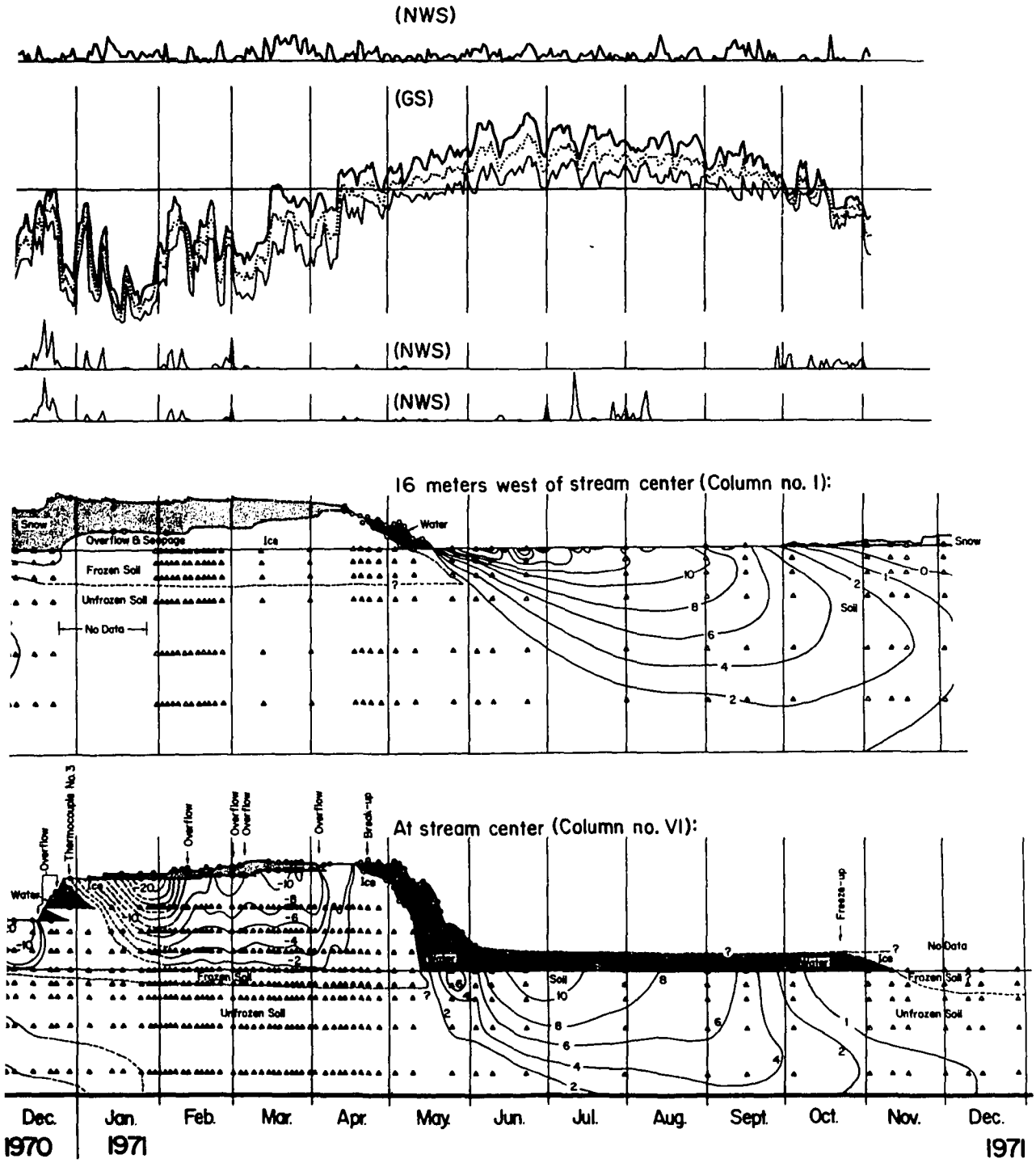

etween temperatures in the aufeis and soil at stream center (column no. VI)
ures in the upper 3 meters of soil, 16 meters west of stream center (column
ghout the period September 1970 through December 1971. Supporting meteor-
a is from both the Goldstream Site (GS) and the National Weather Service,
WS).

3.2.1 Winter 1967-1968

The data coverage for this season was good and was collected by Dr. Benson and students prior to this investigation. Throughout a period of about seven months (9 October to 24 April), 29 temperature profiles were taken at depths of 0, 10, 30, 60, and 100 cm below the ground surface (Pit 1), located about 15 meters west of the stream center. No temperature data from the soil beneath the stream are available for this season, but thermocouples embedded in the aufeis provided good data from the stream itself.

As shown in Figure 18a, consistently sub-freezing air temperatures lasted from 16 October until 21 April, with a minimum of -42°C on 17 January (National Weather Service). This winter was fairly mild; the average annual temperature (July to July) was -2.47°C and the snow fall of 183 cm was about normal.

Adjacent to the stream, the minimum recorded ground temperature was -4.5°C on 8 November, this was during the first major cold spell while the snow cover was still thin, as shown in Figure 18b. Throughout the season, the 0°C isotherm never penetrated much more than 100 cm below the ground surface, and by 1 May, the soil became isothermal at 0°C throughout the depth over which temperature measurements were made.

3.2.2 Winter 1969-1970

Throughout a six-month period (11 November to 1 May), 15 temperature profiles were taken using the same probes as during the previous season: Pit 1 (5 probes) and a vertical selection of 4 aufeis strings.

Consistent sub-zero air temperatures persisted from 19 October to 29 March with a minimum daily mean of -38°C on 16 January. This was the mildest winter recorded at Goldstream; the average annual temperature (July to July) was -1.48°C, and a total snowfall of only 92 cm was observed.

Adjacent to the stream, the soil temperatures were the lowest recorded at Goldstream during the three years of observation due to the unusually thin snow cover which never exceeded 30 cm in thickness. This is because the relatively mild winter was more than compensated by the relative lack of insulation by the snow. On 30 January, the ground surface temperature was -8.2°C with sub-zero temperatures persisting from about 1 November to 1 May. At 1 meter below the ground surface, the temperature reached a minimum of about -1°C in mid-January. Due to a combination of instrumental error and freezing point depression from dissolved minerals in the soil, it is not certain how much deeper the soil actually froze. No data were collected during a six-week period throughout December 1969 and January 1970; temperature fluctuations for this period were estimated on the basis of meteorological data and are shown as dashed lines in Figure 19b.

In the stream center (Figure 19c), the relatively thin ice and the lack of snow produced very high temperature gradients through the ice, and high heat loss from the sediments beneath. Temperatures at the bottom of the ice dropped as low as -8°C; by comparison, the minimum recorded beneath the ice during the previous winter was only -2°C.

Throughout February and March, a small amount of snow remained on the surface, making an effective insulator.

Overflowing in 1969-70 occurred in three main stages: late October, late November, and late March. The one in late November was unusually large compared to the others. As during other winters observed, the overflows quickly raised the temperature of the entire ice mass to 0°C in most cases. The time required for complete removal of the ice in 1970 was four weeks, but only 18 days in 1968.

3.2.3 Hydrological year 1970-1971

The results of 50 profiles taken from 22 October 1970 to 1 November 1971 are represented in Figure 20. The two thermocouple columns selected were no. I, located 16 meters west of the stream center, and no. VI, one meter east of the center. The data coverage was good with the exception of a five-week period in December and January, during which time there was a problem with electrolytic noise. Rapid fluctuations in the elevation of the 0°C isotherm were due to instrumental error, especially during periods of small temperature changes; this made it difficult to estimate the depth of freezing.

Sub-zero air temperatures prevailed from 1 October to 13 April with a minimum daily mean of -50°C on 18 January. This was the most severe winter since that of 1965-1966, and the 370 cm total snowfall exceeded that of any previous winter observed by the Weather Service in Fairbanks.

The snow cover was present from 11 October 1970 until 6 May 1971, and reached a maximum thickness of 108 cm. Its depth profile (Figure 20b), is based on 48 measurements in the vicinity of thermocouple column no. I. Snow data for fall 1971, however, are from National Weather Service records.

The onset of percolating overflow water through the lower layers of snow, commencing in late December, caused considerable densification of the snow, but since the soil was already near 0°C, because of the insulation provided by the deep snow, any additional thermal effect was negligible.

In May and early June 1971, the penetration of the summer heat pulse was temporarily retarded by latent heat exchange as seasonal frost melted; this produced bending of the isotherms in the upper 1 meter of soil. As shown in Figure 15 (a and b), the retardation of the heat pulse was more pronounced nearer to the stream banks, because of greater heat loss from the banks during the winter, and consequently the presence of more ice in the soil near the banks.

Throughout the summer of 1971, the upper soil layers responded to rapid changes in air temperature, but at depths below 1 meter, short term fluctuations were filtered out, resulting in smooth isotherms. The amplitude attenuation and seasonal lag with increasing depth was well pronounced. The maximum ground-surface temperature was 22°C in late June, while at 3 meters, the maximum was only 2.1°C and did not occur until late September, about 95 days later.

In the stream center, the general pattern of events was similar to that observed during previous seasons; namely (1) overflowing during November and December, (2) absorption of snow and warming of ice of 0°C by each overflow, (3) formation of new ice surface by freezing of the overflow water, (4) penetration of low temperatures through the ice after water layer was "pinched out", (5) thermal shielding by the snow cover, and (6) meltwater overflow in April, causing the ice to become isothermal at 0°C. The overflow commencing on 17 December 1970 was unusually extensive - totalling 80 cm.

In the underlying soil, the pattern of isotherms was similar to that observed adjacent to the stream, except for the much smaller amplitude of fluctuation during the summer: The bottom surface reached 11°C in late June, only one half of that observed at the ground surface adjacent to the stream.

CHAPTER 4

ANALYSIS OF THE DATA

Of the thermal parameters studied, only the thermal diffusivity, α, can be determined solely from the temperature data. The specific heat, c, can be estimated on the basis of composition, moisture content, m, and density, ρ. From this, the thermal conductivity, k, is determined by the relationship:

$$k = \alpha c \rho \ . \tag{5}$$

For the determination of α for the various conducting media, three methods were used.

4.1 Four-term Fourier method

By means of Fourier series, any cyclic function (e.g., f(t)) can be expressed as the sum of a sinusoid and its higher harmonics. Carried out to four terms, air temperature, T_o, which is a function of time, t, can be expressed as:

$$T_o = f(t) = T_m + A_1 \cos(\omega t + \theta_1) + A_2 \cos(2\omega t + \theta_2) + A_3 \cos(3\omega t + \theta_3) + A_4 \cos(4\omega t + \theta_4), \tag{6}$$

where: A_1, A_2, A_3, A_4, θ_1, θ_2, θ_3, and θ_4 are the Fourier coefficients (A = amplitude, θ = phase angle); T_m = the mean temperature; and ω = the fundamental frequency of the cycle.

The derivation of the Fourier coefficients (discussed in standard textbook references, such as Carslaw and Jaeger (1959) and Ingersoll and Zobel (1954) results from the full Fourier series for f(t):

$$f(t) = \sum_{n=0}^{\infty}\{C_n \cos(n\omega t) + S_n \sin(n\omega t)\},\ n = 0, 1, 2, \ldots . \quad (7)$$

The coefficients, C_n and S_n, are determined by the expressions:

$$S_n = \frac{2}{q}\sum_{p=0}^{p=q-1} f(\frac{2\pi p}{q}) \sin(\frac{2\pi np}{q}),\ n = 0, 1, 2, \ldots , \quad (8)$$

and

$$C_n = \frac{2}{q}\sum_{p=0}^{p=q-1} f(\frac{2\pi p}{q}) \cos(\frac{2\pi np}{q}),\ n = 0, 1, 2 \ldots . \quad (9)$$

where: $\frac{2\pi p}{q} = \omega t$, p = an integer ranging from 1 to q-1, and q = the number of integration steps throughout main harmonic (e.g., one per month with a total of 12 for an annual cycle). From this, A_n and θ_n are derived:

$$A_n = (S_n^2 + C_n^2)^{1/2},\ n = 0, 1, 2, \ldots , \quad (10)$$

and

$$\theta_n = -\tan^{-1}(\frac{S_n}{C_n}),\qquad n = 0, 1, 2, \ldots . \quad (11)$$

For conduction of heat in a homogenous and isotrophic medium of thermal diffusivity, α, the Fourier conduction equation is obeyed:

$$\frac{dT}{dt} = \alpha(\frac{\partial^2 T}{\partial x^2} + \frac{\partial^2 T}{\partial y^2} + \frac{\partial^2 T}{\partial z^2}) = \alpha\nabla^2 T. \quad (12)$$

Semi-infinite solid: With the surface temperature described by a Fourier series, the temperature, T_z, at depth, z, which satisfies both equations (6) and (12) is (Carslaw and Jaeger, 1959):

$$T_z = \sum_{n=0}^{n=\infty} A_{nz} \exp(-z\sqrt{\frac{n\omega}{2\alpha}}) \cos(n\omega t - z\sqrt{\frac{n\omega}{2\alpha}} + \theta_n). \quad (13)$$

From this, α is determined from the amplitude attenuation with depth:

$$\frac{A_{nz}}{A_{no}} = \exp(-z\sqrt{\frac{n\omega}{2\alpha_n}}), \quad n = 1, 2, 3, \ldots . \tag{14}$$

thus

$$\alpha_n = \frac{n\omega}{2} \{\frac{z}{\ln(\frac{A_{nz}}{A_{no}})}\}^2, \quad n = 1, 2, 3, \ldots . \tag{15}$$

where "z" subscript refers to depth, z, and "o" refers to the medium surface.

Likewise, from the change in phase lag with depth:

$$\Delta\theta_n = -z\sqrt{\frac{n}{2\alpha_n}}, \tag{16}$$

thus

$$\alpha_n = \frac{n\omega}{2} (\frac{z}{\Delta\theta_n})^2, \tag{17}$$

where $\Delta\theta_n$ is the phase difference of the temperature cycle between depth, z, and the surface.

The thermal diffusivity can thus be calculated in a semi-infinite, homogeneous medium from the expected exponential decrease of the temperature amplitude with depth or from the linear change of the phase angle of the temperature wave with depth.

Infinite slab of thickness, x: With the surface temperature represented by a Fourier series, the temperature at depth, $0 \leq z \leq x$ becomes:

$$T_z = \sum_{n=0}^{n=\infty} A_{nz} \sin(n\omega t + \Delta\theta_n + \theta_n),$$

where:
$$A_{nz} = A_n \{\frac{\cosh(2kx - 2kz) - \cos(2kx - 2kz)}{\cosh(2kx) - \cos(2kx)}\}^{1/2} \tag{18}$$

$$k = \sqrt{\frac{n\omega}{2\alpha}}\ , \text{ and}$$

$$\Delta\theta_n = \arg \frac{\sinh \{k(x - z)(1 + i)\}}{\sinh\ kx(1 + i)}$$

(Carslaw and Jaeger, 1959, p. 105).

The amplitude attenuation and phase lag are not only different than in the case of the semi-infinite solid, but the expression of α on this basis is mathematically cumbersome. It is easier to determine α by using trial-and-error values for α in equation (18) until there is agreement with observed amplitude attenuation and phase lag.

4.1.1 Analysis of soil temperatures throughout the annual cycle, November 1970 through October 1971

The only data suitable for the evaluation of α were annual cycles that covered periods of significant temperature change from winter to summer. Also, the sites used for temperature analysis had to be as far removed as possible from the disturbing effects of the stream banks. For this purpose, column no. I, farthest from the stream and column no. VI, in the center of the stream, were used (Fig. 5).

The average monthly temperatures at depths 0, 0.5, 1.0, 2.0, and 3.0 (column no. 1 only) meters were scaled from the data (Fig. 21 and 22), with each month taken to be equal in length. No air temperatures were recorded at the Goldstream site from June to September 1971; throughout this four-month period, data from the National Weather Service (Fairbanks Int. Airport) were used with corrections ranging linearly from -368°C (average departure for April and May) to -1.48°C (average

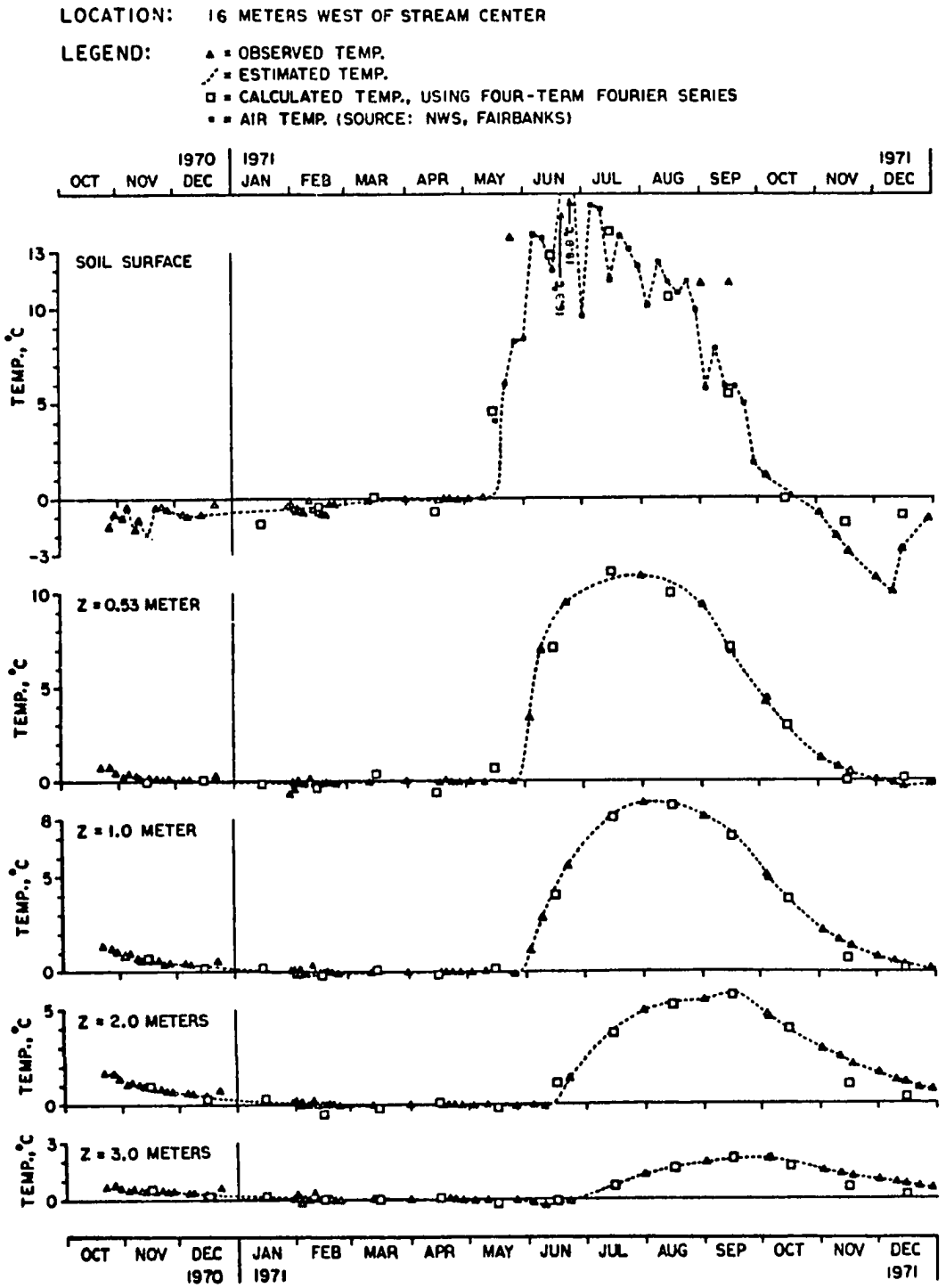

Figure 21. Soil temperatures at column no. I (ground surface, 0.5, 1.0, 2.0, and 3.0 meters depth) from October 1970 through December 1971.

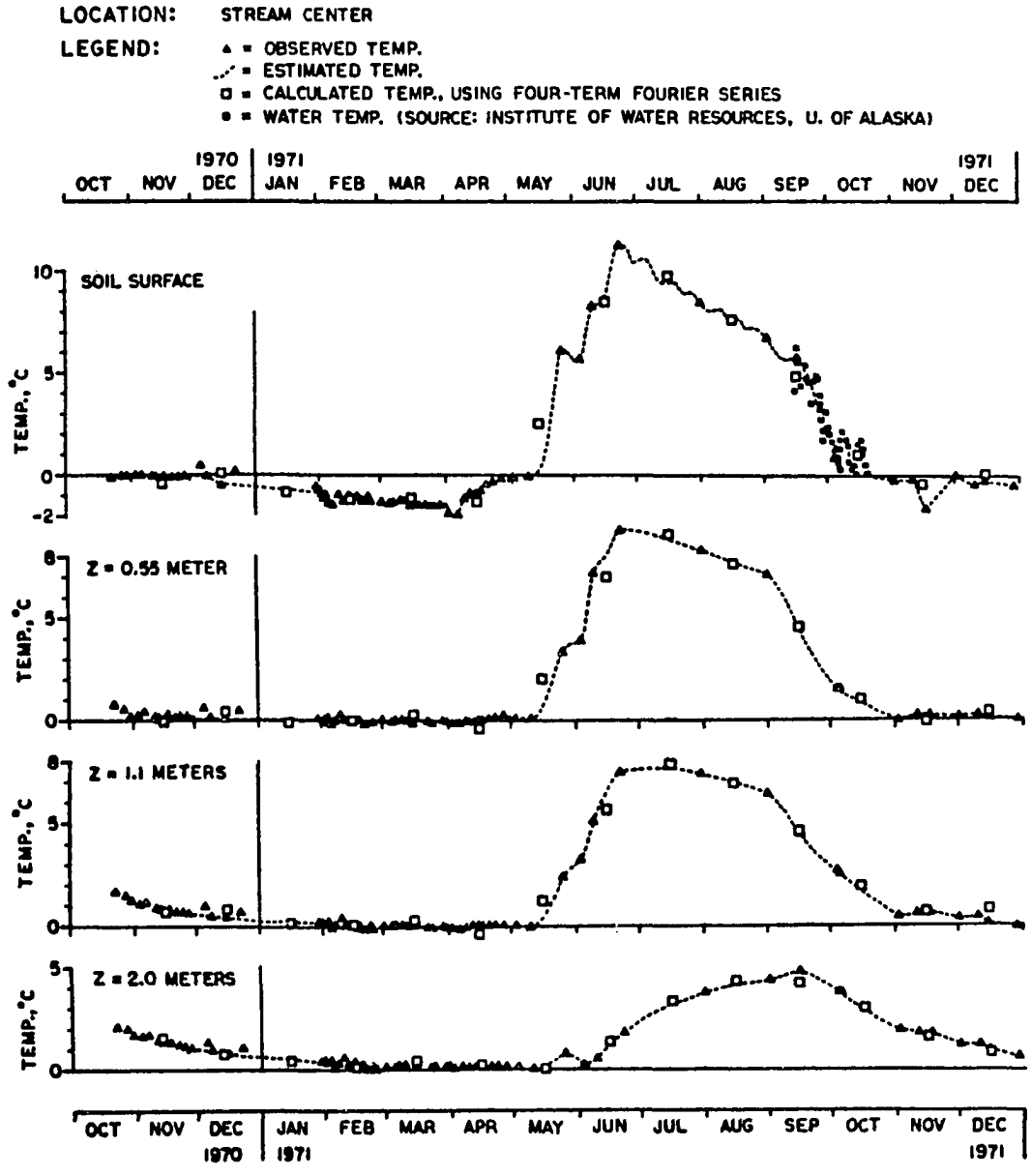

Figure 22. Soil temperatures at column no. VI (stream bottom surface 0.5, 1.1, and 2.0 meters depth) from October 1970 through December 1971.

departure for October and November 1971), to account for the slightly lower temperatures at Goldstream.

Using a twelve month cycle (1 Nov. 1970 to 31 Oct. 1971), the eight parameters - A_1, A_2, A_3, A_4, θ_1, θ_2, θ_3, and θ_4 were derived, using equations (10) and (11), and are shown in Table 4. The phase angles were calculated such that the start of the cycle ($n\omega t = 0$) was on 21 June 1971 to correspond with the summer solstice.

From this, values of α were calculated for n = 1 and n = 2 (Table 5) using both the semi-infinite model (equations (15) and (17)) and the infinite slab model (equation (18)) with 0°C boundary conditions set at 3.5 or 4.0 meters below the surface.

In addition, the thermal diffusivity of the soil, both beneath the stream and farthest from the stream, was estimated by fitting an exponential curve to the observed amplitude attenuation with depth; i.e., the difference between the maximum and minimum temperature envelope shown in Fig. 23.

At both locations - in the stream center and farthest away from the stream, the temperature amplitudes decreased and the phase lags increased with depth, as expected, but, as shown in Table 4, despite negative air temperatures, oil temperatures were positive. Also, the annual air temperature cycle was sinusoidal as shown by low values for A_2, A_3, and A_4 (the amplitudes of the higher harmonics), but in the soil, A_2 was relatively high at all depths.

Judging from the scattering of calculated values for α in Table 5, the application of equations (13) and (18) to the full, 12-month

Table 4. Observed amplitude attenuation of soil temperatures with depth and results of four-term Fourier analysis throughout the annual cycle (November 1970 through October 1971)

			n = 1		n = 2		n = 3		n = 4	
Depth (cm)	T_m (cm)	Obs'd (°C)	A_1 (°C)	θ_1 (°)	A_2 (°C)	θ_2 (°)	A_3 (°C)	θ_3 (°)	A_4 (°C)	θ_4 (°)
(a) Farthest from the stream (column no. I)										
Air	-6.80	-	22.47	-24.2	0.86	87.4	1.42	1.0	2.69	100.5
0	3.63	12.2	6.99	-22.9	3.36	-48.1	0.82	-35.4	0.89	37.0
23	3.81	8.0	6.82	-32.3	3.36	-60.5	1.01	-46.4	0.95	-0.8
53	3.21	5.8	5.27	-43.2	2.55	-79.5	0.63	-69.3	0.62	-16.9
101	2.71	4.5	4.30	-54.5	1.95	-100.8	0.31	-106.4	0.42	-45.3
203	1.69	3.0	2.81	-71.5	1.14	-139.8	0.27	149.6	0.36	-63.1
300	0.58	1.2	0.93	-90.0	0.51	-163.1	0.15	118.7	0.11	-86.4
(b) At center of stream (column no. VI)										
0	2.45	6.7	5.07	-33.7	2.30	-46.0	0.45	-27.0	0.61	22.0
29	2.93	5.7	4.74	-29.1	2.32	-52.6	0.46	-31.9	0.65	23.5
55	2.61	4.7	4.16	-32.6	2.15	-59.9	0.48	-65.7	0.45	22.3
110	2.46	3.9	3.52	-41.8	1.71	-65.1	0.46	-66.4	0.34	7.3
200	1.63	2.4	2.05	-73.0	0.76	-130.0	0.18	-122.0	0.12	-45.7

Table 5. Thermal diffusivities ($10^{-3}cm^2sec^{-1}$) of the soil derived from observed amplitude attenuation with depth and Fourier analysis (n = 1, 2) of soil temperatures throughout the annual cycle (November 1970 through October 1971)

Depth	Obs'd	n = 1				n = 2			
		Semi-inf. solid		Inf. slab 3.5m	Inf. slab 4.0m	Semi-inf. solid		Inf. slab 3.5m	Inf. slab 4.0m
(cm)	Amp.	Amp.	Phase	Amp.	Amp.	Amp.	Phase	Amp.	Amp.
(a)	Farthest from the stream (column no. I)								
0 - 53	0.51	3.50	2.23	3.06	3.21	7.35	1.86	6.36	6.67
53 - 101	3.56	5.54	5.90	5.45	4.70	6.37	3.32	5.40	5.65
101 - 203	6.30	5.72	11.77	∞	13.10	7.19	4.47	17.40	6.40
203 - 300	1.12	0.76	8.98	2.07	0.68	2.90	11.33	∞	2.94
(b)	At center of stream (column no. VI)								
0 - 55	2.40	7.70	∞	7.53	6.57	132.6	10.23	∞	∞
55 - 110	8.65	10.80	11.68	∞	∞	11.49	73.12	12.53	9.95
110 - 200	3.42	2.76	2.72	2.84	2.36	2.45	1.26	2.32	2.17

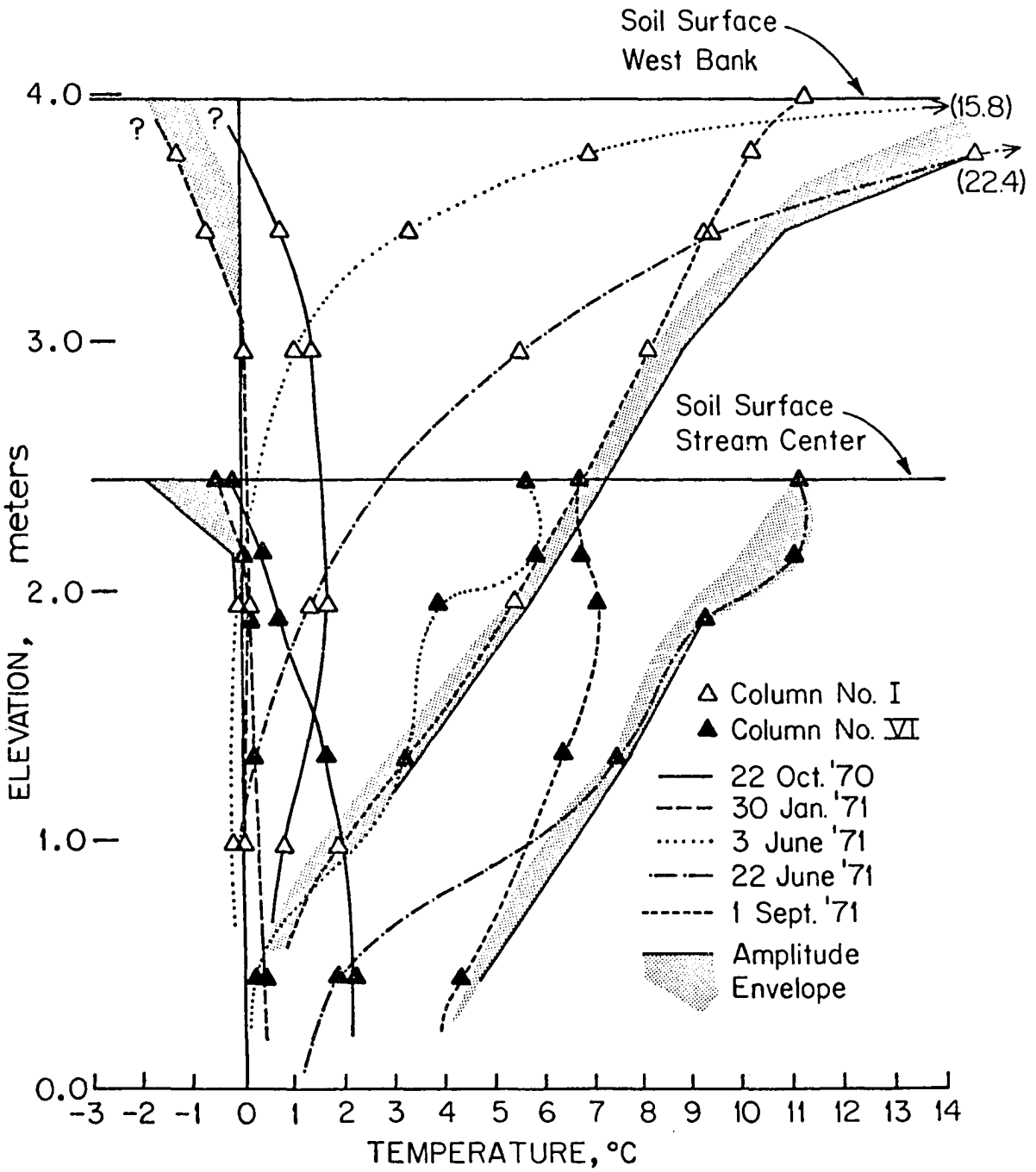

Figure 23. Temperature versus depth profiles in the soil at column no. I, 16 meters west of stream center, and column no. VI, beneath stream center, October 1970 to September 1971.

temperature curves obviously had its limitations, especially for n = 2 and probably even more so for the higher harmonics. Although any cyclic function can be represented by the sum of its harmonics, the insulating effect of the snow and ice cover distorted the annual temperature wave in such a fashion that the second and higher harmonics became more important relative to the first harmonic. Analysis of the data to derive reliable values of α from the lower harmonics ($n \leq 2$) alone was thus inaccurate, as shown in Table 5. Attempts were therefore made to assess the thermal properties of the snow cover and to calculate α for soil from the sinusoidal half-wave summer data only, as described in the next two sections.

4.1.2 Insulating effect of the snow and ice

The soil temperatues throughout 1970-71, as indeed in any other year, were strongly influenced by the presence of a snow cover in winter. The amplitudes of soil temperatures during the winter half of the annual cycle were greatly reduced due to the presence of snow, as shown schematically in Fig. 24.

The known importance of the snow to the thermal regime of the underlying soil led to attempts at determining the thermal diffusivity in undisturbed snow from diurnal temperatures and estimates of specific heat and thermal conductivity, based on published values. Important works dealing with the thermal properties of snow include those by Dorsey (1940) and Mantis (1951).

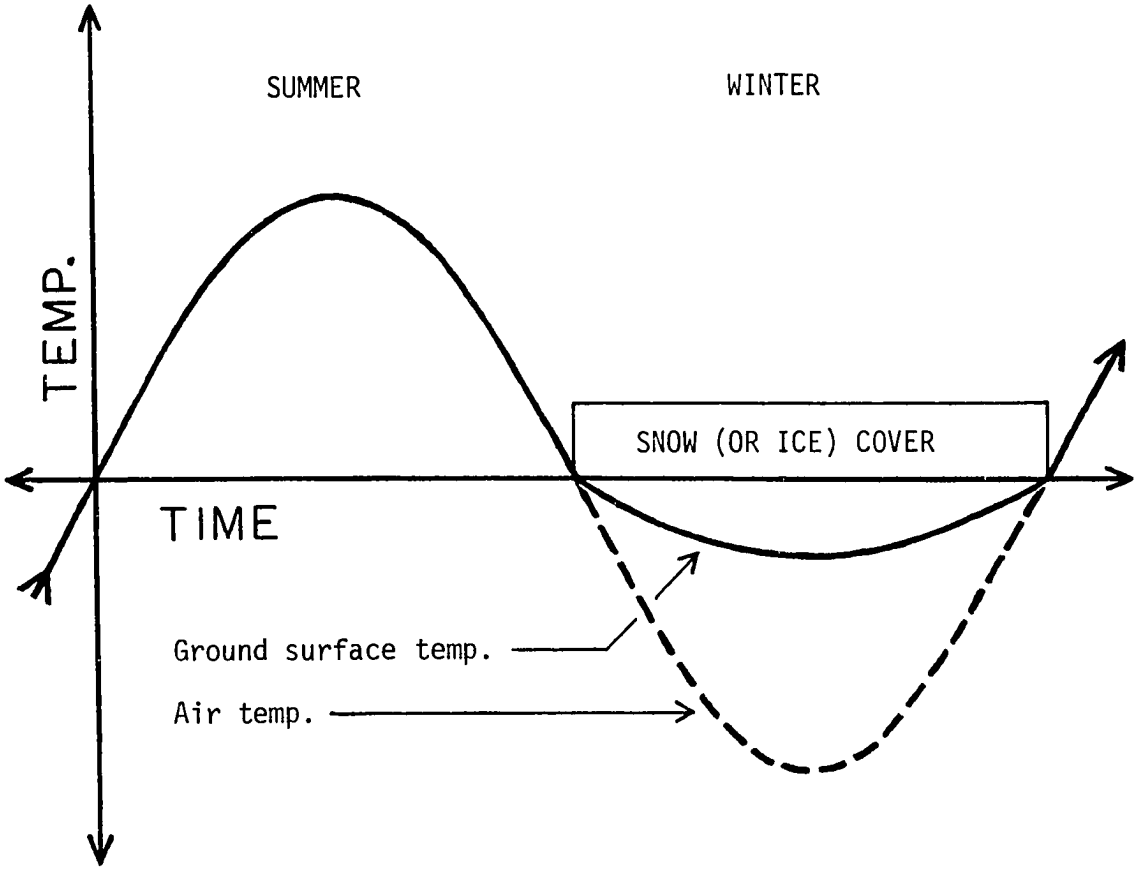

Figure 24. Schematic diagram showing effect of seasonal snow (or ice) cover on ground surface temperature. Although the annual air temperature cycle is sinusoidal, the ground surface temperature is not sinusoidal due to the snow (or ice) which greatly reduces the amplitude of the negative portion of the annual curve.

(1) Thermal diffusivity of the snow

Thermograph measurements of the ambient air temperature and the temperature at the ground surface beneath 27 cm of freshly fallen snow from 7 through 10 Nov. 1970 show a 14-fold reduction in amplitude and phase lags of up to 45° (Fig. 25). A two-term Fourier analysis was made of these curves and the values of α, along with the Fourier coefficients, are presented in Table 6.

In spite of probable non-conductive heat transfer mechanisms and the inhomogeneity of the snow/soil system, the values for α derived on the basis of amplitude attenuation approached the value, 0.004 cm^2sec^{-1}, accepted in the literature (Table 7), but on the basis of phase lag, the values generally came out an order of magnitude too large. The difference in values obtained by the two methods reflects the difficulty of fitting sine waves to the observed values, but the generally high values for α are possibly due to the disturbing effect of moisture transfer upward through the snow, as shown by Benson (1962) and Trabant (1970). These authors determined an average flux of 0.025 g $cm^{-2}day^{-1}$ away from the depth hoar layer of a fully developed snow pack in interior Alaska. In the top layers of snow, air convection constitutes an effective means of additional heat transfer, causing the effective thermal conductivity (and thermal diffusivity) to be several times higher than experimental values (Bey 1951). Another determination of α for snow was made, using temperature data from 27 through 29 March 1971, at which time the snow was 80 cm thick. Using the FORTRAN program (Appendix B), discussed in Chapter 4, theoretical temperature curves were generated, using assumed

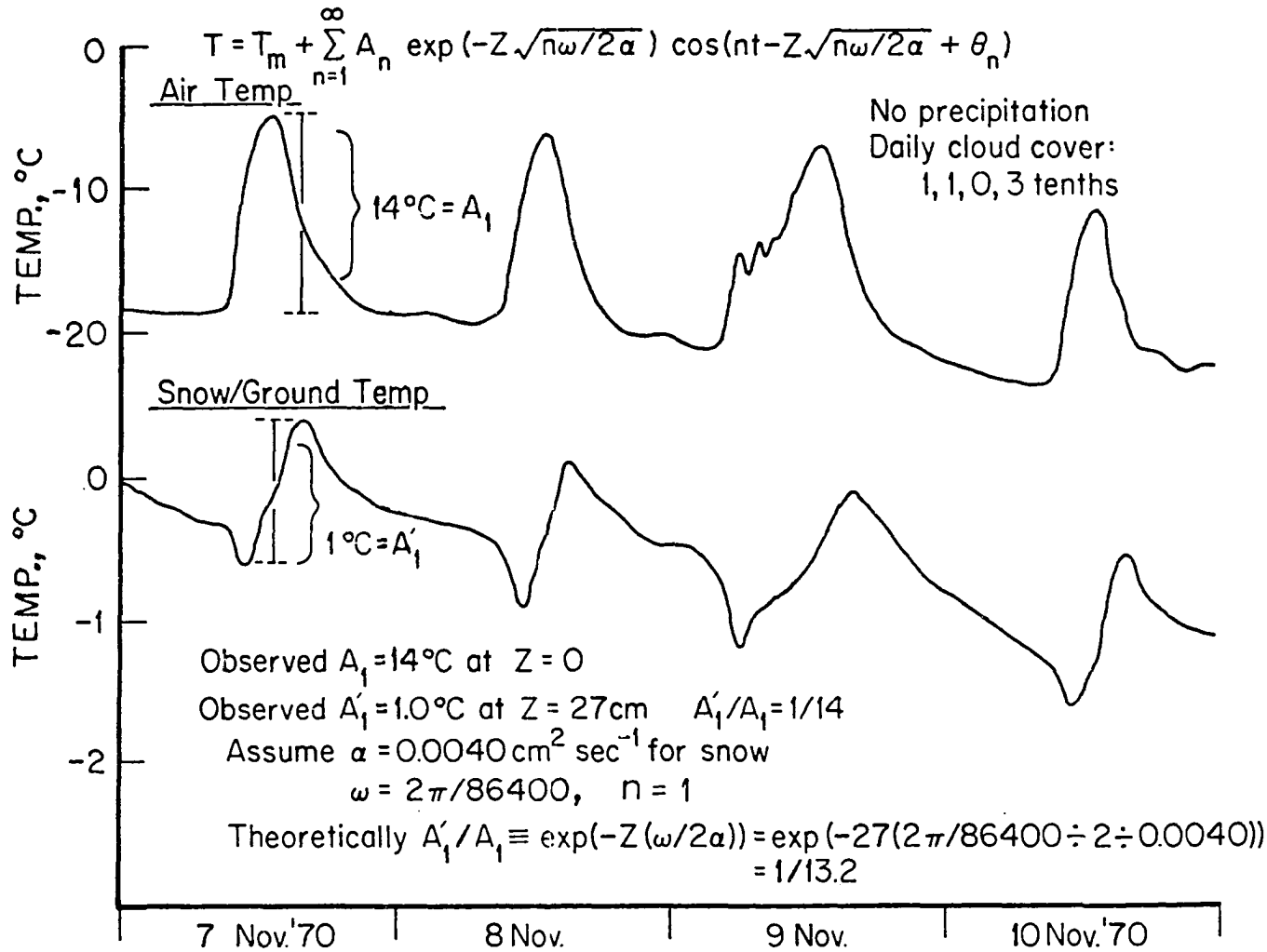

Figure 25. Ambient air temperature and temperature at the ground surface beneath 27 cm of fresh snow, 7 through 10 November 1970.

Table 6. Fourier coefficients and thermal diffusivity ($10^{-3}cm^2sec^{-1}$) of the snow derived from Fourier analysis of diurnal temperature curves above and beneath 27 cm of freshly fallen snow, 7 and 8 November 1970

Harmonic	Depth (cm)	7 Nov. Coefficient		($\alpha 10^{-3}$)	8 Nov. Coefficient		($\alpha 10^{-3}$)
n = 0	0	T_m	-15.29		T_m	-16.92	
	27	T_m	-1.14	-	T_m	-1.36	-
n = 1	0	A_{1o}	5.40		A_{1o}	4.88	
	27	A_{1z}	0.31		A_{1z}	0.20	
		ratio	17.25	3.3	ratio	24.04	2.6
	0	θ_{1o}	-22.5		θ_{1o}	-18.9	
	27	θ_{1z}	-96.9		θ_{1z}	-102.6	
		$\Delta\theta_1$	74.4	15.7	$\Delta\theta_1$		12.4
n = 2	0	A_{2o}	3.20		A_{2o}	3.25	
	27	A_{2z}	0.16		A_{2z}	0.20	
		ratio	19.63	6.0	ratio	16.25	6.8
	0	θ_{2c}	-34.3		θ_{2o}	-33.5	
	27	θ_{2z}	-131.4		θ_{2z}	-102.6	
		$\Delta\theta_2$	97.1	18.4	$\Delta\theta_2$	79.1	27.8
Observed (n = 1)	0	A_o	13.7		A_o	13.6	
	27	A_z	1.08		A_z	1.03	
		ratio	12.7	4.1	ratio	13.2	4.0
	0	θ_o	-15		θ_o	15	
	27	θ_z	-60		θ_z	50	
		$\Delta\theta$	45	42.5	$\Delta\theta$	35	71.0

Amplitudes are in °C and phase lags are in angular degrees (0° = 1200 noon AST).

Table 7. Published values for thermal diffusivity ($10^{-3}cm^2sec^{-1}$) of snow

Density ($g\ cm^{-3}$)	Dorsey (1940) *	Weller & Schwerdtfeger (1968)	
		T = 0°C	T = -50°C
0.125	3.0	-	-
0.19	2.9	-	-
0.32	3.4	4.2	6.7
0.40	3.9	5.0	8.0
0.50	4.8	6.4	10.2
0.60	-	8.7	13.9
0.70	-	10.6	16.9
0.80	-	11.5	18.4
0.917	-	11.8	18.9

* After Van Dusen, 1933 (Dorsey, p. 483).

values of 0.00347 and 0.00694 cm^2sec^{-1} for α. As shown in Figure 26, the curves follow the observed points, but it is not certain which values for α make the best fit. On the basis of observed amplitude attenuation, the value for α in the upper 10 cm of the snow pack, using Eq. (15), was about 0.0038 cm^2sec^{-1}, where A_{1c} and A_{1z} were respectively 16.4°C and 6.2°C (the two subscripts for A refer to the value of n and to the depth in the snow, respectively).

The literature shows large differences in values of α for snow; but generally, α increases linearly with density and decreases with temperature.

(2) Density, specific heat, and thermal conductivity of the snow

Although no measurements of these parameters were made at the Goldstream site for this study, some values determined through other investigations are briefly presented:

(a) Density: Meteorological data from the National Weather Service, Fairbanks, show that newly fallen snow usually has a density between 0.05 and 0.10 g cm^{-3}. As it accumulates, however, it undergoes densification due to gravity settling and moisture transfers (Benson, 1962; Trabant, 1970). The average density of a well developed snow pack in February is about 0.2 g cm^{-3}: ranging from 0.1 g cm^{-3} at the surface to 0.25 g cm^{-3} halfway to the bottom. In the bottom half, the density decreases to about 0.2 g cm^{-3}. Due to the unusually heavy snowfall during the winter of 1970-71, the average density profile was slightly higher than usual; measurements made by Dr. Weller and the author at the Hot Pipe Test Site of the Institute of Arctic Biology, University

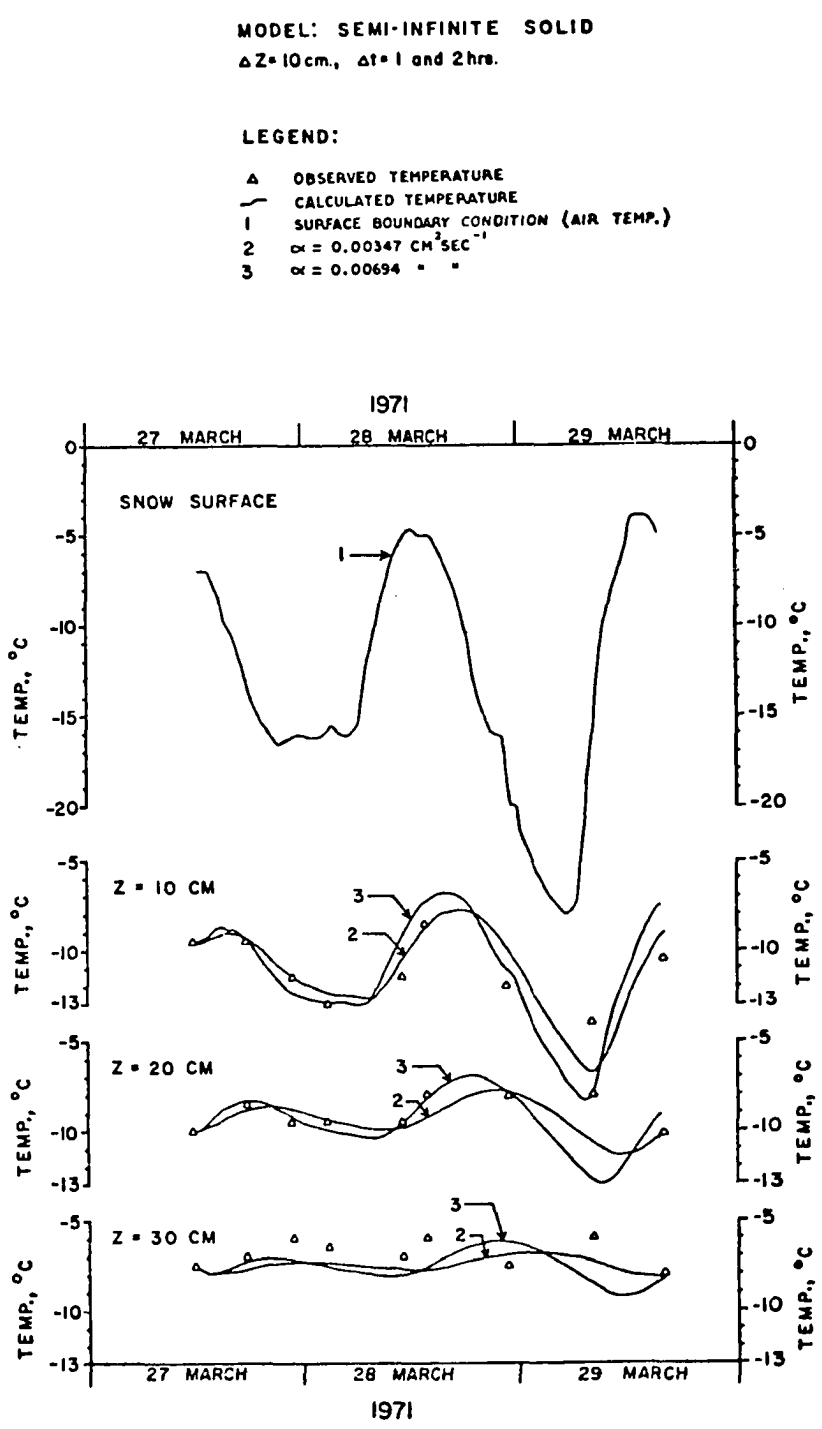

Figure 26. Comparison of observed temperatures in snow with temperatures calculated by numerical step method using infinite slab models of thermal diffusivities, 0.00347 and 0.00694 cm^2sec^{-1}, 27 through 29 March 1971.

Alaska, in mid-February 1971, showed a density ranging from 0.1 g cm^{-3} at the surface, 0.27 g cm^{-3} at mid-depth, and 0.23 g cm^{-3} at the bottom.

(b) Specific heat: The specific heat of ice varies from 0.504 cal $g^{-1}°C^{-1}$ at 0°C to 0.415 cal g^{-1} $°C^{-1}$ at -50°C (Dorsey, 1940, p. 479) and is independent of the density. For simplicity, 0.50 cal $g^{-1}°C^{-1}$ for ice or snow was considered acceptable.

(c) Thermal conductivity: Although the thermal diffusivity of snow ($\simeq$.004 cm^2sec^{-1}) is comparable to that of soil, the thermal conductivity is much lower for snow, due to the low value for $c\rho$; (0.49 cal $g^{-1}°C^{-1}$) x (0.2 g cm^{-3}) = (0.1 cal $cm^{-3}°C^{-1}$); thus, the sudden change in the temperature-gradient across the soil/snow interface in Fig. 31. Published values of k for snow are shown in Table 8.

4.1.3 Analysis of soil temperatures throughout one half of the annual cycle, May 1971 through December 1971

To avoid the disturbing effects of the snow/ice cover and possible latent heat exchanges in the soil, the winter portion of the soil temperature curves was ignored and a Fourier half-wave (6 months) analysis was made of the summer portions only, with the resulting coefficients for n = 0, 1, and 2 shown in Table 9. Using 0°C as the baseline (T_m = 0), the values for A_1 and A_2 turned out to be about double the values of A_1 and A_2 derived from the 12-month analysis (Table 4), but the phase lags generally remained unchanged.

Table 8. Published values for thermal conductivity ($10^{-3}cm^2sec^{-1}$) of snow

Density ($g\ cm^{-3}$)	Van Dusen (1929) *	Devaux (1933) *	Weller & Schwerdtfeger (1968)	
			T = 0°C	T = -50°C
0.11	0.167	0.155	-	-
0.125	0.186	0.179	-	-
0.24	0.363	0.473	-	-
0.45	0.979	1.481	1.25	1.63
0.50	-	-	1.59	2.10
0.60	-	-	2.59	3.42
0.70	-	-	3.68	4.85
0.80	-	-	4.65	6.06
0.917	-	-	5.35	7.10

* Dorsey, 1940, p. 483.

Table 9. Observed amplitude attenuation of soil temperatures with depth and results of two-term Fourier analysis throughout one half of the annual cycle (May 1971 through December 1971)

			n = 1		n = 2		
Depth (cm)	T_m (cm)	Obs'd (°C)	A_1 (°C)	θ_1 (°)	A_2 (°C)	θ_2 (°)	6 mo. period
(a) Farthest from the stream (column no. I)							
0	0 ± 1°C	22.4	13.02	-25.1	7.10	-47.8	May-Oct
23	"	14.7	13.11	-32.9	6.86	-59.5	May-Oct
53	"	10.9	10.47	-43.3	5.17	-79.9	Jun-Nov
101	"	8.9	8.61	-53.7	3.93	-102.6	Jun-Nov
203	"	5.8	5.40	-70.0	2.63	-139.9	Jun-Nov
300	"	2.4	1.88	-85.8	0.96	-167.4	Jul-Dec
(b) At center of stream (column no. VI)							
0	0 ± 1°C	11.4	9.17	-27.2	4.58	-54.1	May-Oct
29	"	11.1	9.49	-26.6	4.61	-53.2	May-Oct
55	"	9.3	8.42	-29.7	4.31	-61.2	May-Oct
110	"	7.7	7.25	-37.5	3.51	-70.9	Jun-Nov
200	"	4.7	4.45	-69.4	1.76	-79.6	Jun-Nov

The values for thermal diffusivity calculated from these 6-month Fourier coefficients came out slightly less scattered than those from the 12-month analysis, as expected, but some scattering was still present (Table 10) mainly because of the asymmetry of the summer heat pulse into the soil. This asymmetry was present because the warming of the soil was delayed by the latent heat required to melt ice in the soil. In 1971, the air temperature first reached 0°C in April, but positive temperatures did not begin to penetrate the soil until late May (Figs. 21 and 22).

4.2 Numerical models using a step method based on the Fourier Conduction equation

With semi-infinite solids and slabs under uniform boundary conditions, the "x" and "y" terms become zero when the z axis is made perpendicular to the body and thus the Fourier conduction equation (12) reduces to:

$$\frac{dT}{dt} = \alpha \frac{d^2T}{dz^2} . \qquad (19)$$

The body is assumed to be homogeneous and isotropic and is divided into a suitable number of equal layers, each of thickness, Δz, and thermal diffusivity, α.

For each successive time increment, Δt, the change in temperature at each layer is calculated using a step method described in standard text books dealing with heat transfer (e.g. Ingersoll and Zobel, 1954). Briefly, any two adjacent layers, (n) and (n - 1) undergo a temperature change of ΔT during time, Δt, caused by the different temperature

Table 10. Thermal diffusivities ($10^{-3}cm^2sec^{-1}$) of the soil derived from observed amplitude attenuation with depth and Fourier analysis (n = 1, 2) of soil temperatures throughout one half the annual cycle (May 1971 through December 1971)

Depth	Obs'd	n = 1				n = 2			
		Semi-inf. solid		Inf. slab 3.5m	Inf. slab 4.0m	Semi-inf. solid		Inf. slab 3.5m	Inf. slab 4.0m
(cm)	Amp.	Amp.	Phase	Amp.	Amp.	Amp.	Phase	Amp.	Amp.
(a)	Farthest from the stream (column no. I)								
0 - 53	0.5	5.9	2.8	5.03	4.98	5.6	1.8	5.04	5.30
53 - 101	5.6	6.0	7.0	6.52	5.14	6.1	2.8	5.19	5.44
101 - 203	5.6	4.8	12.8	∞	5.22	12.8	2.4	∞	∞
203 - 300	1.2	0.8	12.3	∞	0.75	1.8	8.2	∞	1.64
(b)	At center of stream (column no. VI)								
0 - 55	7.3	41.4	158.0	6.78	6.15	163.0	39.2	∞	∞
55 - 110	8.4	13.5	16.2	∞	10.00	14.3	21.0	∞	13.48
110 - 200	3.3	3.4	2.6	5.05	2.80	3.4	11.8	2.92	3.02

gradients in the two layers: $(T_{n+1} - T_n)/\Delta z$ and $(T_n - T_{n-1})/\Delta z$. Heat flowing through layer, n, is then expressed as:

$$Q_n = \frac{k(T_{n+1} - T_n)}{\Delta z} . \tag{20}$$

Likewise, heat flowing through layer n-1 is:

$$Q_{n-1} = \frac{k(T_n - T_{n-1})}{\Delta z} . \tag{21}$$

The net heat flux into the system is thus:

$$\Delta Q = Q_n - Q_{n-1} = \frac{k(T_{n+1} - 2T_n + T_{n-1})}{\Delta z} . \tag{22}$$

To find ΔT, the alternative expression for ΔQ is given:

$$\Delta Q = \frac{c\rho\ (\Delta z)\ (\Delta T)}{\Delta t} , \tag{23}$$

where: c = specific heat, and

ρ = density of the medium.

Substituting for ΔQ in equation (22), equation (23) yields:

$$\frac{(\Delta z)(\Delta T)}{\Delta t} = \frac{k(T_{n+1} - 2T_n + T_{n-1})}{c\rho\ \Delta z} . \tag{24}$$

Since $\alpha = k/c\rho$ (Eq. (5)), the terms are rearranged to give:

$$\Delta T = \alpha\left(\frac{T_{n+1} - 2T_n + T_{n-1}}{\Delta z^2}\right)\ \Delta t \simeq \alpha \frac{\partial^2 T}{\partial z^2}\, dt. \tag{25}$$

In order to maintain mathematical stability, ΔT cannot exceed the expression:

$$\Delta T \simeq \left(\frac{T_{n+1} + T_{n-1}}{2}\right) - T_n$$

(i.e., the shaded area shown in Fig. 27 must not extend past the dotted line). Thus,

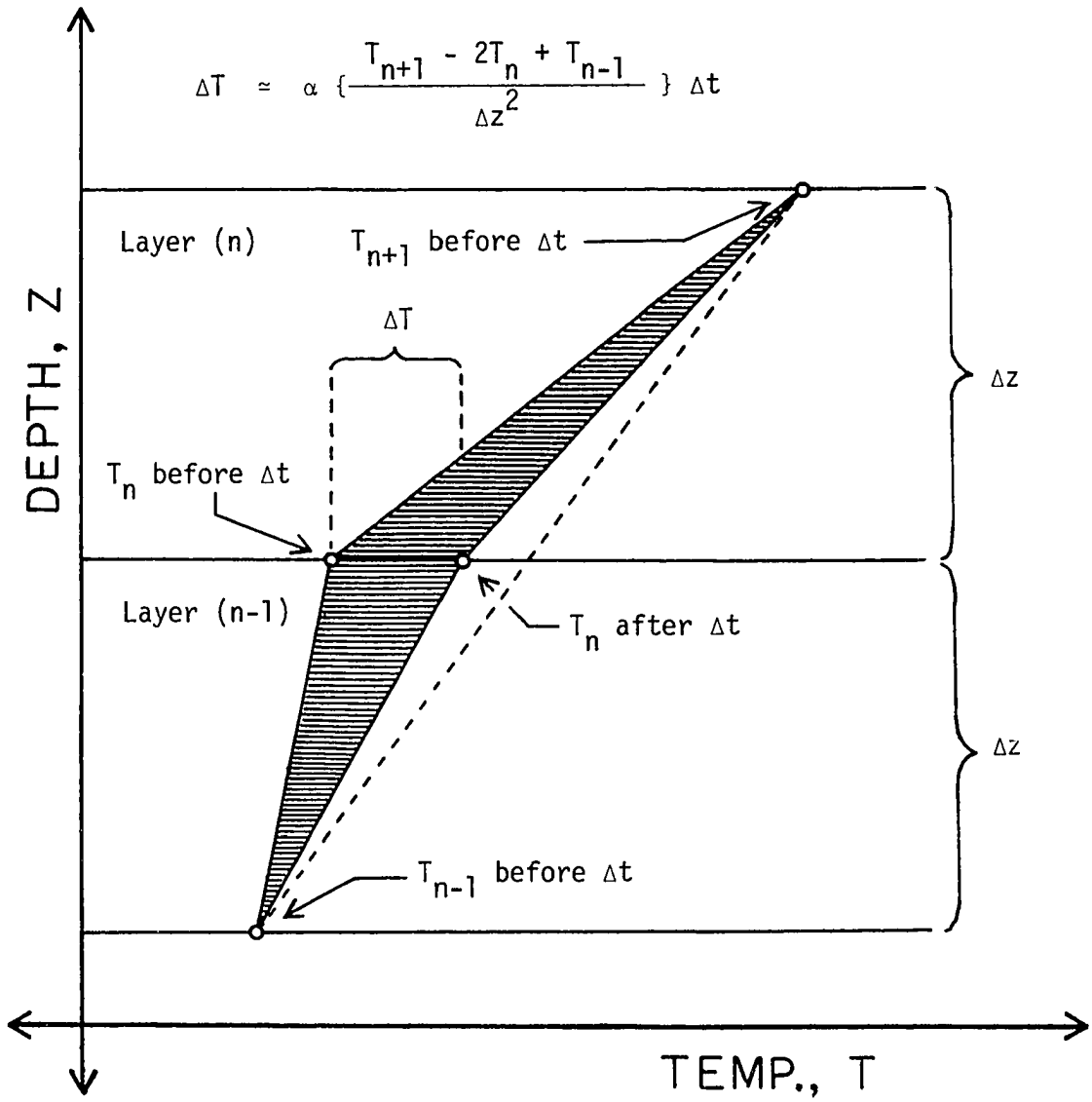

Figure 27. Two layered medium undergoing temperature change as a result of the difference in linear temperature gradients across each of the two layers.

$$\alpha \left(\frac{T_{n+1} - 2T_n + T_{n-1}}{\Delta z^2}\right) \Delta t \leq \left(\frac{T_{n+1} + T_{n-1}}{2} - T_n\right), \qquad (26)$$

or:

$$\alpha \left(\frac{\Delta t}{\Delta z^2}\right) \leq \frac{1}{2} \qquad (27)$$

The increments, Δz and Δt must then be selected to insure that the relationships (26) or (27) hold true throughout the simulation. The usual method of computation, given a known initial depth profile at time, t, and known boundary temperatures at time, $t + \Delta t$, is to calculate ΔT, using equation (25), for every other layer, beginning at the surface and working along z as far as necessary or until the lower boundary is reached. The same procedure is then repeated for the odd numbered layers before going on to the next increment, Δt.

A computer program in FORTRAN IV was written for this study to facilitate the numerous calculations required. Shown in Appendix B, the program was provided with an automatic repetition for various trial values of α, and will stop whenever equation (26) is not satisfied.

4.2.1 Unfrozen soil, October 1970 through December 1970

Using time intervals of 4 days and depth intervals of 50 cm, a series of curves were generated with the aid of the FORTRAN Program, beginning with the known temperature profile of 22 October 1970. Using 0.004 and 0.006 $cm^2 sec^{-1}$ for thermal diffusivity, the soil to 4 meters depth was assumed to be an infinite, homogeneous slab. In Fig. 28, the calculated temperatures at depths, 0.5, 1.0, 2.0 and 3.0 meters are compared with observed temperatures from column no. I, farthest from

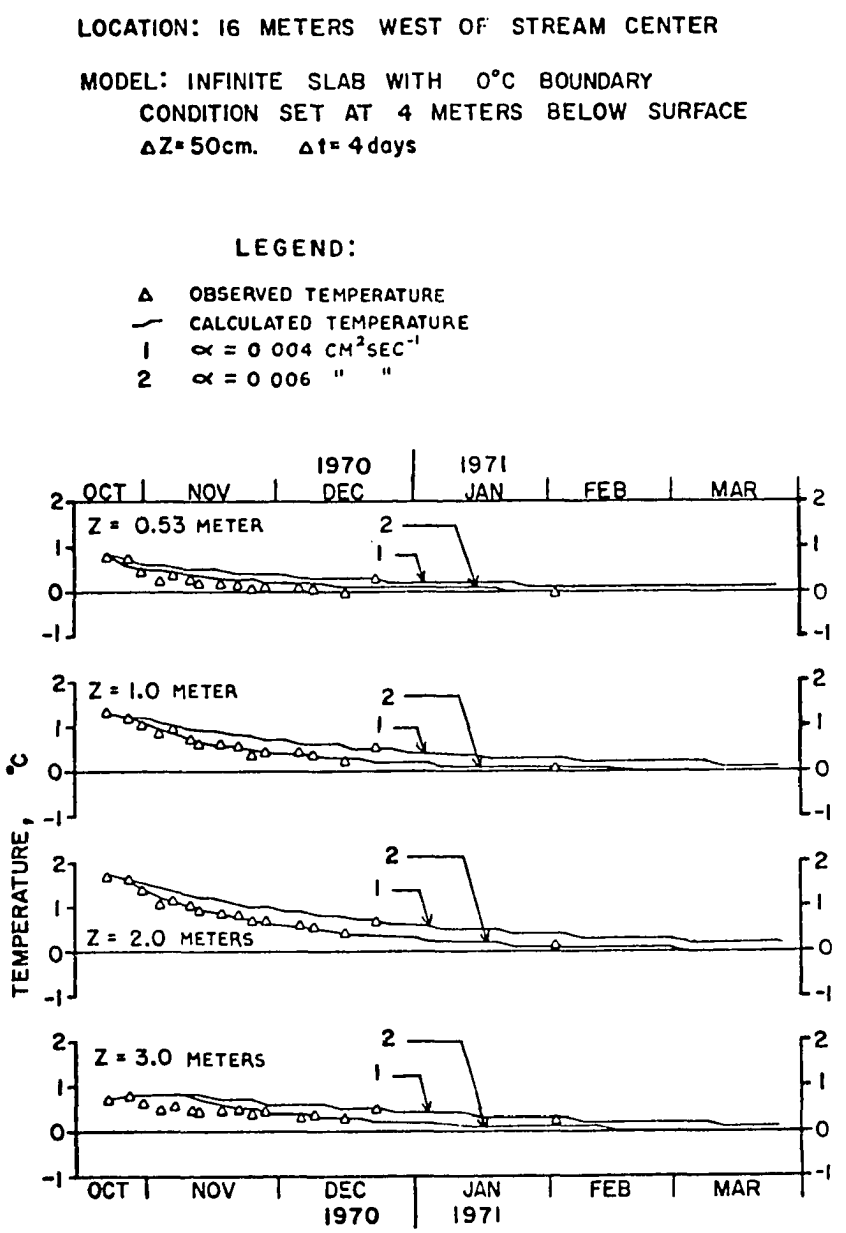

Figure 28. Comparison of observed temperatures in soil at column no. I (16 meters west of stream center) with temperatures calculated by numerical step method, using infinite slab models of thermal diffusivities, 0.004 and 0.006 cm^2sec^{-1}, fall 1970.

the stream. Throughout the three month cooling period, the observed data followed the curve for α = 0.006 cm^2sec^{-1} rather closely at 1 meter and 2 meters, but appeared to reflect higher thermal diffusivities at 0.5 and 3.0 meters.

Since the calculated temperature curves at each depth begin at one point, the spacing between the curves throughout the first several 4-day time periods is small and is not regarded as a significant indicator of the actual thermal diffusivity of the medium.

4.2.2 Unfrozen soil, May 1971 through December 1971

From January through May 1971, the temperature changes in the soil, both beneath and adjacent to the stream, were too slight for determining, but with the summer heat pulse during the remainder of 1971, the FORTRAN program was repeated using thermal diffusivities of 0.004 and 0.006 cm^2sec^{-1} farthest from the stream (Fig. 29) and 0.008, 0.010, and 0.012 cm^2sec^{-1} beneath the stream (Fig. 30).

(1) Column no. I, 16 meters west of the stream center: By successive approximations infinite slab models were used of the soil down to 3.5 and 4.0 meter depths. The observed temperatures followed the hypothetical slab temperatures with a diffusivity of 0.004 cm^2sec^{-1} during the first half of the summer, rose to 0.006 cm^2sec^{-1} during late summer, but fell back to 0.004 cm^2sec^{-1} by late fall of 1971. The temporary increase in diffusivity could have been due to additional heat transfer by water movement throughout the saturated soil. As discussed in Chapter 5, this was especially prominent at 2 meters depth.

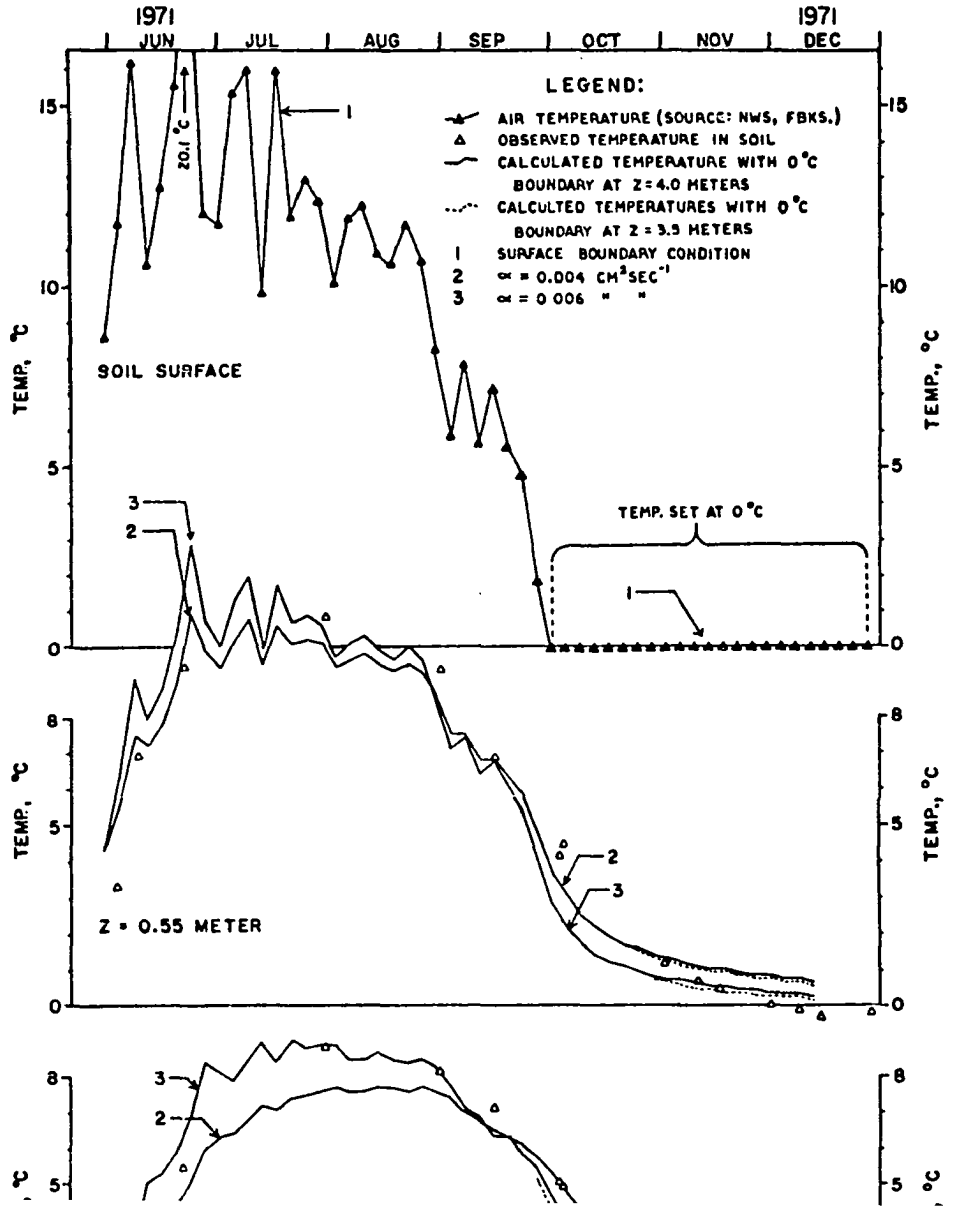

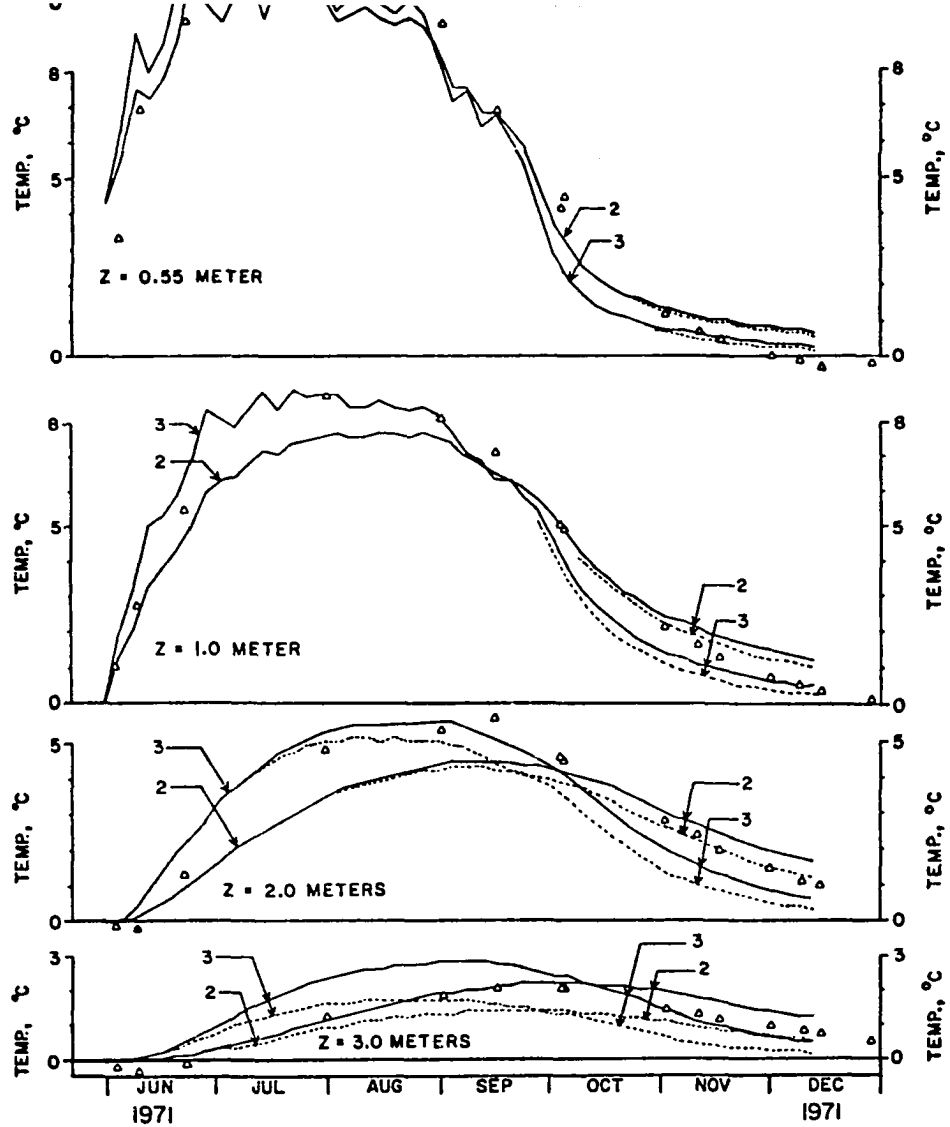

Figure 29. Comparison of observed temperatures in soil at column no. I (16 meters west of stream center) with temperatures calculated by numerical step method, using infinite slab models of thermal diffusivities, 0.004 and 0.006 $cm^2 sec^{-1}$, summer and fall 1971.

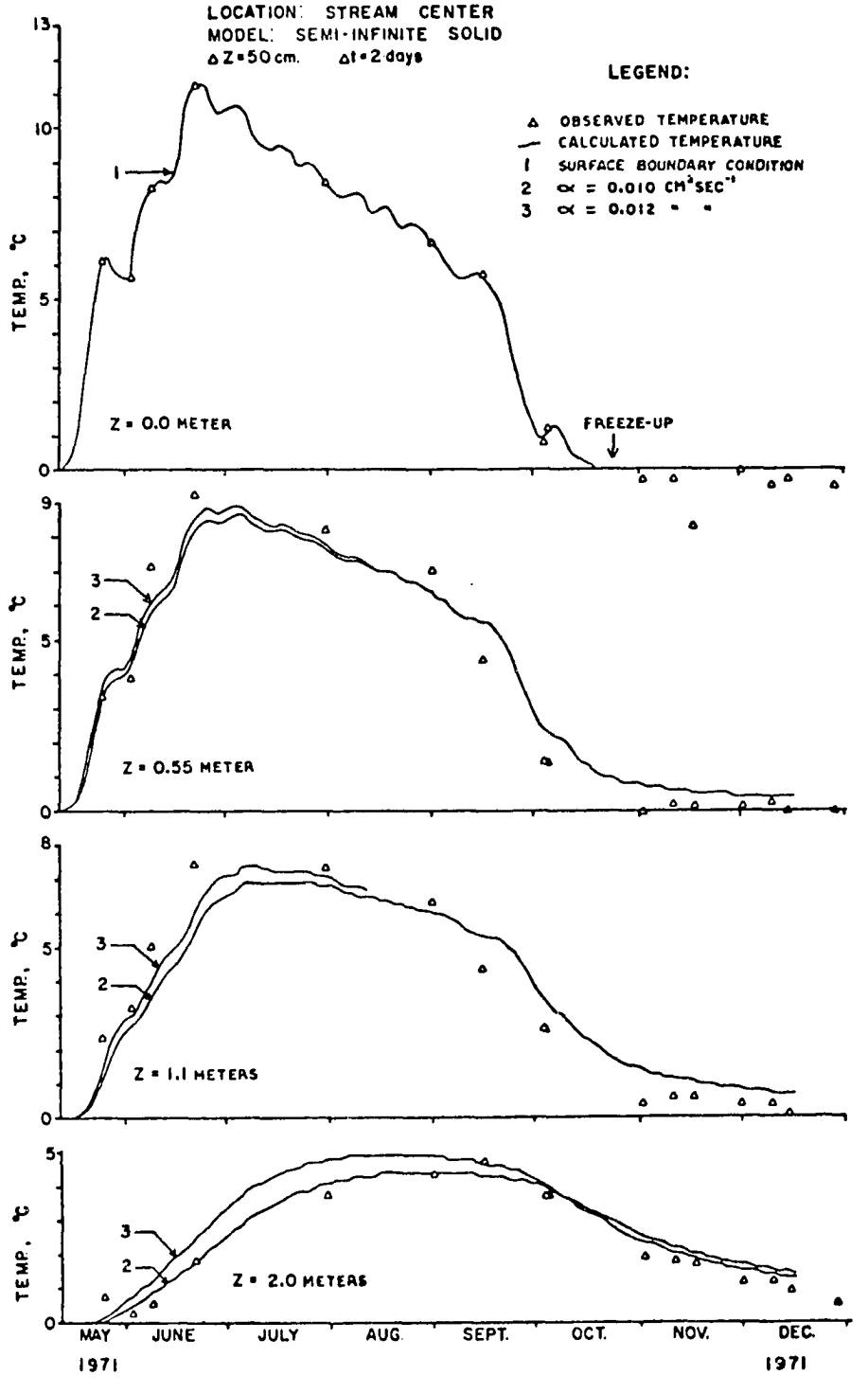

Figure 30. Comparison of observed temperatures in soil at column no. VI (beneath stream center) with temperatures calculated by numerical step method, using semi-infinite models of thermal diffusivities, 0.008, 0.010, and 0.012 cm^2sec^{-1}, summer and fall 1971.

The difference between the 3.5 meter and 4.0 meter slab models is not noticeable in the upper meter of soil, but at a depth of 3 meters, the difference was considerable. In Fig. 29, the data followed the 4.0 meter model temperature curve through September, but fell toward the 3.5 meter model curve from October through December (α = 0.004 cm^2sec^{-1}).

(2) Column no. VI, beneath the stream center: Using a semi-infinite solid as the model, the temperature curves generated at 0.5, 1.0, and 20 meter depths show the thermal diffusivity in the sediments to be considerably higher than away from the stream. Using time intervals of two days to insure mathematical stability, the upper meter of soil exceeded values of α of 0.012 cm^2sec^{-1} while at 2 meters depth, the observed temperatures were generally lower than those generated with a diffusivity of 0.008 cm^2sec^{-1} (Fig. 30). These high values for α, once again, were probably caused by additional heat transfer due to water movement, as discussed in Chapter 5.

4.3 Differential analysis using the Fourier conduction equation

This approach is similar to the numerical method discussed above in that the Fourier conduction equation (Eq. (19)) is used, but in this case, the thermal diffusivity, α, is derived directly from the data by numerically determining the double derivative of the temperature with respect to time, and taking the quotient of these two values for each depth and time increment.

Thus,

$$\frac{dT}{dt} = \alpha \frac{d^2T}{dz^2} \tag{28}$$

or:

$$\alpha = \frac{\frac{dT}{dt}}{\frac{d^2T}{dz^2}} . \tag{29}$$

In arithmetic form, equation (29) reduces to:

$$\alpha = \frac{\frac{\Delta T}{\Delta t}}{\frac{\Delta^2 T}{\Delta z^2}} = \frac{(T_{n,m+1} - T_{n,m-1})\ (\Delta z^2)}{(T_{n+1,m} - 2T_{n,m} + T_{n-1,m})\ (2\Delta t)} , \tag{30}$$

where n and m are the subscripts for the depth increment, Δz, and time increment, Δt, respectively.

The depth and time increments are made small enough to resolve large changes in the temperature derivatives, yet large enough to avoid an unnecessary number of computations.

Assuming α is constant throughout several layers of Δz, equation (30) can be integrated with respect to depth ($z_p \leq z \leq z_q$), given the temperature gradients at z_p and z_q. Thus, at time, m:

$$\Delta Q = k\ (\frac{\Delta T_{q,m}}{\Delta z})_z - (\frac{\Delta T_{p,m}}{\Delta z})_z = c\rho \sum_{n=p}^{n=q} (\frac{\Delta T_{n,m}}{\Delta t})_t\ \Delta z , \tag{31}$$

or:

$$\alpha = \frac{k}{c\rho} = \frac{\sum_{n=p}^{n=q} (\Delta T_{n,m})_t\ (\Delta z)^2}{(\Delta T_{q,m})_z - (\Delta T_{p,m})_z\ (\Delta t)} , \tag{32}$$

and

$$\alpha = \frac{\Delta z^2 \sum_{n=p}^{n=q} (T_{n,m+1} - T_{n,m-1})}{\Delta t\ (T_{q+1,m} - T_{q-1,m} - T_{p+1,m} + T_{p-1,m})} , \tag{33}$$

where p and q are subscripts for the bottom and top layers, respectively.

Throughout the above derivations, the heat transfer mechanism was assumed to be conduction only. The addition of extra terms to account for non-conductive heat transfer mechanisms is discussed in Chapter 5.

4.3.1. Unfrozen soil, October 1970 through November 1970

With the onset of freezing at the surface, this period was marked by a gradual cooling of the soil from 1.7°C to 1.1°C (beneath the stream). The expressions, $\Delta T/\Delta t$ and $\Delta^2 T/\Delta x^2$, were determined graphically from temperature versus time curves (Figs. 21 and 22) and from temperature versus depth profiles, using depth intervals of 20 cm and time intervals of 5 days. α was then derived by using equation (30), and the results are shown in Table 11.

Although the measured temperature differences were small, the data coverage was good, and smoothing of the numbers gave diffusivity values of about 0.003 $cm^2 sec^{-1}$ throughout the upper 2.0 meters of soil away from the stream. Beneath the stream, however, the values came out much more scattered, ranging from 0.002 to 0.005 $cm^2 sec^{-1}$ (below the depth of 1 meter), while in the upper meter of sediments, they were totally meaningless, due to a reversal in the expected curvatures of the temperature profiles, thus implying negative values of diffusivity. For example, with heat obviously leaving the soil, as shown by negative values for $\Delta T/\Delta t$, the corresponding values for $\Delta^2 T/\Delta x^2$ should have also been negative to yield positive values for α. In other words, a temperature profile, under these conditions should have been convex

Table 11. Thermal diffusivities ($10^{-3}cm^2sec^{-1}$) of the soil derived by differential analysis of soil temperatures from column no. I (16 meters west of stream center) and column no. VI (beneath stream center), November 1970 and June 1971

	1 - 30 November 1970		30 May - 28 June 1971	
Depth (cm)	Stream bank	Stream center	Stream bank	Stream center
0	-	-	-	16.9
20	-	-	1.6	16.9
40	3.36	∞	2.8	23.7
60	2.90	∞	3.6	266.2
80	2.90	∞	4.6	∞
100	2.92	5.25	4.5	∞
120	3.03	2.53	3.5	∞
140	3.08	2.22	3.6	∞
160	3.05	2.63	3.8	6.1
180	3.07	2.90	4.3	1.2
200	3.32	2.85	5.2	0.8
220	3.33	-	4.7	-
240	3.17	-	6.0	-
260	2.93	-	6.0	-
280	2.40	-	-	-
300	1.60	-	-	-

toward the direction of increasing temperatures. As shown in Figure 31, they were obviously curved the opposite way at about 1 meter depth. This suggests either the inapplicability of equations (29) and (30) on account of heat transfer mechanisms other than conduction, or else the thermocouple probes in the upper meter of soil were all reading too high.

Throughout October and November, water was observed beneath the ice; thus, it is reasonably correct to fix the bottom surface temperatures at 0°C, as shown in Fig. 31b.

Due to the errors involved with measuring small temperature changes, however, the derivation of accurate data was impossible; thus, the values for α shown in Table 11 are uncertain. To help rule out the possibility of the anomalous results being due solely to erroneous data, the analysis was repeated for the larger and more accurate temperature changes during the following June.

4.3.2. Unfrozen soil, June 1971

This period was marked by rapid penetration of heat into the soil with surface temperatures increasing from 9.2°C to 19.5°C (farthest from the stream) and from 6.0°C to 11.1°C (beneath the stream) throughout the thirty day period from 27 May to 26 June 1971.

Using 20 cm depth intervals and five day time intervals, the same graphical procedure used above was employed to yield values for thermal diffusivity ranging from about 0.0020 at the surface to 0.0060 $cm^2 sec^{-1}$ at a depth of 260 cm farthest from the stream (Table 11), which were up to twice as high as those during October 1970.

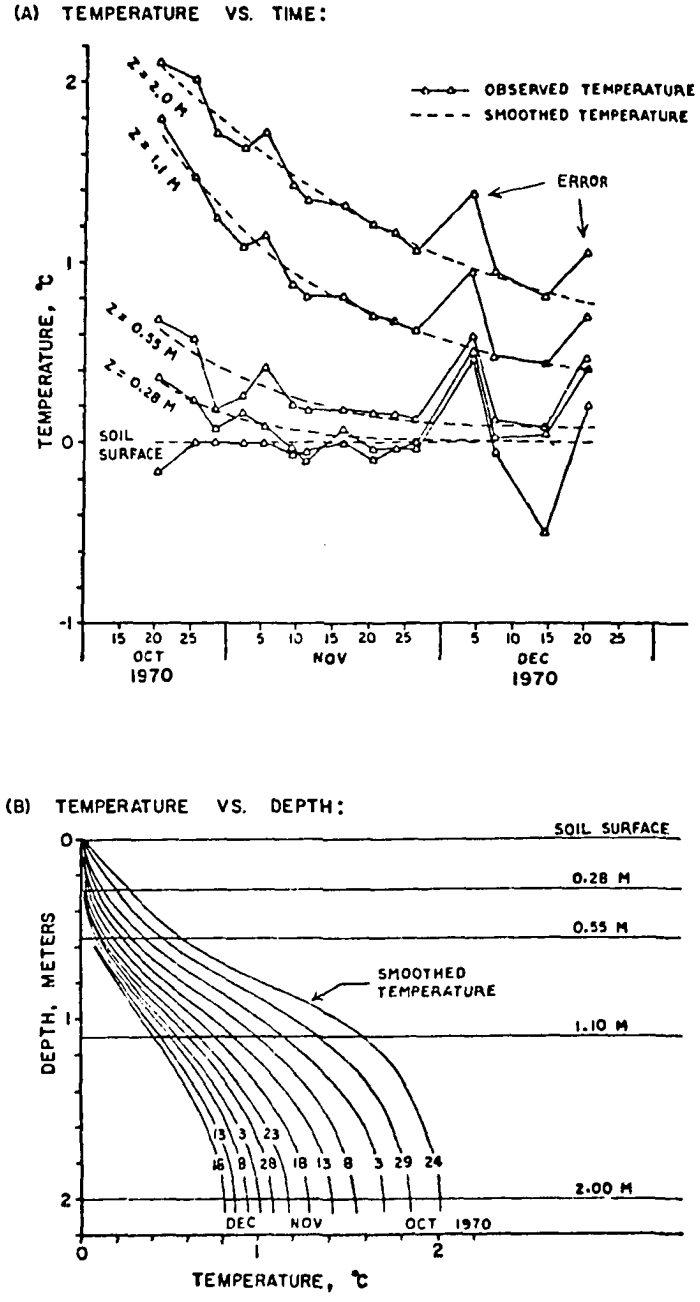

Figure 31. Soil temperatures at column no. I, 16 meters west of stream center. (a) observed temperature versus time. (b) smoothed temperature versus depth. 22 October through 21 December 1970.

Beneath the stream, however, the values were meaningless for the most part just as they were during October 1970, due once again to inflection points in the temperature versus depth profiles. Since heat was obviously penetrating the soil, the curves should have been concave in the direction of increasing temperature, but as shown in Fig 23, they were curved in the opposite way in the upper 1.5 meters of the soil (e.g., 3 June 1971). Below 1.5 meters, however, the values were plausible, even though scattered.

A sample calculation sheet is included (Table 12) showing the smoothed values for temperature and derived diffusivity for each depth and time increment. Use of equation (33) gave an average diffusivity of 0.0056 cm^2sec^{-1} from 1.0 to 3.0 meters throughout a twenty day time period (4 through 13 June 1971).

4.4 Summary of analysis

The three methods for determining thermal diffusivity of the soil, described in the previous three sections, were all based on the assumption that conduction was the only means of heat transfer. As shown in Table 13, all three methods were effective for the soil temperatures at column no. I, farthest from the stream, but at column no. VI, beneath the stream, the thermal diffusivities scattered widely and were generally an order of magnitude higher in the upper one meter of sediments than elsewhere throughout the soil cross-section. The average value throughout the upper 3 meters of soil was 4.9 cm^2sec^{-1}.

Table 12. (a) Smoothed soil temperatures versus depth from thermocouple column no. I using 20 cm depth intervals and 5-day time intervals from 25 May 1971 through 28 June 1971. (b) Thermal diffusivities ($10^{-3}cm^2sec^{-1}$) calculated from (a) by differential analysis using Fourier conduction equation

Depth (cm)	25-29 May	30 May 03 June	04-08 June	09-13 June	14-18 June	19-23 June	24-28 June	
(a)	Soil Temperature (°C)							
0	9.22[1]	9.06[1]	14.61[1]	14.39[1]	12.56[1]	17.00[1]	19.50[1]	
20	2.00	4.95	9.50	11.35	11.35	12.90	14.10	
40	0.60	3.05	6.40	8.65	9.60	10.30	11.15	
60	0.10	1.90	4.35	6.40	7.65	8.25	9.10	
80	0.03	1.12	3.95	4.60	5.90	6.65	7.50	
100	-0.11	0.60	1.85	3.10	4.35	5.28	6.20	
120	-0.11	0.25	0.95	1.93	3.05	4.13	5.10	
140	-0.11	0.05	0.30	1.10	2.08	3.15	4.25	
160	-0.11	-0.02	0.05	0.50	1.40	2.33	3.45	
180	-0.11	-0.06	-0.05	0.07	0.85	1.66	2.70	
200	-0.11	-0.09	-0.14	-0.13	0.45	1.13	2.05	
220	-0.10	-0.11	-0.17	-0.20	0.19	0.72	1.45	
240	-0.10	-0.13	-0.19	-0.25	0.05	0.41	0.95	
260	-0.09	-0.15	-0.21	-0.28	-0.10	0.17	0.55	
280	-0.09	-0.16	-0.23	-0.29	-0.20	-0.02	0.25	
300	-0.08	-0.17	-0.25	-0.30	-0.27	-0.18	-0.01	
(b)	Thermal diffusivity ($10^{-3}cm^2sec^{-1}$)							Avg.
0	-	-	-	-	-	-	-	-
20	-	1.6	1.6	2.6	1.3	0.7	-	1.6
40	-	3.6	2.4	3.3	3.8	1.1	-	2.8
60	-	5.3	3.3	3.4	4.3	1.5	-	3.6
80	-	5.2	5.4	4.5	4.8	3.3	-	4.6
100	-	5.0	5.8	3.4	4.0	4.2	-	4.5
120	-	2.8	3.2	3.2	3.1	5.3	-	3.5
140	-	-	1.2	3.8	3.3	5.9	-	3.6
160	-	-	1.6	3.7	3.4	6.3	-	3.8
180	-	-	-	1.8	4.9	6.1	-	4.3
200	-	-	-	-	4.2	6.2	-	5.2
220	-	-	-	-	3.6	5.8	-	4.7
240	-	-	-	-	-	6.0	-	6.0
260	-	-	-	-	-	6.0	-	6.0
280	-	-	-	-	-	-	-	-
300	-	-	-	-	-	-	-	-

[1] Surface temperature taken from National Weather Service data (Fairbanks International Airport). Five-day average reduced by 3.0°C to account for cooler conditions in Goldstream Valley.

Table 13. Summary of results from three methods employed for determining thermal diffusivity ($10^{-3}cm^2sec^{-1}$) of the soil (a) away from stream and (b) beneath stream

Depth (cm)	Method I Fourier Analysis 12 month (Table 5) Range	Mean	Method I Fourier Analysis 6 month (Table 7) Range	Mean	Method II Numerical Analysis (Figs. 26-28) Range	Mean	Method III Differential Analysis (Table 9) Range	Mean
(a) Column no. I, 16 meters from stream center								
0 - 50	0.5-7.4	3.8	0.5-5.6	4.1	4 - 7	5.5	1.6-3.4	2.7
50 - 100	3.3-6.4	5.1	2.8-7.0	5.5	4 - 6	5.0	2.9-4.6	3.5
100 - 200	4.5- ∞	9.0*	2.4- ∞	7.3*	4 - 6	5.0	2.9-5.2	3.5
200 - 300	0.7- ∞	3.8*	0.8- ∞	3.8*	4 - 6	5.0	1.6-6.0	4.0
(b) Column no. VI, at stream center								
0 - 50	2.4- ∞	27.8*	6.2- ∞	60.3*	10-16	13.0	25.0- ∞	25.7*
50 - 100	8.6- ∞	19.7*	8.4- ∞	13.8*	12-16	14.0	5.2- ∞	17.0*
100 - 200	1.3-3.4	2.5	2.6-11.8	4.2	8-10	9.0	0.9- ∞	2.3*

* Average of non-infinite numbers only.

In summary, the Fourier analysis was made, treating the conducting medium as a semi-infinite, homogeneous medium and solving for α by using the amplitude attenuation and phase lag with depth of the temperature cycle. Infinite slab models of the soil to depths of 3.5 and 4.0 meters were also used to account for a possible, lower 0°C boundary. Due to the disturbance of the sinusoidal shape of the temperature cycle by the insulating snow cover on the banks and the multilayered system of snow, ice and water in the stream bed, the analysis was repeated using only the summer half wave. Although the scattering of the diffusivity values was reduced somewhat (in the stream center), the secondary amplitudes (n = 2) were still relatively important and the warm temperature pulses were asymmetrical due to the seasonal lag in their penetration into the soil.

To completely eliminate the winter disturbance of the temperature cycles and to gain better control over initial temperature boundary conditions, numerical step models, employing the Fourier conduction equation were used, assuming various test values for α and comparing calculated temperatures (using the FORTRAN program) with observed temperatures. Although the observed data from summer 1971 were scattered about any one theoretical curve, the unfrozen soil to 3.5 and 4.0 meters depth generally behaved as an infinite slab away from the stream and as a semi-infinite solid beneath the stream. For each depth range, the soil was assumed to have the same thermal diffusivitiy throughout its entire thickness. This method, unlike the Fourier method, indicated the variation of the thermal diffusivity through time.

To resolve changes in thermal diffusivity with depth as well as through time, a third method was employed, which entailed the graphical determination of d^2T/dz^2 and dT/dt, for various depth and time increments, the calculation of α directly, using the Fourier conduction equation. This proved to be the most effective of the three methods away from the stream, where reliable values of α were obtained with the least amount of scatter. In the stream center however, the assumption of conduction being the sole means of heat transfer had serious limitations as shown by the anomalous curvatures of the observed temperature versus depth profiles (Figs. 23 and 31). Estimates of the thermal diffusivity were based solely on the first two methods in this case.

Due to the importance of snow as an insulator for the soil, several attempts were made to determine its diffusivity. Freshly fallen snow, according to Fourier analysis of temperatures throughout a two day period, ranged from 0.003 to 0.006 cm^2sec^{-1} with a mean of 0.004 cm^2sec^{-1}.

In summary, factors affecting the effective thermal diffusivity and in turn, modifying the temperature pattern in the soil away from the stream are: (1) insulation by the snow, (2) latent heat exchanges due to soil freezing and thawing, and (3) presence of permafrost. Beneath the stream, on the other hand, the main factors include: (1) insulation by ice and snow, (2) overflows, (3) latent heat exchanges due to freezing and thawing of the aufeis and soil and (4) heat transfer by water movement through the soil.

In addition to the scattering of the thermal diffusivities by the various influencing factors mentioned above and discussed in Chapter 5,

it is important to note that some of the scattering was also due to observational, instrumental, and interpretive errors. For example, diurnal fluctuations of air and water temperatures have undoubtedly caused some of the data points in the surface layers of the soil to be nonrepresentative. For instance, a daily fluctuation of $\pm$ 10°C at the surface causes a change of 10 $\exp(-50\sqrt{n\omega/2\alpha})$ or $\pm$ 0.85°C at a depth of 50 cm, assuming that thermal diffusivity α = 0.005 cm^2sec^{-1}, n = 1, and $\omega = 2\pi\ day^{-1}$. For this reason (elimination of diurnal temperature fluctuations), the temperature curves at 0.2 meters were ignored throughout this analysis.

Also, as indicated earlier, the accuracy of the potentiometer/thermocouple network was estimated to be $\pm$ 0.3°C, provided that the ice bath was uniformly at 0°C. Slight warming of the ice bath with the resulting increase in the reference temperature was probably the cause of the apparent dip in temperature (about -0.5°C) at 2.0 meters depth during June 1971 (Figs. 21 and 22). Finally, there was some subjectivity involved in the interpolation and smoothing of the temperature curves. By nature, an analysis of temperature data to find the thermal diffusivity is such that a small perturbation in the data causes a large scattering of the diffusivity values, especially with small temperature changes.

In spite of these obstacles, the general pattern has emerged that the thermal diffusivities are much higher in the stream bed and the various factors responsible for this are discussed in the next chapter.

CHAPTER 5

DISCUSSION AND CONCLUSIONS

The results from Chapter 4 show the difficulty of determining the thermal characteristics of a sub-arctic stream bed where conditions of pure conduction in a homogeneous, infinite medium do not apply. In this case, one must consider non-conductive effects and the nonhomogeneous nature of the layered medium, in which the heat transfer takes place.

Non-conductive effects include: (1) latent heat exchanges in the soil and at the ice/water interface, (2) mass transfers, such as groundwater movement, absorption of rainwater, and air convection through the soil, and (3) radiation through the ice, snow, and water. Also important is the vertical displacement of medium boundaries, such as (1) snow accumulation and ablation, (2) changes in depth of freezing in soil and water, and (3) stream overflows, which periodically remove the insulating snow cover from the aufeis.

These and other factors which affect the thermal regime around the stream bed are now discussed.

5.1 Thermal parameters of the soil

Due to the great variation in soil type, texture, and composition, published values for thermal diffusivity, specific heat, and thermal conductivity show variation over a large range. A few generalizations, as they pertain to the low-organic silt in Goldstream valley, nevertheless, are as follows.

5.1.1 Unfrozen soil

(1) Thermal diffusivity, α, and moisture content, w: The determination of α from the temperature data, using three different methods, is discussed in Chapter 4, and the values derived are summarized in Table 13. Generally, α was found to increase with depth from about 0.002 cm^2sec^{-1} at the surface to 0.006 cm^2sec^{-1} at 3 meters, which compares favorably with values in the literature (Table 14).

The main factor affecting α is moisture content. For example, Kersten (1952, p. 169) cites a 50% increase in α for average soil when moisture is increased from 0 to 15%. The grey colored silt at the Goldstream site is saturated with moisture, and drill data from the Alaska Department of Highways show moisture content ranging from 37% to 75% by dry weight. Silts of such a high moisture content are above the liquid limit, as attested by the ease with which the thermocouple holes were established by ramming with the steel rod. The very high percentages were from samples either of high organic content (top soil) or in a frozen state containing ice lenses. A representative moisture content for unfrozen silt of low organic content ($\leq$ 10%) in Goldstream valley is then considered to be 50 $\pm$ 5% by dry weight (Alaska Department of Highways, 1974).

In addition to moisture content, the dry density, ρ_d, and dry specific heat, c_d, of the soil are equally important in determining the thermal diffusivity.

Table 14. Thermal parameters of the soil: comparison of values estimated at Goldstream Creek with those published in the literature

Type and Location	Moisture Content (% of dry wt.)	Wet Density ρ_m g cm^{-3}	Wet Specific Heat, c_m cal $g^{-1}°C^{-1}$	Thermal Diff. α $10^{-3}cm^2sec^{-1}$	Thermal Cond. k $cal(10^{-3}cm^2sec°C)^{-1}$	Reference
Sandy clay	15	0.78	0.33	3.7	2.2	Ingersoll & Zobel (1954)
Wet sand	-	1.7-2.3	0.2-0.6	4-10	2-6	Geiger (1965)
Wet clay	-	1.7-2.2	0.3-0.4	6-16	2-5	Geiger (1965)
Dry sand	0	1.4-1.7	0.1-0.4	2-5	0.4-0.7	Geiger (1965)
Dry clay	0	-	0.1-0.4	0.5-2.0	0.2-1.5	Geiger (1965)
Fai. silt/loam (at 0°C)	0	-	0.17	-	-	Kersten (1952)
Average soil	-	2.5	0.19	4.6	2.3	Carslaw & Jaeger (1959)
Pure ice (0°C)	-	0.917	0.49	11.8	5.35	Dorsey (1940)
Snow	-	0.2	0.49	3.0	0.3	Dorsey (1940)
Silt at CRREL permafrost tunnel, Fairbanks						
Wet silt	32-139	1.2-1.8	-	-	-	Sellmann (1972)
Dry silt	0	0.5-1.4	-	-	-	Sellmann (1972)
Saturated silt at Goldstream						
West bank:						
Surface	50±5*	1.7**	0.45**	2.0	1.5**	-
Z = 3 m	50±5	1.7**	0.45**	6.0	4.6**	-
Stream bed:						
Surface	50±5	1.7**	0.45**	15	11**	-
Z = 2 m	50±5	1.7**	0.45**	6	5	-
Frozen silt	50±5	1.6**	0.28**	-	-	-

* Alaska Department of Highways, 1974.
** Estimated.

(2) Density: Soil consists of three basic ingredients: solid particles, water, and air. Due to the negligible weight of air, the density of moist soil, ρ_m, is:

$$\rho_m = \rho_d (1 + w), \text{ (after Geiger, 1965, p. 28),} \tag{34}$$

where ρ_d = dry density, and w = moisture content (percent of dry weight/100). Equation (34) implies that the volume concentration of solid particles remains the same while the water fills available pore space between the particles. Assuming this, the amount of pore space, V_v, is:

$$V_v = 1 - \frac{\rho_d}{\rho_s}, \tag{35}$$

and the saturation moisture content, W_{max}, can be shown to be:

$$W_{max} = \frac{\rho_w(\rho_s - \rho_d)}{\rho_s \rho_d}, \tag{36}$$

where ρ_w = density of water and ρ_s = density of the solid particles.

The wet or dry density of the silt at Goldstream Creek was not measured; however, Sellmann (1972) gives an average value of 0.87 g cm^{-3} for the dry density of silt at the CRREL permafrost tunnel (near Fairbanks, Alaska), but this seems very low. Taking a value of 2.6 g cm^{-3} for ρ_s at Goldstream (Alaska Department of Highways, 1974) the pore space, V_v, would have to be 67% which reflects particle bridging higher than that expected at Goldstream. For the silt to be saturated at W_{max} = 50%, the dry density would have to be 1.1 g cm^{-3}, which seems more reasonable. By equation (34), the wet density of the silt is then considered to be:

$$\rho_m = 1.7 \text{ g cm}^{-3}.$$

(3) Specific heat: A characteristic value of specific heat for soil is 0.19 or 0.20 cal $g^{-1}°C^{-1}$ (Kersten, 1952, p. 161). The value for Dry Fairbanks silt loam is 0.164 (at -18°C), increasing linearly to 0.194 (at 60°C). For fine quartz sand, Baver (1948, p. 296) cites 0.192 cal $g^{-1}°C^{-1}$. The most important factor affecting specific heat is moisture, and for wet soil, the specific heat given by Kersten (1952, p. 162) is:

$$c_m = \frac{(c_d + w)}{(1 + w)}, \tag{37}$$

where: c_d = specific heat of dry soil.

The silt at Goldstream valley is considered to have the same dry specific heat as that of Fairbanks silt loam:

$$c_d = 0.17 \text{ cal } g^{-1}°C^{-1} \text{ (at 0°C)}$$

thus giving $c_m = 0.45$ cal $g^{1}°C^{-1}$ with a 50% moisture content.

(4) Thermal conductivity: From equation (5), thermal conductivity for wet soil is derived from the thermal diffusivity that was determined from the temperature data in Chapter 4. Also, using equations (34) and (35):

$$k_m = \alpha c_m \rho_m = \alpha \rho_d (c_d + w). \tag{38}$$

For silt with 50% moisture, a representative value for thermal conductivity would thus be equal to $(\alpha c_m \rho_m)$ or $\alpha(0.45)(1.7) = (0.76)\alpha$. Estimated values for α, ρ_m, c_m, and k_m at the study site are shown in Table 14 and are compared with values published elsewhere.

5.1.2 Frozen soil

(1) Thermal diffusivity: The data are not sufficient for the direct determination of thermal diffusivity of frozen soil by the methods outlined in Chapter 4, but it is known that the thermal diffusivity of frozen soil is genrally higher than for unfrozen soil. Opposing this tendency is the gradual reduction of moisture in the uppermost layers throughout the winter, due to mass transfer of water into the overlying snow. Trabant (1970, p. 33) observed a moisture reduction in the top 10 cm of soil which was between 25 and 30% in October through November, but only 7 to 9% in March at the Experimental Farm site, University of Alaska.

(2) Density: The effect of freezing on soil density is relatively small. For saturated soil, the density decreases since the density of pure ice (ρ_i = 0.917) is less than that of water. The density, ρ_f, for frozen soil can be given as:

$$\rho_f = \rho_d (1 + 0.917\ w). \tag{39}$$

(3) Specific heat: Likewise, the specific heat of moist soil decreases upon freezing. By substituting the specific heat of ice, 0.5 cal $g^{-1}{}^{\circ}C^{-1}$, in equation (35),

$$c_f = \frac{(c_d + 0.5\ w)}{(1 + w)}\ , \text{(Kersten, 1952).} \tag{40}$$

(4) Thermal conductivity: According to Kersten (1948 and references), freezing does not produce any change in k for dry solids, but with moisture contents of up to 12%, fine soils have lower k upon freezing while above 12%, the thermal conductivity is greater than in

the unfrozen state. On the average, for all types of moist soils ($w \geq 12\%$), k increases about 50% upon freezing.

Using expressions, (5), (39), and (40), the thermal conductivity of frozen soil can be approximated by:

$$k_f = \frac{\alpha \rho_d (c_d + 0.5\ w)(1 + 0.917\ w)}{(1 + w)} . \qquad (41)$$

For silt of 50% moisture, the thermal conductivity would equal the thermal diffusivity multiplied by $c_f \rho_f$, which gives $\alpha(0.28)(1.6) = (0.46)\ \alpha$. Values for α, ρ_f, c_f, and k_f are shown in Table 14.

The pattern of heat transfer can be far more complex than the above expressions imply, which assume conduction to be the only transfer mechanism. The literature treats this subject only inadequately. The following are attempts to outline some processes that affect heat transfer in the soil.

5.2 Thermal regime away from the stream

5.2.1 Seasonal snow cover

The effect of the snow cover in retarding the penetration of the winter cold pulse into the soil was ascertained by a check-and-control experiment performed at the Goldstream site by Dr. Benson and Mr. Kreitner in 1967-68. Using the thermocouple network located 8.4 meters from the west bank, the snow was carefully protected from disturbance at Pit no. 1, while at Pit no. 2, the snow was removed from the soil after every snow-fall so that the soil surface remained exposed to the air (Fig. 32).

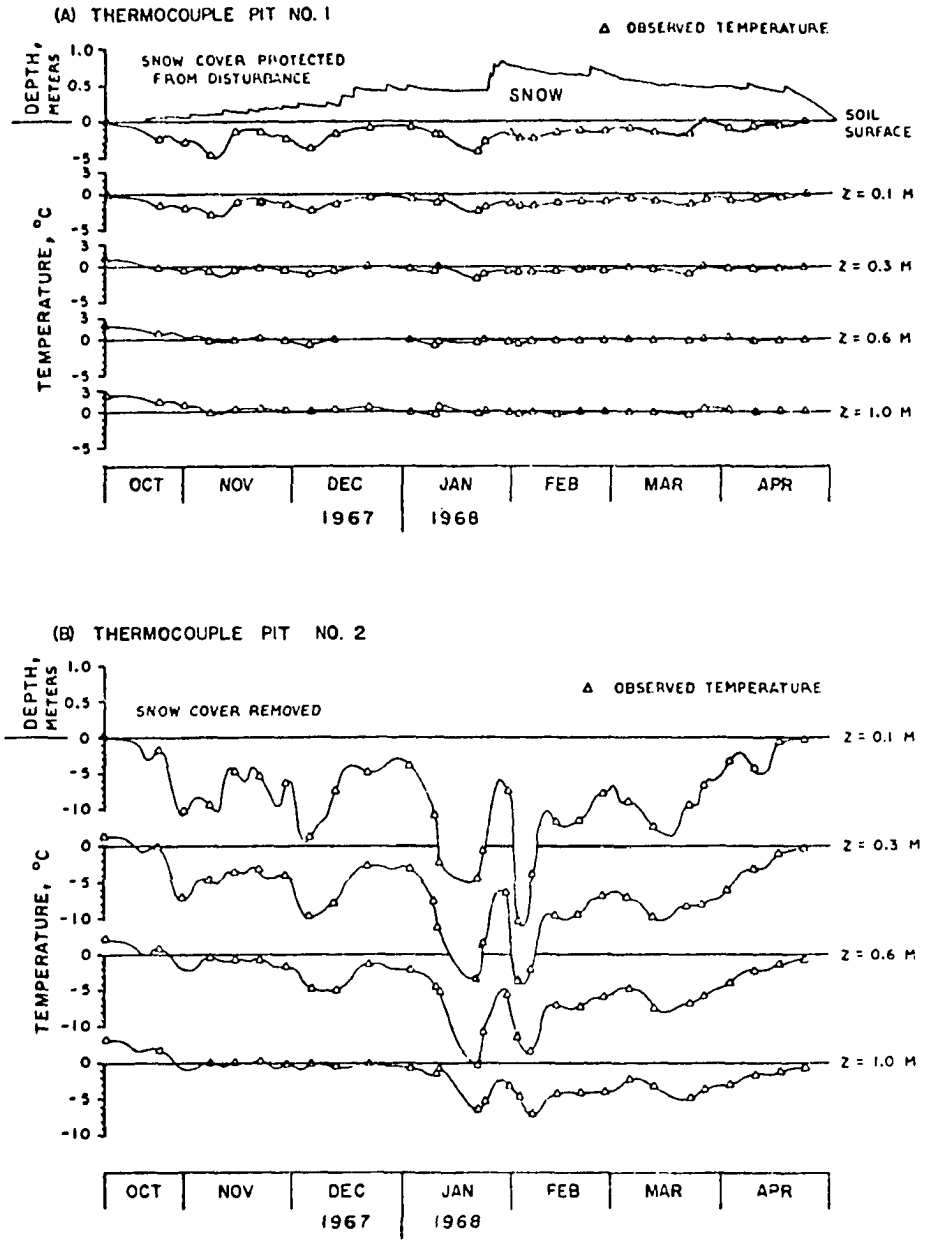

Figure 32. Effect of snow cover on soil temperatures. (a) pit no. 1, beneath snow cover protected from disturbance, and (b) pit no. 2, over which the snow was continuously removed. Winter 1967-68.

Temperature measurements taken throughout the seven month period (9 October 1967 to 24 April 1968) at both pits show the resulting large difference in the amount of cold pulse penetration. Consistently sub-zero air temperatures lasted from 16 October to 21 April, with the lowest daily average temperature of -42°C occurring on 17 January (NWS, Fairbanks).

At pit no. 1 (protected), the snow prevented the ground surface from cooling below -4.5°C (recorded on 8 November) while at 100 cm depth, the temperature always remained above 0°C. At pit no. 2, on the other hand, the surface temperature presumably remained near the ambient air temperature, while at 10 cm and 100 cm depth, the minimum recorded temperatures were respectively -25.2°C (3 February) and -7.1°C (7 February).

The effect of the snow is further shown in Fig. 33 with a selection of three sets of temperature-depth profiles. The high insulation value of the snow is evidenced by the large temperature gradients.

5.2.2 Soil freezing

Due to the high latent heat of fusion of ice (79.67 cal g^{-1}), the moisture in the soil acts as a large heat reservoir which, along with the snow cover, helps to retard the penetration of the winter cold pulse (Fig. 32).

Obviously the use of equations (15) and (16) had its limitations since only conduction was assumed. Thus, by acting as a barrier to

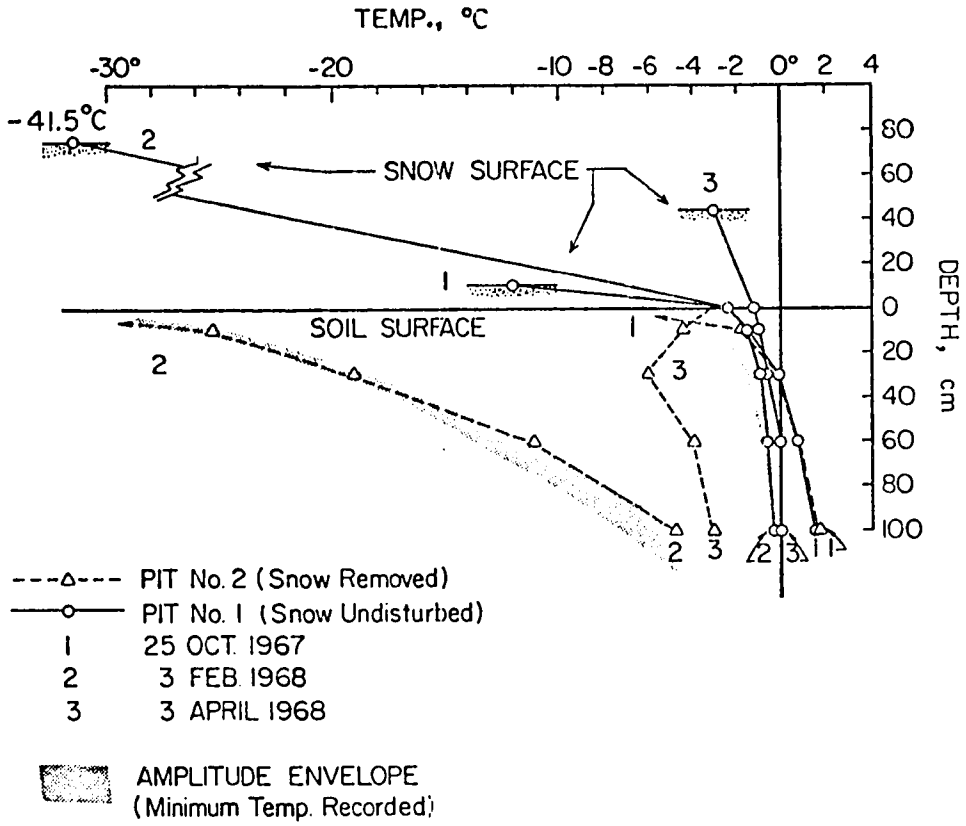

Figure 33. Effect of snow cover on soil temperatures. Temperature versus depth profiles at pits no. 1 (where snow was protected) and no. 2 (where snow was removed), winter 1967-68.

surface temperature changes, the top meter of soil had an effective thermal diffusivity that was effectively low, hence the low values for $\alpha(n = 1)$ from 0 to 0.5 meters in Tables 5 and 10.

Due to uncertainty regarding snow density, thermal conductivity of frozen soil, and freezing point depression for soil, no attempt was made to calculate the depth of freezing throughout the winter season. From the lowest position of the 0°C isotherm (Figs. 18, 19, and 20), the maximum depths of freezing during the winters of 1967-68, 1969-70, and 1970-71, were respectively about 1, 1+, and 0.6 meters.

5.2.3 Permafrost

The existence of permafrost was established from drill data of the Alaska Department of Highways and from probing through the silt at thermocouple column no. IX. (p. 4; Fig. 6). Further evidence of the permafrost was provided by the unusually low values for thermal diffusivity at thermocouple column no. I at 3 meters depth, with the medium assumed to be a semi-infinite solid (Tables 5 and 10). A 0°C boundary provided by permafrost at a certain depth would have caused the temperature amplitudes to attenuate more rapidly with depth than expected in a semi-infinite solid. Different infinite slab models were employed, and the best fitting results were from boundary conditions placed at either 3.5 or 4.0 meters below the soil surface (Tables 5, 10; Fig. 27). Consequently, according to Equation (13). the derived thermal diffusivities from 2.0 to 3.0 meters depth, were larger and closer to

acceptable values. Permafrost thus probably affected the diffusivity and thermal regime below 3.0 to 4.0 meters depth.

5.3 Thermal regime at the stream center

5.3.1 Aufeis cover

Although the snow cover on the aufeis was considerably thinner than on the banks, the large thickness of ice in conjunction with the snow and flowing water, both beneath and over the ice, made an effective insulator against the cold pulse penetration into the underlying sediments. Consequently, the stream bottom surface, on the average, has not undergone much more cooling than the soil surface away from the stream during the three winters of observation - 1967-68, 1969-70, 1970-71, as shown in Figs. 18, 19, 20, 21, and 22.

The aufeis cover without snow or water tended to act as a heat sink, due to its relatively high thermal conductivity, as shown by the rapid penetration of negative isotherms to the soil during early December 1970 and late January 1971 (Fig. 20). The presence of snow on top of the ice had a striking effect, causing the ice to warm rapidly toward a new steady state temperature profile. A good example of this was the sudden fall of about 38 cm of snow beginning on January 1968 which not only provided insulation but fell during a period of relatively high air temperatures, thus adding heat to the system (Fig. 18). The cold spells of mid-January and early-February were of equal intensity, yet due to the snow the ice temperature was much higher during the second cold spell than during the first.

As shown in Table 8, the thermal conductivity of ice is about 16 times that of snow with a density of 0.2 g cm^{-3} or about 32 times that of snow with a density of 0.1 g cm^{-3}; thus, the addition of the 38 cm of snow (with an assumed density of 0.15 g cm^{-3}) to 150 cm of ice increased the insulation quality of the system by about 600%.

More striking was the occurrence of overflows, which temporarily but totally shielded the underlying ice from the cold. Usually occurring in November and December of each season, each overflow caused the ice surface to rise to 0°C immediately and, during the time required for the overflow to freeze, the entire ice body became essentially isothermal at 0°C. This situation closely approximated the ideal case of an infinite slab bounded at the top and bottom by 0°C and given an initial temperature ranging linearly from 0°C at the bottom to a negative temperature, T_o, at the top. The mathematical expression, given by Carslaw and Jaeger (1959) is:

$$T_z = \frac{2T_o}{\pi} \sum_{n=1}^{n=\infty} \frac{(-1)^{n-1}}{n} \exp(-n^2\theta) \sin\left(\frac{n \pi z}{x}\right), \quad n = 1, 2, 3, \ldots . \quad (42)$$

where: T_z = temperature at depth, z,

T_o = initial surface temperature,

$\theta = \alpha\pi^2 t/x^2$,

t = time (sec),

α = thermal diffusivity of ice = 0.0118 $cm^2 sec^{-1}$ (Table 14),

and x = thickness of the slab (cm).

Using the overflow commencing on or about 11 December 1967 as an example, the air temperature was -37°C with an ice thickness of 100 cm. The time required for the ice to warm past -1.0°C at mid-depth, according to equation (42) was 3.14 days. The time required for the 33 cm of overflow water to freeze according to Michel's equation (Michel, 1971, p. 77, eq. 82) was 9 days, by which time the lower 100 cm of ice had warmed to within -0.0027°C. Only after the water was completely frozen was it possible for the low temperatures to penetrate the ice again. Due to the saturation of snow by the overflow, the subsequent removal of heat or "penetration of cold" was usually rapid, as shown by the overflow commencing on 20 November 1970 (Fig. 20).

An attempt was made to determine the thermal diffusivity of ice from the temperature data available, using the numerical step method (Appendix B) as discussed in Chapter 4. From theoretical temperature curves generated throughout six separate time periods (generally lasting two to three weeks each), it was found that the best fitting curve in each case indicated a thermal diffusivity much higher than 0.0118 cm^2sec^{-1}, the maximum possible for pure ice. Since the aufeis contained layers of air bubbles, caused by inclusion of snow by the overflows, the thermal diffusivity was expected to be less than 0.0118 cm^2sec^{-1} (Table 8). As shown in Fig. 34 (showing the results from 9 to 27 April 1971), the ice became isothermal much more rapidly than it would have if conduction were the only means of heat transfer; non-conductive heat transfer mechanisms were present, a possible example having been convection of air and/or water through cracks and holes in the ice.

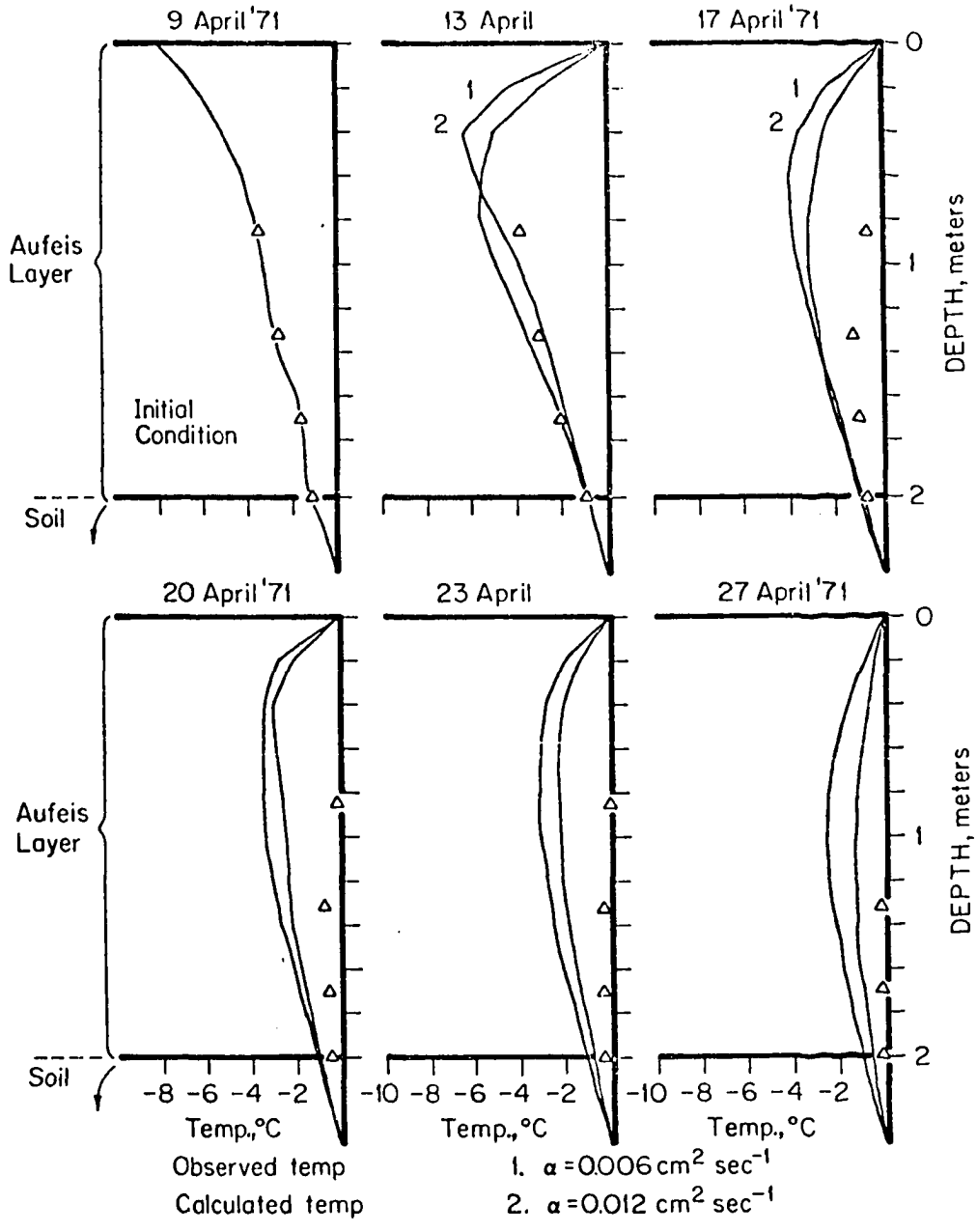

Figure 34. Comparison of observed temperatures in aufeis with those calculated by numerical step method, using infinite slab models of thermal diffusivities, 0.006 and 0.012 $cm^2 sec^{-1}$, 9 through 27 April 1971.

5.3.2 Heat transfer by water movement

The Fourier amplitudes for the temperatures at column no. I (farthest from the stream) decreased 34% from the ground surface to 1 meter depth, but in the stream center the decrease was only 21%, thus giving very high values for thermal diffusivity according to equations (15), (16), and (18) (Tables 4, 5, 9, and 10). The numerical step method, also discussed in Chapter 4, yielded very high values for α in the stream sediments. From the third method (differential analysis), the results were, for the most part, completely incompatible with the assumption of conduction being the only means of heat transfer. Notwithstanding inaccuracies in the data, the existence of negative $\frac{dT/dt}{d^2T/dz^2}$ and α, due to anamolous curvatures of the temperature profiles require explanation. The high values for α derived from the more reliable methods are undoubtedly due to additional heat transfer by water movement, but can this cause the expression, $\frac{dT/dt}{d^2T/dz^2}$, to be negative?

In an attempt to answer this, the following mathematical considerations are made. If there is any convection of water at all, it is most apt to be in the horizontal direction downstream, due to ground water seepage. In addition, horizontal movement of water (between the stream bed and the banks) and net vertical movement (due to changes in the hydrostatic pressure head) are undoubtedly present, as shown in studies by Kane (1975, p. 25 and 32) and Kane et al. (1973). Due to the movement of water around the soil particles, there is the possibility

of dispersion or scattering (i.e., intermingling of individual water molecules). Together, the net movement (convection) and dispersion (scattering) of water aid in the transfer of heat through the sediments; thus, at least two additional terms should be added to the basic conductive heat-flow equation:

$$Q = Q_c + Q_v + Q_d, \tag{43}$$

where: Q = total heat flux,

Q_c = heat flux due to conduction,

Q_v = heat flux due to convection of water, and

Q_d = heat flux due to dispersion of water.

The derivation of an expression for Q_v and Q_d in terms of mass flux, temperature, depth and time is beyond the scope of this study; however, Q_c is directly proportional to the wet thermal conductivity, K_m, and the temperature gradient, ∇T:

$$Q_c = K_m \nabla T \tag{44}$$

therefore:

$$Q = K_m \nabla T + Q_v + Q_d \tag{45}$$

The change in temperature of a parcel of material is related to the gradient of Q as follows:

$$\nabla \cdot Q = c_m \rho_m \left(\frac{\partial T}{\partial t}\right) \tag{46}$$

where: c_m = wet specific heat, and

ρ_m = wet density of the soil.

Substituting for Q in equations (46) and (45):

$$\nabla \cdot Q = c_m \rho_m \left(\frac{\partial T}{\partial t}\right) = \nabla \cdot (K_m \nabla T + Q_v + Q_d) \tag{47}$$

thus giving:

$$\frac{\partial T}{\partial t} = \alpha \nabla^2 T + \frac{\nabla \cdot (Q_v + Q_d)}{c_m \rho_m} \qquad (48)$$

where: $\alpha = K_m / c_m \rho_m$.

Without data on ground water movement and without better control over the temperature data, the complete evaluation of equation (48) remains largely a matter of conjecture.

5.4 Conclusions

The thermal regime of a sub-arctic stream, such as Goldstream Creek, was observed to be complex and significantly different from that adjacent to the channel. The system consists of multiple layers of inhomogeneous media, whose boundaries fluctuate through space and time.

On either side of the stream, snow was underlain by frozen silt, mainly saturated unfrozen silt, and permafrost at a depth of about 4 meters. In the stream, snow was underlain by ice (water or frozen soil), unfrozen soil, and possibly permafrost. The stream is close to an end member of stream freezing types, ranging from groundwater seeps to large rivers that freeze only at the surface.

The summer temperatures in the stream bed and at the ground surface were 11°C and 22°C respectively during the year 1970-71. During the winter they were the same: -2°C.

Thus with the small amount of water present, Goldstream Creek tends to be a heat source during the winter and a heat sink during the summer, but to a lesser extent than large bodies of water, such as rivers and

lakes. Generally, throughout the annual cycle, the isotherms follow topographic contours of the well defined banks which rise about 1.8 meters above the flat bottom.

The tendency for the stream to serve as a summer heat sink was largely counteracted at depth by very rapid heat penetration into the sediments caused possibly by additional heat transfer due to water movement. From data collected during the winter 1971-72, Kane (1975) concluded that water movement takes place between the stream below the permafrost. Whether this occurs during the summer is not known, but Kane's studies show the complicated and little-understood nature of groundwater movement in the valley. If this movement takes place, non-conductive heat transfer would be very important as a factor, thus making the conduction models used in the study totally inapplicable. Verification of the existence of heat transfer by water movement requires further investigation to rule out the possibility of faulty thermocouple connections.

The existence of permafrost at a depth of about 4 meters (away from the stream) was indicated by Alaska Highway Department drill data and probing of the soil with a steel rod. This is consistent with the thermal data which was best fit by infinite slab models with boundary conditions set at 4.0 meters. Also, while the soil cooled during the fall, the temperature profiles consistently had a maximum at 2 meters depth.

From season to season, the differences in winter conditions have been significant. For example, the winter of 1969-70 was milder than

that of 1970-71, but in spite of this the winter cold pulse penetrated more deeply due to the unusually thin snow cover which never exceeded 30 cm on the ground. Likewise, the aufeis was only 100 cm thick during most of the winter. As a result, the minimum soil surface temperatures in 1969-70 were -8.2 °C adjacent to the stream, and -8.0 °C beneath the aufeis. During 1970-71 the corresponding minimum values were both -2 °C.

5.5 Suggestions for further study

In view of the complex nature of the heat balance in and near a sub-arctic stream, the following recommendations for a similar, future study are made:

(1) A comprehensive study should be carried out on the heat and mass fluxes throughout the annual cycle in streams of several sizes.

(2) The study should take account of: (a) latent heat exchanges, (b) advancing boundaries due to freezing and thawing, (c) fluctuations of stream water level, and (d) changes in the thickness and density of snow. These factors, of course, would add considerable complexity to the simplest numerical step procedure.

(3) A purely mathematical model is too complex and impractical; thus a numerical model, patterned after the simple models used in this study would be more suitable. A numerical step procedure is preferable.

(4) Due to the vast number of calculations required, a computer program, similar in approach to the FORTRAN program written for this

study is suggested. For each time increment, the changes throughout a layered system of mediums should be determined in two alternating stages: (a) changes in medium boundaries at constant temperature, and (b) changes in temperature with fixed medium boundaries.

(5) Finally, in spite of the large amount of data collected for this study, there is greater need for data control: (a) continuous or frequent, automatic recording of temperature to ascertain and correct for diurnal fluctuations, (b) density measurements of the snow throughout the winter season, (c) laboratory determination of soil moisture content, dry density, and thermal conductivity, and (d) at least several measurements of the rate of groundwater movement through the soil.

APPENDIX A

SAMPLE DATA SHEET

Data sheets were prepared for the project to systematically contain data originally entered into field notebooks. As shown in the sample sheet (Fig. 35), space was provided to include a log of events, potentiometer readings, meteorological information and additional data pertaining to snow, ice, and water conditions.

Potentiometer readings were expressed both in microvolts and equivalent degrees centigrade. Probe numbers, as displayed on the switch panel, included A0 through A23 (columns no. I, II, III, and IV), C0 through C23 (columns no. V, VI, VII, and VIII), and E0 through E8 (columns no. IX and X).

Meteorological information consisted of wind and sky conditions and present air temperature according to both the mercury thermometer ("Air T.") and thermograph ("Graph I"). Also entered were present temperature from the secondary thermograph probe ("Graph II") and previous daily high and low air temperature.

Readings of snow thickness were made on the ground (above columns no. I, II, III, VIII, IX, and X), the aufeis, and on three snow tables. Table I was located near the hut (Fig. 5), while Tables II and III (not shown) were situated close to Ballaine Road on the east bank.

GOLDSTREAM CREEK

1135 Arrived at site.
Thermograph OK.
Ice: same as yesterday. No overflows.
Installed thermocouple strand #1 on ice.
Junctions E12-E17 located 25 ± 5 cm downstream from stakes 45-VII respectively.
Spacing between junctions: 130 3 cm.

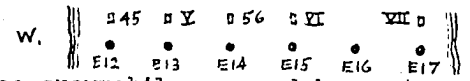

Three snowmobiles passed by upstream just after we froze slush over thermocouple strand. Acid test! No harm done.
1300 Began temperature readings using Esterline Angus recorder - much handier than L&N.
1400 Ended temperature measurements.
1415 Left site

#	μV	T°C	#	μV	T°C	#	μV	T°C
A0	-56	-1.5	C0	0	0.0	E0	-52	-1.4
1	-4	-0.1	1	0	0.0	1	-6	-0.2
2	34	0.9	2	10	0.3	2	0	0.0
3	46	1.2	3	43	1.1	3	23	0.6
4	62	1.6	4	72	1.9	4	23	0.6
5	26	0.7	5	-513	-13.6	5	21	0.6
						6	-5	-0.1
A6	-72	-1.9	C6	0	0.0			
7	-3	-0.1	7	9	0.2	E7	43	1.1
8	9	0.2	8	22	0.6	8	24	0.6
9	22	0.6	9	57	1.5			
10	23	0.6	10	77	2.0	A0	-60	-1.6
11	22	0.6	11	0	0.0	1	-25	-0.6
						2	22	0.6
A12	-72	-1.9	C12	0	0.0	3	47	1.2
13	-24	-0.6	13	2	0.0	4	62	1.6
14	10	0.3	14	23	0.6	5	34	0.9
15	25	0.6	15	35	0.9			
16	33	0.9	16	48	1.2			
17	46	1.2	17	-1	0.0			
A18	-38	-1.0	C18	-113	-3.0			
19	0	0.0	19	-3	-0.1			
20	21	0.6	20	-1	0.0			
21	27	0.7	21	0	0.0			
22	49	1.3	22	0	0.0			
23	33	0.9	23	0	0.0			

DATA	
Time AST	1135
D. of W.	Tue
Date	27 Oct
Year	1970
Party	SWC
"	BLH
"	-
"	-
WEATHER	
Sky	Clear
Wind	Calm
Air T.	-14.2
Graph I	-14.2
Graph II	-2.7
High T.	-11.0
Low T.	-26.8
Misc.	
SNOW	
Table I	35.5
" II	-
" III	-
Stake I	27
" II	30
" III	25
" IIX	24
" IX	28
" X	34
On ice	6?
New snow	0
WATER	
Temp.	-
Level GP	-
Sample #	-
Conduct.	-
Current	-
ICE	
Level GP	37
Stake 45	-
" V	-
" 56	-
" VI	-
" VII	-
Thickness	-
Elevation	280?
MISC	

Figure 35. Sample data sheet.

Finally, hydrological data included water temperature, water level (according to the gauge post), electrical conductivity of water samples, and ice level as read from the gauge post and from stakes located over the thermocouple cross-section (stakes V, VI, and VII). In addition, stakes 45 (between IV and V), and 56 (between V and VI) were also employed.

APPENDIX B

FORTRAN PROGRAM FOR TEMPERATURE CALCULATION, USING NUMERICAL STEP METHOD

A program, written in FORTRAN IV (Fig. 36), was a considerable aid in performing the numerous calculations required. Based on the Fourier conduction equation (equation 12 in text), the step method employed in this study is discussed in standard textbooks on heat transfer (eg. Ingersoll and Zobel, 1954) and is briefly covered in Chapter 4, Part 2 (equations (19) through (27)). The main features of the program are summarized by the following flow diagram, list of symbols, and data card sequence.

```
1 MAR 69 BUFF40 FORTRAN IV-F                                    --C001--   DATE 04/05/72

      C
      C     A PROGRAM FOR CALCULATING TEMPERATURE FLUCTUATIONS IN A SEMI-INFINITE
      C         HOMOGENEOUS MEDIUM OF KNOWN THERMAL DIFFUSIVITY WITH GIVEN
      C           SURFACE TEMPERATURES.
      C
      C     FOR THIS, THE NUMERICAL APPROACH IS TAKEN DUE TO ITS ACCURACY
      C       AND SIMPLICITY
      C
0001          DIMENSION TEMP(4,200), A1(10), DATA(10), Z(21)
0002        1 READ(1,2)(DATA(I),I=1,10),DZ,DT,NZ,NT,(A1(J),J=1,8)
0003        2 FORMAT(4A4,F4.2,5A4,2F4.0,2I4,8F3.0)
0004          IF(A1(1))50,50,3
0005        3 JM=NT/10+1
0006          DO 6 I=1,2
0007          DO 5 J=1,JM
0008          K=10*J-9
0009          L=10*J
0010          READ(1,4)(TEMP(I,M),M=K,L)
0011        4 FORMAT(10F8.2)
0012        5 CONTINUE
0013        6 CONTINUE
0014          IM=NZ/10+1
0015          DO 7 I=1,IM
0016          J=10*I-9
0017          K=10*I
0018        7 READ(1,4)(TEMP(3,L),L=J,K)
0019          I=NZ+1
0020          Z(1)=0.
0021          AS=1800.*DT/(DZ**2)
0022          DO 8 J=2,21
0023        8 Z(J)=Z(J-1)+DZ
0024          IA=0
0025        9 IA=IA+1
```

Figure 36. Listing of computer program, written in FORTRAN IV, for calculating temperature changes in semi-infinite solids (and infinite slabs), using numerical step procedure.

```
0026            A2=A1(IA)/10000.
0027            A4=A2*A3
0028            IF(A2)1,1,10
0029         10 WRITE(3,11)(DATA(J),J=1,10),DZ,NZ,DT,NT,A2,(Z(K),K=1,21)
0030         11 FORMAT('1','LOCATION -- ',4A4/' BEGINNING TIME-- ',F4.1,3A4/
                C' TYPE OF MEDIUM-- ',2A4/' DEPTH INCREMENT-- ',F4.0,' CENTIMETERS'
                C/' NUMBER OF DEPTH INCREMENTS-- ',I4/' TIME INCREMENT-- ',F4.0,
                C' HOURS'/' NUMBER OF TIME INCREMENTS-- ',I4/' THERMAL DIFFUSIVITY
                COF THE MEDIUM-- ',F6.5//' TIME',T30,'DEPTH-- CENTIMETERS'//
                C' DAY  HOUR',3X,21F5.0/)
0031            IDAY=1
0032            HOUR=DATA(5)
0033            IF(2*A2*A3-1.)14,14,12
0034         12 WRITE(3,13)
0035         13 FORMAT(////////////////T30,'CANNOT DO THIS ONE'//
                CT30,'CHOSEN DEPTH AND TIME INCREMENTS DO NOT FULFILL STABILITY'/
                CT33,'REQUIREMENT FOR GIVEN THERMAL DIFFUSIVITY'////////////
                CT30,'SORRY ABOUT THAT'///)
0036            GO TO 9
0037         14 IF(NZ-20)32,35,35
0038         32 DO 33 K=NZ,20
0039         33 TEMP(3,K+1)=TEMP(3,1)
0040         35 WRITE(3,15)IDAY,HOUR,(TEMP(3,J),J=1,21)
0041         15 FORMAT(I2,I3,2X,F4.1,3X,21F5.1)
0042            DO 37 J=1,1
0043         37 TEMP(4,J)=TEMP(3,J)
0044            J=NT
0045            DO 30 K=2,J
0046            TEMP(4,I)=TEMP(1,K)
0047            TEMP(4,I)=TEMP(2,K)
0048            M=2*(I/2)-1
0049            DO 18 L=3,M,2
0050         18 TEMP(4,L)=TEMP(4,L)+A4*(TEMP(4,L-1)-2*TEMP(4,L)+TEMP(4,L+1))
0051            IF(2*(NZ/2)-NZ)41,40,40
0052         40 M=M+2
0053         41 DO 20 L=3,M,2
0054         20 TEMP(4,L-1)=TEMP(4,L-1)+A4*(TEMP(4,L-2)-2*TEMP(4,L-1)+TEMP(4,L))
0055            IF(NZ-20)22,25,25
0056         22 DO 23 L=NZ,20
```

Figure 36, cont'd.

```
0057        23 TEMP(4,L+1)=TEMP(2,K)
0058        25 HOUR=HOUR+DT
0059        26 IF(HOUR-24.)26,27,27
0060        27 HOUR=HOUR-24.
0061           IDAY=IDAY+1
0062           GO TO 26
0063        28 WRITE(3,15)IDAY,HOUR,(TEMP(4,L),L=1,21)
0064        30 CONTINUE
0065           GO TO 9
0066        50 STOP
0067           END

*     IN *MAIN*,
*     PROGRAM STORAGE USES 03570 BYTES
*     SYMBOL TABLE STORAGE USES 01304 BYTES
*     DIMENSIONED DATA STORAGE USES 03364 BYTES

*     STORAGE REMAINING IS 72858 BYTES
*     END OF COMPILATION 24.05.24.59

*     PROGRAM EXECUTION
```

Figure 36, cont'd.

B.1 Flow Diagram

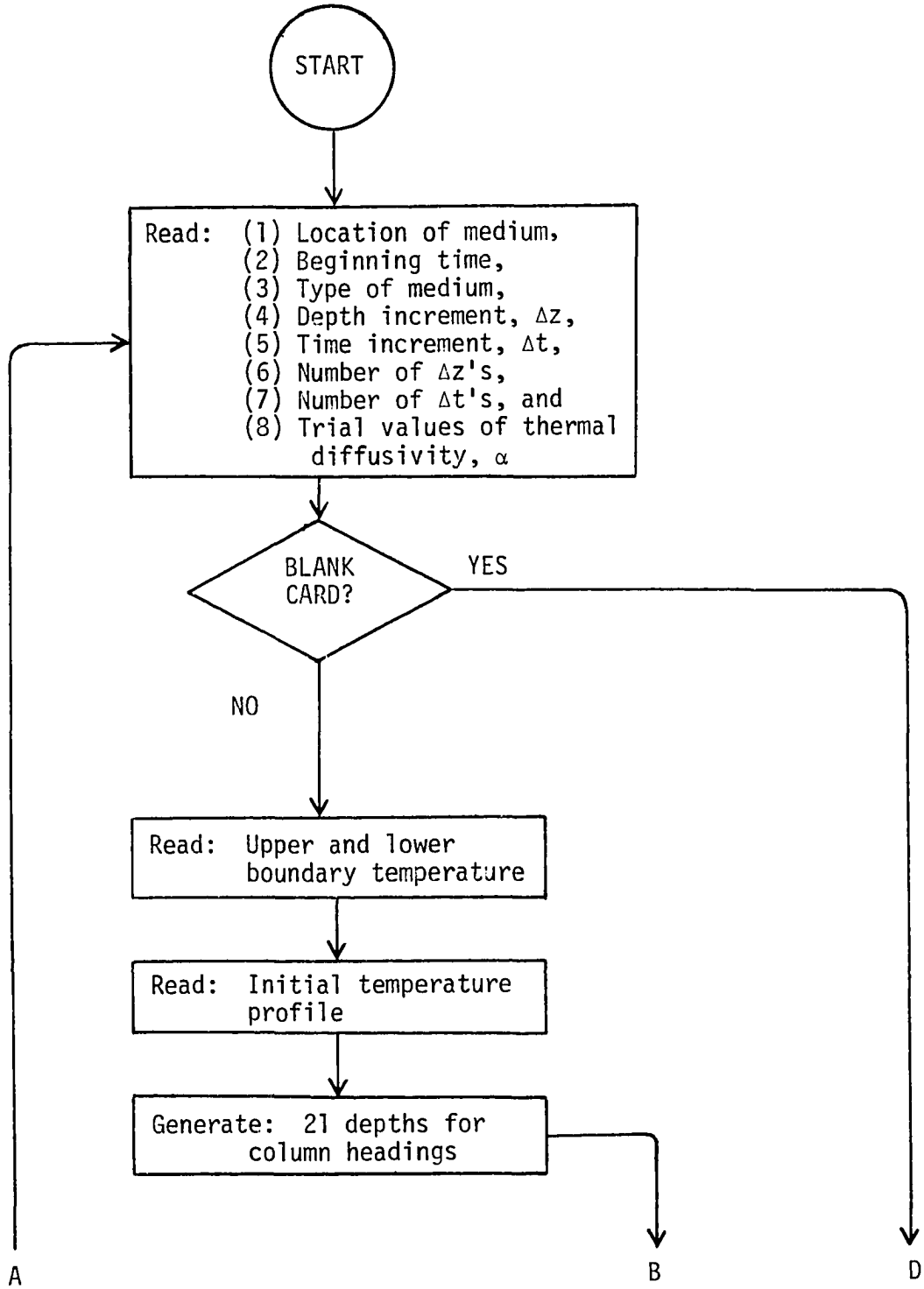

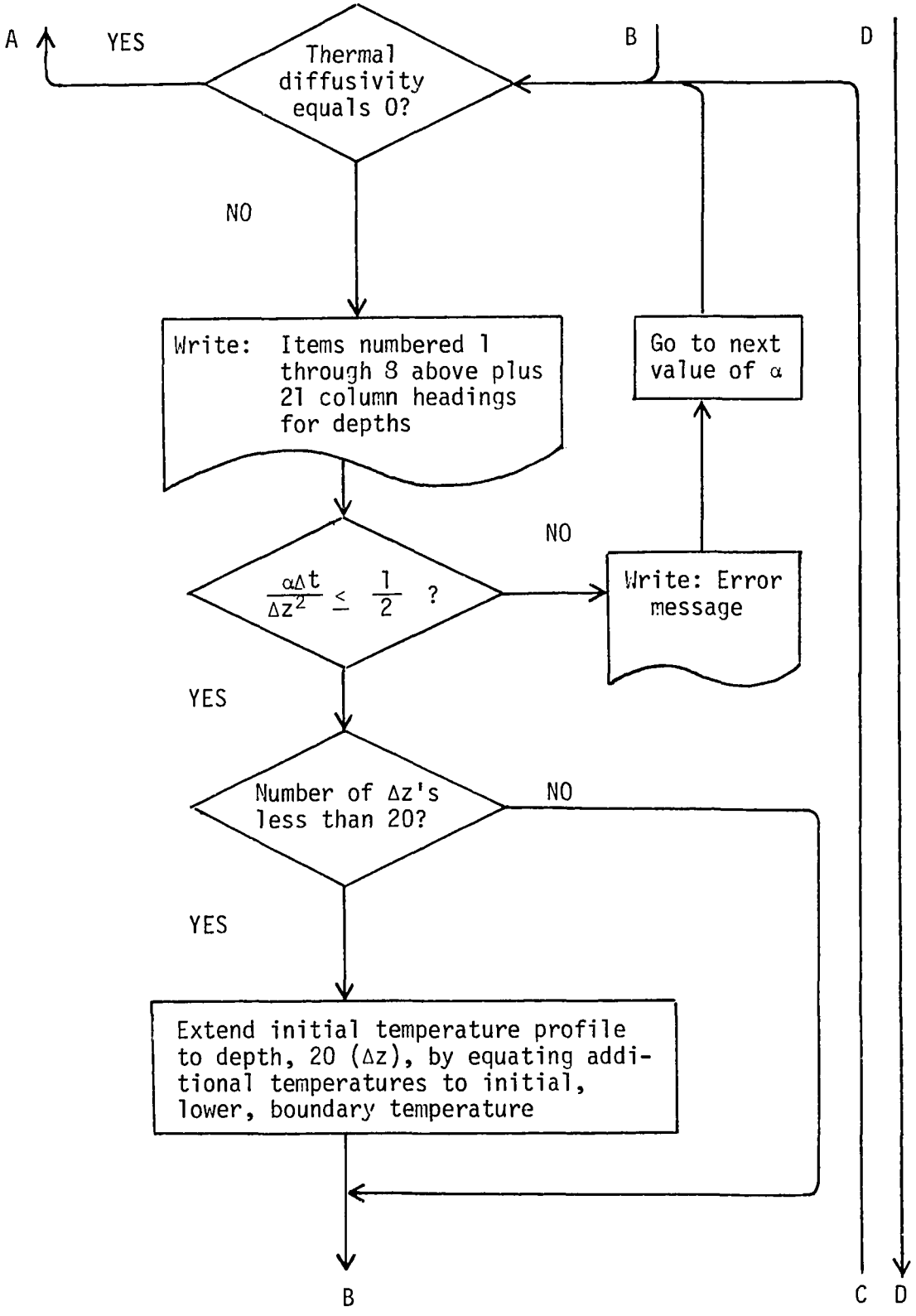

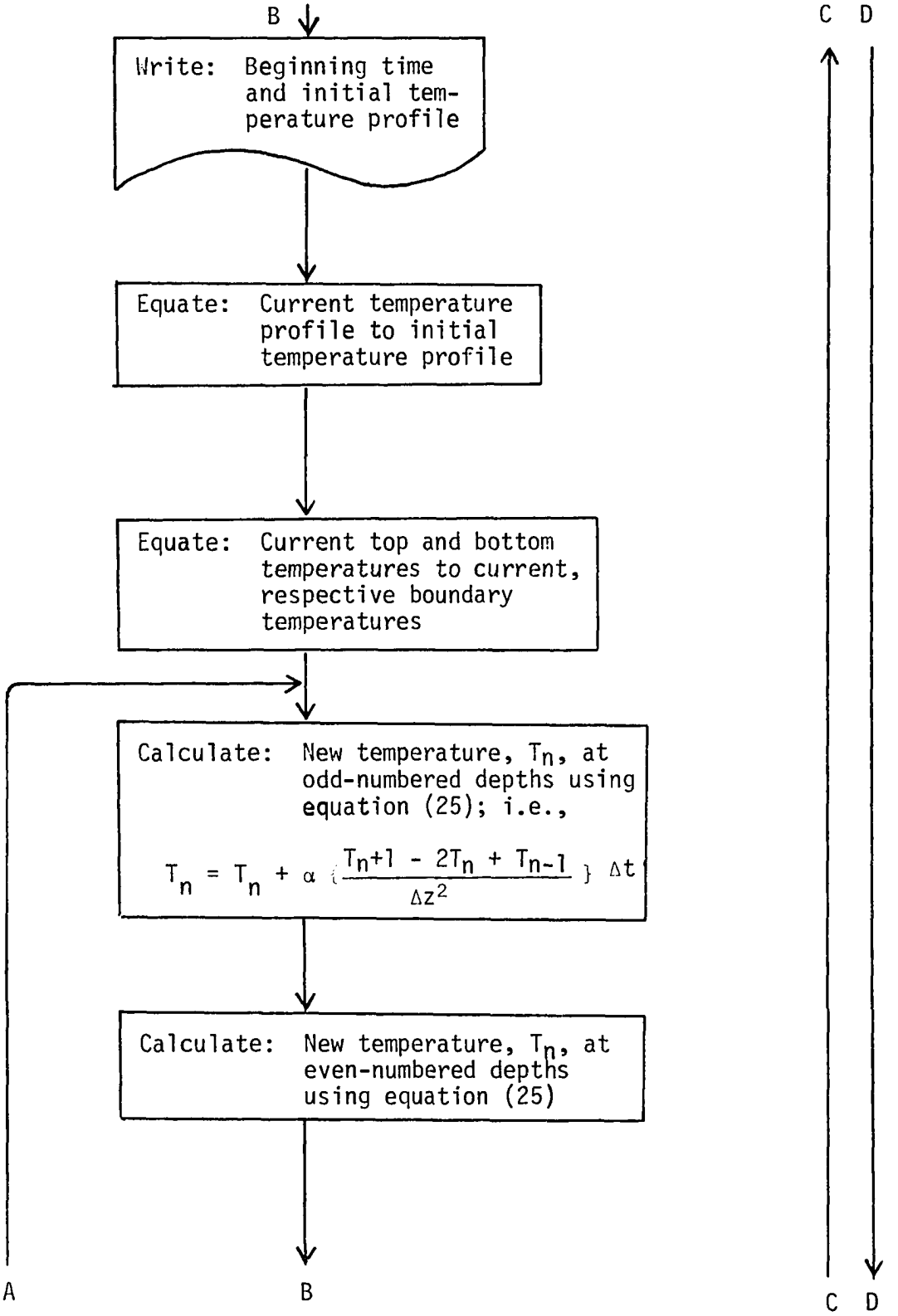

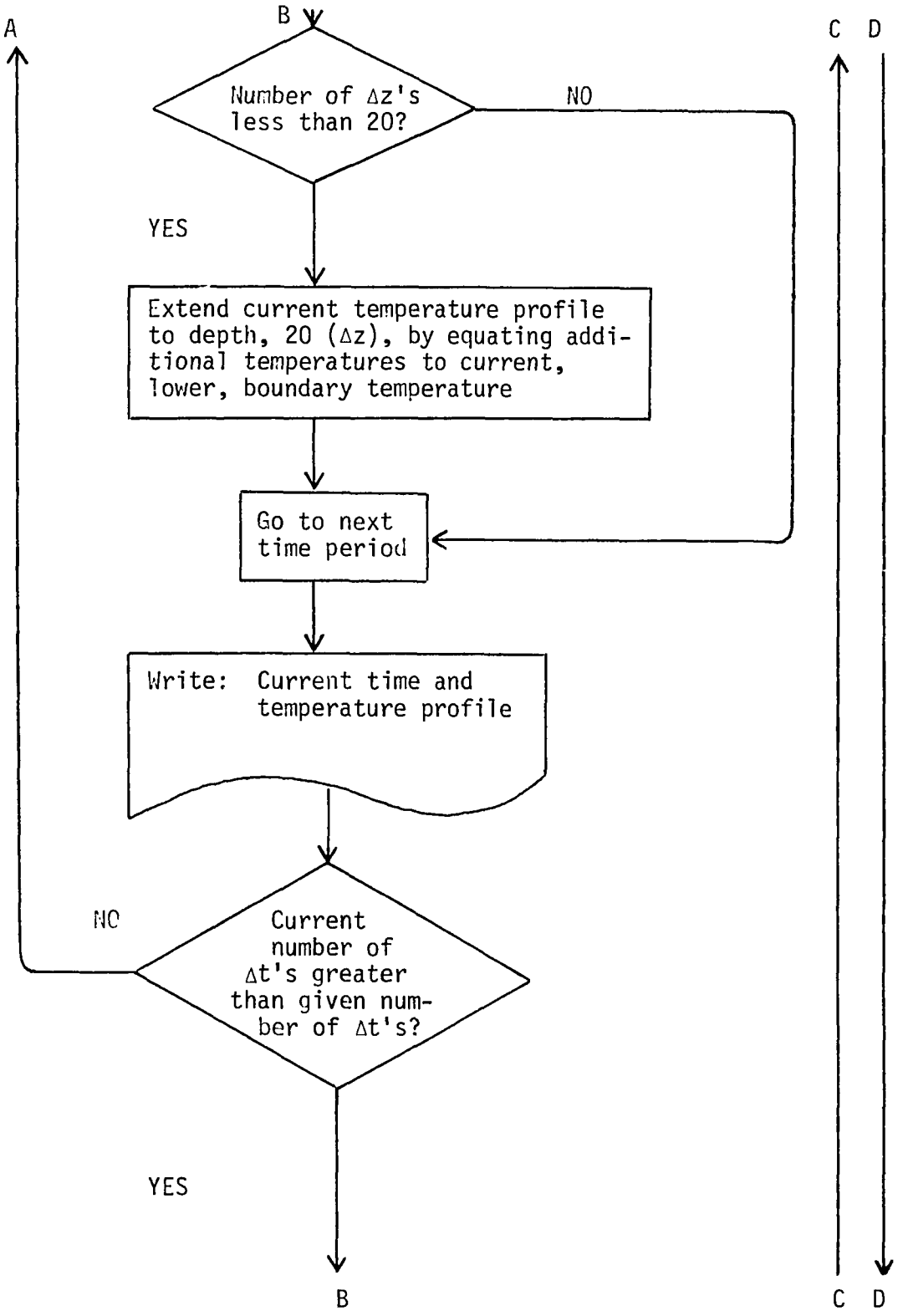

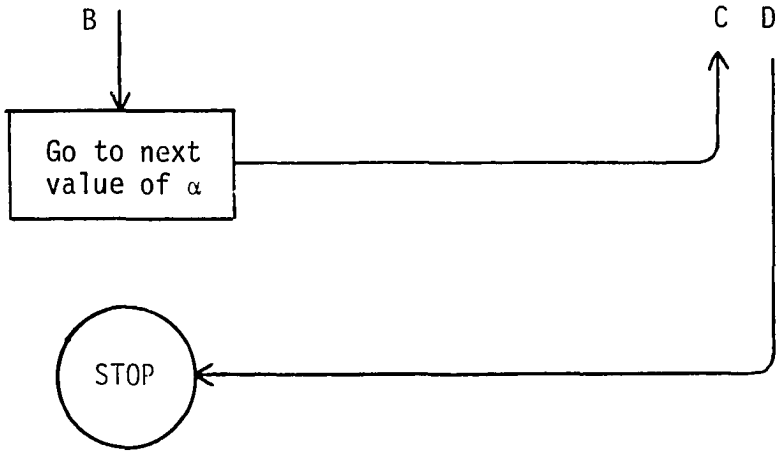

B.2 List of symbols (in order of appearance in program)

DATA(1-10)	Supporting information; namely, location (DATA(1-4)), beginning time (DATA(5)), beginning date (DATA(6-8)), and type of medium (DATA(9-10)).
DZ	Given depth increment, Δz
DT	Given time increment, Δt
NZ	Given number of depth increments throughout medium
NT	Given number of time increments throughout period of calculation
A1(1-8)	Given values of thermal diffusivity, α, in units of $10^{-4}cm^2sec^{-1}$ (factor of 10^{-4} eliminates unnecessary zeros on data card)
TEMP(1, 1-200)	Given temperatures, T_1, at upper boundary of medium throughout time period
TEMP(2, 1-200)	Given temperatures, T_{NZ+1}, at lower boundary of medium throughout time period (for semi-infinite solid, use suitably large number for NZ not to exceed 200)

JM	Number of data cards required for either TEMP(1,1-200) or TEMP(2,1-200); i.e., NT/10 rounded to next higher integer
TEMP(3, 1-200)	Initial or previous temperature profile, T_n
IM	Number of data cards required for TEMP(3, 1-200); i.e., NZ/10 rounded to next higher integer
A3	1800(DT/DZ^2) which equals: $\frac{\Delta t}{2\Delta z^2}$
Z(1-21)	Multiples of DZ, ranging from 0 cm to 20(DZ) or 20(Δz)
IA	Current subscript of A1(1-8)
A2	Thermal diffusivity, α, expressed in cm^2sec^{-1} or 10^{-4}(A1(IA))
A4	A2 x A4 or $\frac{\alpha\Delta t}{2\Delta z^2}$ which must be equal to or less than 0.5 to maintain stability of calculation
IDAY	Current day (numbered from beginning day)
HOUR	Current hour of day
TEMP(4-200)	Current temperature profile, T_n
I, J, K, L, and M	Indices for do-loops

B.3 Data Card Sequence

The following sequence of cards was used for execution of the program shown in Fig. 37:

Card(s)	Spaces	Format	Values Punched
1	1-16	4A4	Location of medium ("CENTER OF STREAM")
	17-20	F4.2	Beginning hour, tenths, and hundredths ("0.00")
	21-32	3A4	Beginning day and year ("12 MAY 1971")
	33-40	2A4	Type of medium ("SOIL")
	41-44	F4.0	Depth increment in cm ("50.")
	45-48	F4.0	Time increment in hour(s) ("48.")
	49-52	I4	Number of depth increments ("20")
	53-56	I4	Number of time increments ("110")
	57-80	8F3.0	Trial sequence of thermal diffusivities in units of $10^{-4}cm^2sec^{-1}$ ("040.", etc.) Note: Interruption of sequence by zeros or blanks will cause the program to stop or skip remaining values in sequence.
JM=12	1-80	10F8.2	Upper boundary temperatures in ^oC, with 10 temperatures to each card ("0.0", "0.2", "0.5", etc.)
JM=12	1-80	10F8.2	Lower boundary temperatures in ^oC, with 10 temperatures to each card (all cards left blank).
IM=3	1-80	10F8.2	Initial temperature profile in ^oC, with 10 temperatures to each card (all zeros).
1	1-80	-	Blank card to stop program

29 = Total number of cards

LOCATION -- CENTER OF STREAM
BEGINNING TIME-- 0.0 12 MAY 1971
TYPE OF MEDIUM-- SOIL
DEPTH INCREMENT-- 50. CENTIMETERS
NUMBER OF DEPTH INCREMENTS-- 20
TIME INCREMENT-- 48. HOURS
NUMBER OF TIME INCREMENTS-- 110
THERMAL DIFFUSIVITY OF THE MEDIUM-- .00400

TIME		DEPTH-- CENTIMETERS												
DAY	HOUR	0.	50.	100.	150.	200.	250.	300.	350.	400.	450.	500.	550.	600.
1	0.0	0.0	0.0	0.0	0.0	0.0	0.0	0.0	0.0	0.0	0.0	0.0	0.0	0.0
3	0.0	0.2	0.0	0.0	0.0	0.0	0.0	0.0	0.0	0.0	0.0	0.0	0.0	0.0
5	0.0	0.5	0.1	0.0	0.0	0.0	0.0	0.0	0.0	0.0	0.0	0.0	0.0	0.0
7	0.0	1.4	0.3	0.0	0.0	0.0	0.0	0.0	0.0	0.0	0.0	0.0	0.0	0.0
9	0.0	2.7	0.6	0.0	0.0	0.0	0.0	0.0	0.0	0.0	0.0	0.0	0.0	0.0
11	0.0	4.4	1.0	0.1	0.0	0.0	0.0	0.0	0.0	0.0	0.0	0.0	0.0	0.0
13	0.0	5.8	1.6	0.2	0.0	0.0	0.0	0.0	0.0	0.0	0.0	0.0	0.0	0.0
15	0.0	6.2	2.1	0.4	0.1	0.0	0.0	0.0	0.0	0.0	0.0	0.0	0.0	0.0
17	0.0	5.9	2.4	0.6	0.1	0.0	0.0	0.0	0.0	0.0	0.0	0.0	0.0	0.0
19	0.0	5.7	2.6	0.8	0.2	0.0	0.0	0.0	0.0	0.0	0.0	0.0	0.0	0.0
21	0.0	5.6	2.8	0.9	0.3	0.1	0.0	0.0	0.0	0.0	0.0	0.0	0.0	0.0
23	0.0	6.3	3.1	1.1	0.4	0.1	0.0	0.0	0.0	0.0	0.0	0.0	0.0	0.0
25	0.0	7.4	3.4	1.3	0.5	0.1	0.0	0.0	0.0	0.0	0.0	0.0	0.0	0.0
27	0.0	7.9	3.9	1.5	0.6	0.2	0.0	0.0	0.0	0.0	0.0	0.0	0.0	0.0
29	0.0	8.3	4.1	1.7	0.7	0.2	0.1	0.0	0.0	0.0	0.0	0.0	0.0	0.0
31	0.0	8.4	4.4	1.9	0.8	0.2	0.1	0.0	0.0	0.0	0.0	0.0	0.0	0.0
33	0.0	8.4	4.6	2.1	0.9	0.3	0.1	0.0	0.0	0.0	0.0	0.0	0.0	0.0
35	0.0	8.5	4.8	2.2	1.0	0.3	0.1	0.0	0.0	0.0	0.0	0.0	0.0	0.0
37	0.0	9.6	5.2	2.4	1.1	0.4	0.2	0.0	0.0	0.0	0.0	0.0	0.0	0.0
39	0.0	10.6	5.6	2.6	1.2	0.5	0.2	0.1	0.0	0.0	0.0	0.0	0.0	0.0
41	0.0	11.1	5.9	2.8	1.4	0.5	0.2	0.1	0.0	0.0	0.0	0.0	0.0	0.0
43	0.0	11.2	6.3	3.1	1.5	0.6	0.3	0.1	0.0	0.0	0.0	0.0	0.0	0.0
45	0.0	11.2	6.5	3.3	1.6	0.7	0.3	0.1	0.0	0.0	0.0	0.0	0.0	0.0
47	0.0	10.7	6.7	3.5	1.8	0.8	0.3	0.1	0.0	0.0	0.0	0.0	0.0	0.0
49	0.0	10.4	6.8	3.7	1.9	0.8	0.4	0.1	0.1	0.0	0.0	0.0	0.0	0.0
51	0.0	10.5	6.9	3.9	2.0	0.9	0.4	0.2	0.1	0.0	0.0	0.0	0.0	0.0
53	0.0	10.6	7.0	4.0	2.2	1.0	0.5	0.2	0.1	0.0	0.0	0.0	0.0	0.0
55	0.0	10.6	7.1	4.2	2.3	1.1	0.5	0.2	0.1	0.0	0.0	0.0	0.0	0.0
57	0.0	10.3	7.2	4.3	2.4	1.2	0.6	0.2	0.1	0.0	0.0	0.0	0.0	0.0
59	0.0	9.8	7.2	4.5	2.6	1.3	0.6	0.3	0.1	0.0	0.0	0.0	0.0	0.0
61	0.0	9.5	7.1	4.6	2.7	1.4	0.7	0.3	0.1	0.0	0.0	0.0	0.0	0.0
63	0.0	9.4	7.1	4.7	2.8	1.4	0.7	0.3	0.1	0.1	0.0	0.0	0.0	0.0
65	0.0	9.4	7.1	4.7	2.9	1.5	0.8	0.4	0.2	0.1	0.0	0.0	0.0	0.0
67	0.0	9.5	7.1	4.8	3.0	1.6	0.9	0.4	0.2	0.1	0.0	0.0	0.0	0.0
69	0.0	9.4	7.1	4.9	3.1	1.7	0.9	0.4	0.2	0.1	0.0	0.0	0.0	0.0
71	0.0	9.2	7.1	4.9	3.1	1.8	1.0	0.5	0.2	0.1	0.0	0.0	0.0	0.0
73	0.0	8.9	7.1	5.0	3.2	1.9	1.0	0.5	0.2	0.1	0.0	0.0	0.0	0.0
75	0.0	9.0	7.0	5.0	3.3	1.9	1.1	0.5	0.3	0.1	0.1	0.0	0.0	0.0
77	0.0	8.9	7.0	5.1	3.4	2.0	1.1	0.6	0.3	0.1	0.1	0.0	0.0	0.0
79	0.0	8.7	7.0	5.1	3.4	2.1	1.2	0.6	0.3	0.1	0.1	0.0	0.0	0.0
81	0.0	8.4	6.9	5.1	3.5	2.1	1.2	0.7	0.3	0.2	0.1	0.0	0.0	0.0
83	0.0	8.1	6.8	5.2	3.5	2.2	1.3	0.7	0.4	0.2	0.1	0.0	0.0	0.0
85	0.0	8.0	6.8	5.2	3.6	2.3	1.4	0.7	0.4	0.2	0.1	0.0	0.0	0.0
87	0.0	8.0	6.7	5.2	3.6	2.3	1.4	0.8	0.4	0.2	0.1	0.0	0.0	0.0
89	0.0	8.1	6.7	5.2	3.7	2.4	1.5	0.8	0.4	0.2	0.1	0.0	0.0	0.0
91	0.0	8.1	6.7	5.2	3.7	2.4	1.5	0.8	0.5	0.2	0.1	0.0	0.0	0.0
93	0.0	7.8	6.6	5.2	3.7	2.5	1.6	0.9	0.5	0.2	0.1	0.1	0.0	0.0

Figure 37. Sample execution of FORTRAN program, showing temperatures (°C) in a semi-infinite solid.

APPENDIX C

PROGRAMS FOR HEWLETT-PACKARD-25 HAND CALCULATOR

In addition to the use of FORTRAN IV, summarized in Appendix B, the present-day availability of programmable, hand calculators provided much convenience in performing numerous, repetitive calculations. As with many models presently on the market, the Hewlett-Packard 25 model, with a memory capacity of program steps, 8 addressable registers, and 4 stack registers, was adequate.

With details of operation covered in the manufacturer's instruction manual, the following is a resume of the programs and procedures that were devised for the evaluation of four equations discussed in the text.

C.1 Depth of Freezing in Soil

(1) Purpose: To calculate change in depth of freezing (from Z_1 to Z_2) soil with moisture content, w, and thermal conductivity, K_f. Soil is covered with snow of thickness, Z_s, and thermal conductivity, K_s, and T is the average subfreezing temperature throughout the time period, Δt. Also, let ρ_I and L represent density and latent heat of fusion of ice respectively:

$$Z_2 = \{(\frac{Z_s K_f}{K_s} + Z_1)^2 + \frac{2 T K_f \Delta t}{w \rho_I L}\}^{1/2} - \frac{Z_s K_f}{K_s}$$

(see text, pp. 14-16; after Michel, 1971).

(2) Program:

01	RCL 6	09	÷	17	x	25	+
02	g x=0	10	RCL 4	18	x y	26	g x^2
03	GTO 13	11	÷	19	RCL 0	27	+
04	R↓	12	STO 6	20	x	28	f
05	RCL 5	13	x	21	RCL 1	29	RCL 3
06	RCL 2	14	RCL 0	22	÷	30	-
07	÷	15	x	23	STO 3	31	STO 7
08	RCL 3	16	2	24	RCL 7		

(3) Procedure:

(a) Store the following values in memory registers:

R0	K_f	R4	L
R1	K_s	R5	Δt
R2	w	R6	-
R3	ρ	R7	Z_1

(b) Key in the sequence:

Z_s, ENTER, T, and R/S

(c) With Z_2 displayed, repeat (b) for each successive Δt.

NOTE: If w or Δt vary, clear R6 before next calculation.

After each calculation, the following values are automatically stored in the registers:

R3 $Z_s K_f / K_s$

R6 $\Delta t / w \rho_I L$

R7 Z_2

Z_2 is identical to Z_1 for the next time period, and there is no need to enter Z_1 into R7 between each calculation.

C.2 Four-term Fourier Series

(1) Purpose: To evaluate temperature, T, as a cyclic function of time, t, where T is expressed as the sum of the mean temperature, T_m, and first, second, third, and fourth-order sinusoids. Let ω represent

the frequency of the first-order sinusoid, and A_1, A_2, A_3, A_4, Θ_1, Θ_2, Θ_3, and Θ_4 be the Fourier coefficients (A = amplitude, Θ = phase angle).

$$T = T_m + A_1 \cos(\omega t + \Theta_1) + A_2 \cos(2\omega t + \Theta_2) + A_3 \cos(3\omega t + \Theta_3) + A_4 \cos(4\omega t + \Theta_4)$$

(see text, pp. 57-58)

(2) Program:

01	R↓	11	x	21	+	31	RCL 7
02	R↓	12	+	22	RCL 5	32	1
03	ENTER	13	RCL 3	23	9	33	2
04	RCL 1	14	6	24	0	34	0
05	3	15	0	25	+	35	+
06	0	16	+	26	STO 5	36	STO 7
07	+	17	STO 3	27	f cos	37	f cos
08	STO 1	18	f cos	28	RCL 4	38	RCL 6
09	f cos	19	RCL 2	29	x	39	x
10	RCL 0	20	x	30	+	40	+

(3) Procedure:

(a) Store the following values in memory registers:

R0	A_1	R4	A_3
R1	Θ_1	R5	Θ_3
R2	A_2	R6	A_4
R3	Θ_2	R7	Θ_4

(b) Key in the sequence:

T_m, ENTER, ENTER, ENTER, R/S

(c) With T displayed, press R/S for each successive Δt

NOTE: Δt automatically equals 30^o where 360^o equals the duration of the main cycle. To change Δt, key in the following sequence:

GTO 04, Δt, GTO 13, $2\Delta t$, GTO 22, $3\Delta t$, GTO 31, and $4\Delta t$.

C.3 Amplitude Attenuation of Sinusoidal Temperature Pulse with Depth in an Infinite Slab

(1) Purpose: To calculate the ratio between the amplitude of temperature fluctuation, A_z, at depth, z, in an infinite, homogeneous slab and the amplitude of fluctuation at the surface, A_o. Let x be the thickness of the slab, ω be the frequency of temperature variation, α = thermal diffusivity of the medium, and n = any positive integer:

$$\frac{A_z}{A_o} = \left\{\frac{\cosh(2kx - 2kz) - \cos(2kx - 2kz)}{\cosh(2kx) - \cos(2kx)}\right\}^{1/2}$$

where $k = \sqrt{n\omega/2\alpha}$

(see text, pp. 59-60; source: Carslaw and Jaeger, 1959).

(2) Program:

01	g 1/x	13	R↓	25	g e^x	37	RCL 5
02	RCL 1	14	RCL 3	26	x	38	RCL 6
03	x	15	CHS	27	RCL 6	39	STO 5
04	RCL 2	16	RCL 4	28	f cos	40	R↓
05	x	17	+	29	2	41	STO 6
06	f $\sqrt{x}$	18	x	30	x	42	f CLX
07	STO 0	19	STO 5	31	-	43	GTO 21
08	ENTER	20	f CLX	32	RCL 7	44	÷
09	ENTER	21	RCL 6	33	g x≠0	45	0
10	RCL 4	22	g e^x	34	GTO 44	46	STO 7
11	x	23	RCL 6	35	x⇄y	47	R↓
12	STO 6	24	CHS	36	STO 7	48	f $\sqrt{x}$

(3) Procedure:

(a) Store the following values in memory registers:

R0	-	R4	x
R1	2n	R5	-
R2	ω	R6	-
R3	z	R7	-

(b) Key in the sequence:

α, R/S

(c) With A_z/A_o displayed, repeat (b) for different values of α.

NOTE: The key, g rad, must be pressed in the beginning of the calculation so that all angles will be expressed in terms of radians.

After each calculation, the following values are automatically stored in the registers:

R0 2k
R5 2k(x - z)
R6 2kx

C.4 Temperature Variation in an Infinite Slab

(1) Purpose: To calculate temperature, T_z, at time, t, and depth, z, in an infinite, homogeneous slab of thickness, x. Let the slab be bounded at both top and bottom by 0^oC with an initial temperature profile ranging linearally from 0^oC at the bottom to T_o at the top. Also, let α equal the thermal diffusivity of the medium:

$$T_z = \frac{2T_o}{\pi} \sum_{n=1}^{n=\infty} \frac{(-1)^{n-1}}{n} \exp(-n^2\Theta) \sin\left(\frac{n\pi z}{x}\right)$$

where $\Theta = \alpha\pi^2 t/x^2$

(see text, pp. 111-112; source: Carslaw and Jaeger, 1959).

(2) Program:

01	RCL 3	13	g x^2	25	÷	37	x
02	g π	14	x	26	f sin	38	RCL 0
03	g x^2	15	RCL 4	27	x	39	x
04	x	16	x	28	RCL 5	40	2
05	RCL 1	17	CHS	29	÷	41	x
06	g x^2	18	g e^x	30	RCL 5	42	g π
07	÷	19	RCL 5	31	2	43	÷
08	STO 6	20	g π	32	÷	44	RCL 7
09	RCL 5	21	x	33	g frac	45	+
10	1	22	RCL 2	34	4	46	STO 7
11	+	23	x	35	x		
12	STO 5	24	RCL 1	36	-1		

(3) Procedure:

(a) Store the following values in memory registers:

R0	T_o	R4	t
R1	x	R5	-
R2	z	R6	-
R3		R7	-

(b) Press R/S

(c) With successive approximations of T_z displayed, press R/S repeatedly until display does not change.

NOTE: After each calculation, the following values are automatically stored in the registers:

R5	n
R6	$\alpha\pi^2/x^2$
R7	approx. T_z

If a value is already stored in R6, the first nine program steps can be bypassed by pressing GTO 09 instead of GTO 00 before execution.

If α or x change, clear R6 before next calculation.

REFERENCES

Alaska Department of Highways (1974). Foundation report, Goldstream Creek at Ballaine Road, bridge no. 1009, project no. S-0646(3), interior district. 6 p. W. H. Slater, chief geologist. Fairbanks, Alaska.

Altberg, W. J. (1936). Twenty years of work in the domain of underwater ice formation (1915-1935). IN: Bulletin 23, pp. 373-407. International Union of Geodesy and Geophysics, International Association of Scientific Hydrology.

Baver, L. D. (1948). Soil Physics. 384 p. John Wiley and Sons, Inc., New York, New York. Chapman and Hall, Ltd., London, England.

Bear, J. (1972). Dynamics of Fluids in Porous Media. 756 p. American Elsevier Publishing Company, Inc., New York, New York.

Benson, C. S. (1962). Stratigraphic studies of the snow and firn of the Greenland ice sheet. SIPRE research report 70. 93 p. Snow, Ice and Permafrost Research Establishment (now USA CRREL), Corps of Engineers, U.S. Army. Hanover, New Hampshire.

_____. (1966). A study of the freezing cycle in an Alaskan stream. IN: 1966 annual report, pp. 100-117. Institute of Water Resources, University of Alaska, Fairbanks, Alaska.

_____. (1967). A study of the freezing cycle in an Alaskan stream. IN: 1967 Annual report, pp. 19-22. Institute of Water Resources, University of Alaska, Fairbanks, Alaska.

_____. (1968). A study of the freezing cycle in an Alaskan stream. IN: 1968 annual report, pp. 13-21. Institute of Water Resources, University of Alaska, Fairbanks, Alaska.

_____. (1973). A study of the freezing cycle in an Alaskan stream, a completion report. 31 p. Institute of Water Resources, University of Alaska, Fairbanks, Alaska.

Bey, P. P. (1951). The heat economy of the snow pack. IN: Review of the properties of snow and ice. SIPRE technical report 4, pp. 73-81. H. T. Mantis, editor. Snow, Ice and Permafrost Research Establishment (now USA CRREL), Corps of Engineers, U.S. Army. Hanover, New Hampshire.

Brewer, M. C. (1958). The thermal regime of an arctic lake. IN: Trans. Amer. Geophys. Union, Vol. 39, pp. 278-284.

Carslaw, H. S., and J. C. Jaeger (1947, 1959). Conduction of Heat in Solids. 386 p. Oxford University Press, London, England. Melbourne, Australia.

Corbin, S. W., and C. S. Benson (1972). The winter thermal regime of Goldstream Creek, Alaska. IN: Proceedings of the 22nd Alaskan Science Conference, p. 163. Amer. Assoc. for the Adv. of Science, Alaska Division. College, Alaska. August 1971.

Crawford, C. B. (1952). Soil temperature, a review of the literature. IN: Frost Action in Soils. A Symposium, Highway Res. Board, Spec. Report No. 2, pp. 17-41. Nat. Acad. of Sci., Washington, D.C., January 1951.

Dingman, L. S., W. F. Weeks and Y. C. Yen (1967). The effects of thermal pollution on river ice conditions - a general method of calculation. USA CRREL research report 206, part 1. 33 p. USA CRREL, Corps of Engineers, U.S. Army. Hanover, New Hampshire.

Dorsey, N. E. (1940). Properties of Ordinary Water Substance. 356 p. Reinhold Pub. Corp., New York, New York.

_____. (1948). The freezing of supercooled water. IN: Trans. of Amer. Philosop. Soc., Vol. 38, part 3, pp. 247-328.

Geiger, R. (1965). The Climate Near the Ground. 600 p. Harvard University Press, Cambridge, Massachusetts.

Gilfilian, R. E. (1973). Winter history of a small sub-arctic Alaskan stream. M.S. thesis. 119 p. University of Alaska, Fairbanks, Alaska.

Gilfilian, R. E., W. L. Kline, T. E. Osterkamp, and C. S. Benson (1972). Ice formation in a small Alaskan stream. IN: Proceedings of the International Symposium on the Role of Snow and Ice in Hydrology, pp. 505-513. World. Met. Organiz., Banff, Canada, September 1972.

Goldstein, R. J., and B. L. Hansen (1951). Thermal properties. IN: Review of the properties of snow and ice. SIPRE technical report 4. pp. 52-59. H. T. Mantis, editor. Snow, Ice and Permafrost Research Establishment (now USA CRREL), Corps of Engineers, U.S. Army. Hanover, New Hampshire.

Ingersoll, L. R., O. J. Zobel and A. C. Ingersoll (1954). Heat Conduction - with Engineering, Geological, and Other Applications. 316 p. Revised edition, Univ. of Wisconsin Press, Madison, Wisconsin.

Kane, D. L. (1975). Hydraulic mechanism of aufeis growth. Ph.D. thesis. 118 p. Univ. of Minnesota, Minneapolis, Minnesota.

Kane, D. L., R. F. Carlson and C. E. Bowers (1973). Groundwater pore pressures adjacent to sub-arctic streams. IN: North American Contribution to the Second International Permafrost Conference. pp. 453-458. Nat. Acad. of Sci., Yakutsk, USSR, July 1973.

Kersten, M. S. (1948). The thermal conductivity of soils. IN: Proceedings, Highway Research Board, Vol. 28, pp. 391-409.

_____. (1952). Thermal properties of soils. IN: Frost Action in Soils, a Symposium. Highway Research Board, Special Report No. 2, Nat. Acad. of Sci. Washington, D.C., January 1951.

_____. (1963). Thermal properties of frozen ground. IN: Permafrost - International Conference, Nat. Acad. of Sci., Nat. Res. Council. Lafayette, Indiana. pp. 301-304.

Kreitner, J. D. (1969). The petrofabrics of aufeis in a turbulent Alaskan stream. M. S. thesis, 59 p. University of Alaska, Fairbanks, Alaska.

Kreitner, J. D., and C. S. Benson (1970). The freezing cycle in a small turbulent stream. IN: Proceedings of the 20th Alaskan Science. pp. 332-333. Amer. Assoc. for the Adv. of Science, Alaska Division. College, Alaska. August 1969.

Lachenbruch, A. H. (1970). Some estimates of the thermal effects of a heated pipeline in permafrost. 23 p. U.S. Geological Survey Circular 632. U.S.G.S., U.S. Dept. of Interior, Washington, D.C.

Mantis, H. T., editor (1951). Review of the properties of snow and ice. SIPRE technical report 4. 156 p. Snow, Ice and Permafrost Research Establishment (now USA CRREL), Corps of Engineers, U.S. Army. Hanover, New Hampshire.

Michel, B. (1968). Morphology of frazil ice. IN: Physics of Snow and Ice, Proceedings of the International Conference on Low Temperature Science, Col. 1, part 1, pp. 119-136. Institute of Low Temperature Science, Hokkaido Univ., Sapporo, Japan, August 1966.

_____. (1971). Winter regime of rivers and lakes. USA CRREL, Cold Regions Science and Engineering, Monograph III-B1a. 139 p. USA CRREL, Crops of Engineers, U.S. Army. Hanover, New Hampshire.

Osterkamp, T. E., R. E. Gilfilian, and C. S. Benson (1972). Observations of stage, disc arge, pH, and electrical conductivity during periods of ice formation in a small subarctic stream. IN: Trans. Amer. Geophysical Union, Vol. 11, No. 2, pp. 268-272.

Pounder, E. R. (1965). Physics of Ice. 143 p. Pergamon Press, New York, New York.

Sellmann, P. V. (1972). Geology and properties of materials exposed in the USA CRREL permafrost tunnel. Special report 177. 18 p. USA CRREL, Corps of Engineers, U.S. Army. Hanover, New Hampshire.

Trabant, D. C. (1970). Diagenesis of the seasonal snow cover in interior Alaska. M. S. thesis. 48 p. University of Alaska, Fairbanks, Alaska.

Weller, G. E., and P. Schwerdtfeger (1970). Thermal properties and heat transfer processes of the snow of the central antarctic plateau. IASH Publication No. 86, p. 284. The International Symposium on Antarctic Glaciological Exploration. Hanover, New Hampshire, August 1968.

Williams, J. R. (1965). Ground water in permafrost regions - annotated bibliography. U.S. Geological Survey Water Supply Paper 1972. 294 p. USGS, U.S. Dept. of the Interior, Washington, D.C.

_____. (1970). Ground water in the permafrost regions of Alaska. U.S. Geological Survey Prof. Paper 696. 83 p. USGS, U.S. Dept. of the Interior, Washington, D.C.